

From the  
Comprehensive Pneumology Centre (CPC)  
of the Ludwig-Maximilians-Universität München  
Director: PD Dr. Anne Hilgendorff and Dr. Ali Önder Yildirim

---

# The lung fibroblast surface proteins PDGFR $\alpha$ and CDCP1 as profibrotic mediators in pulmonary fibrosis

---

Dissertation  
zum Erwerb des Doctor of Philosophy (Ph.D.)  
an der Medizinischen Fakultät der  
Ludwig-Maximilians-Universität München

submitted by  
Nina Noskovičová  
from  
Bratislava, Slovakia

on  
February 2018

Supervisor: Prof. Dr. Oliver Eickelberg

Second evaluator: Prof. Dr. Heiko Adler

Dean: Prof. Dr. Reinhard Hickel

Date of oral defense: August 16, 2018

## AFFIDAVIT

I, Nina Noskovičová, hereby declare, that submitted thesis entitled

*„The lung fibroblast surface proteins PDGFR $\alpha$  and CDCP1 as profibrotic mediators  
in pulmonary fibrosis”*

is my own work. I have only used the sources indicated and have not made unauthorized use of services of a third party. Where the work of others has been quoted or reproduced, the source is always given,

I further declare that the submitted thesis or parts thereof have not been presented as parts of an examination degree at any other university.

Munich, 17.08.2018

Noskovičová Nina

---

Place/Date

---

Signature doctoral candidate

*"Never be afraid to try something new, because life gets boring when you stay within the limits of what you already know"*



---

**TABLE OF CONTENT**

<b>ABBREVIATIONS</b> .....	<b>1</b>
<b>SUMMARY</b> .....	<b>7</b>
<b>1 INTRODUCTION</b> .....	<b>9</b>
<b>1.1 Idiopathic pulmonary fibrosis (IPF)</b> .....	<b>9</b>
1.1.1 Clinical presentation of IPF .....	9
1.1.2 Diagnosis of IPF .....	9
1.1.3 Treatment strategies of IPF .....	11
1.1.4 Histopathologic features of IPF .....	12
1.1.5 Pathogenesis of IPF .....	13
<b>1.2 Lung fibroblasts</b> .....	<b>14</b>
1.2.1 Fibroblasts in wound healing .....	15
1.2.2 Activated fibroblasts in IPF .....	16
1.2.3 Molecular mechanisms regulating fibroblasts activation.....	17
1.2.4 Transforming growth factor-beta (TGF $\beta$ ) signaling .....	18
1.2.4.1 Smad-dependent signaling .....	19
1.2.4.2 Smad-independent signaling .....	20
<b>1.3 Fibroblasts surface proteins</b> .....	<b>21</b>
1.3.1 Platelet-derived growth factor receptor-alpha (PDGFR $\alpha$ ).....	22
1.3.2 Cub domain containing protein 1.....	24
<b>2 OBJECTIVES</b> .....	<b>25</b>
<b>3 MATERIALS AND METHODS</b> .....	<b>26</b>
<b>3.1 Materials</b> .....	<b>26</b>
3.1.1 Chemicals and reagents .....	26
3.1.2 Consumables.....	27
3.1.3 Cell culture media.....	28

---

3.1.4	Small interfering RNA (siRNA)	28
3.1.5	DNA constructs	29
3.1.6	Inhibitors and antagonists	29
3.1.7	Antibodies	29
3.1.8	Human primers	32
3.1.9	Kits	32
3.1.10	Laboratory equipment	33
3.1.11	Software	34
<b>3.2</b>	<b>Methods</b>	<b>34</b>
3.2.1	Isolation of primary human lung fibroblasts	34
3.2.2	Cryopreservation of primary human lung fibroblasts	35
3.2.3	Thawing frozen cells	35
3.2.4	Cell culture experiments	35
3.2.4.1	Growth factor stimulation	35
3.2.4.2	siRNA-mediated reverse transfection	36
3.2.4.3	Plasmid DNA transfection	36
3.2.4.4	Luciferase reporter assay	37
3.2.4.5	Cell treatment with inhibitors	38
3.2.4.6	Cell treatment with 2-phospho-L-ascorbic acid	38
3.2.4.7	Cell adhesion assay	38
3.2.4.8	Cell invasion assay	38
3.2.4.8.1	Preparation of collagen G Gels	38
3.2.4.8.2	3D collagen-based invasion assay	39
3.2.5	Protein analysis	39
3.2.5.1	Protein extraction from primary fibroblasts	39
3.2.5.2	Protein concentration from cell supernatants	39

3.2.5.3	SDS-PAGE and immunoblotting .....	40
3.2.5.4	Immunoprecipitation .....	41
3.2.5.5	Sircol collagen assay .....	42
3.2.5.6	Immunofluorescence staining of primary human lung fibroblast .....	43
3.2.5.7	Immunofluorescence staining of spherically-shaped primary human lung fibroblasts ...	43
3.2.5.8	Live-cell staining.....	43
3.2.5.9	Immunofluorescence staining of paraffin-embedded tissue sections .....	44
3.2.5.10	Flow cytometry.....	45
3.2.6	RNA expression analysis .....	45
3.2.6.1	RNA isolation.....	45
3.2.6.2	cDNA synthesis by Reverse Transcription.....	45
3.2.6.3	Quantitative Real-Time Polymerase Chain Reaction (qRT-PCR) .....	46
<b>4</b>	<b>RESULTS.....</b>	<b>48</b>
	<b>Chapter A: TGF<math>\beta</math> regulates cell surface marker expression.....</b>	<b>48</b>
4.1	TGF $\beta$ decreases PDGFR $\alpha$ expression in pHLFs .....	48
4.2	TGF $\beta$ downregulates CDCP1 expression in pHLFs.....	49
	<b>Chapter B: Functional consequence of altered surface marker expression.....</b>	<b>52</b>
4.3	<b>Characterization of PDGF signaling in lung fibroblasts and analysis of potential cross-talk to TGF<math>\beta</math> signaling.....</b>	<b>52</b>
4.3.1	PDGF ligands promote downstream PDGF signaling in lung fibroblasts .....	52
4.3.2	PDGF-AB increases invasion properties of primary human lung fibroblasts.....	53
4.3.3	PDGF-AB and PDGF-DD enhance PDGF signaling independently of TGF $\beta$ .....	54
4.3.4	PDGF signaling is increased in the absence of PDGFR $\alpha$ .....	55
4.3.5	The activity of tyrosine kinase inhibitor is attenuated in the absence of PDGFR $\alpha$ .....	58
4.3.6	Knockdown of PDGFR $\alpha$ together with TGF $\beta$ increases myofibroblasts differentiation and ECM production.....	60
4.4	<b>Identifying the role of CDCP1 in myofibroblast differentiation of human lung fibroblasts .</b>	<b>61</b>

4.4.1	SiRNA-mediated silencing of CDCP1 affects its cell surface and total protein levels in phLFs .....	61
4.4.2	CDCP1 inhibits cell adhesion of phLFs.....	62
4.4.3	Absence of CDCP1 enhances the expression of $\alpha$ SMA and ECM proteins .....	63
4.4.4	CDCP1 inhibits canonical TGF $\beta$ signaling in lung fibroblasts.....	66
4.4.5	TGF $\beta$ regulates CDCP1 expression via non-canonical TGF $\beta$ signaling pathway .....	67
4.4.6	TGF $\beta$ decreases CDCP1 expression levels via ubiquitin-independent proteasomal degradation .....	68
<b>5</b>	<b>DISCUSSION.....</b>	<b>71</b>
<b>5.1</b>	<b>Fibroblasts cell-surface proteome in response to profibrotic TGF<math>\beta</math>.....</b>	<b>71</b>
<b>5.2</b>	<b>TGF<math>\beta</math> effect on PDGF receptor expression in phLFs.....</b>	<b>72</b>
<b>5.3</b>	<b>PDGF ligand-receptor binding affinities in phLFs.....</b>	<b>73</b>
<b>5.4</b>	<b>PDGF signaling in human lung fibroblasts.....</b>	<b>74</b>
<b>5.5</b>	<b>PDGF signaling in cell invasion.....</b>	<b>74</b>
<b>5.6</b>	<b>Targeting PDGF signaling in IPF .....</b>	<b>75</b>
<b>5.7</b>	<b>TGF<math>\beta</math>-mediated expression changes of CDCP1 in phLFs .....</b>	<b>76</b>
<b>5.8</b>	<b>TGF<math>\beta</math> potentially drives an ubiquitin-independent degradation of CDCP1 in the proteasome .....</b>	<b>77</b>
<b>5.9</b>	<b>CDCP1 as a negative regulator of TGF<math>\beta</math> signaling .....</b>	<b>78</b>
<b>6</b>	<b>CONCLUSION AND FUTURE DIRECTIONS.....</b>	<b>80</b>
<b>7</b>	<b>REFERENCES .....</b>	<b>82</b>
<b>8</b>	<b>LIST OF TABLES.....</b>	<b>104</b>
<b>9</b>	<b>LIST OF FIGURES.....</b>	<b>105</b>
	<b>ACKNOWLEDGEMENTS.....</b>	<b>106</b>

**ABBREVIATIONS****A**

$\alpha$ SMA	Alpha-Smooth Muscle Actin
AEC	Alveolar Epithelial Cells
AKT	AKR mouse thymoma kinase
ALK5	Activin-Like Kinase 5
APS	Ammonium peroxodisulfate
APC-conjugated	Allophycocyanin-conjugated
ATS	American Thoracic Society

**B**

BCA	Bicinchoninic acid assay
BSA	Bovine serum albumin

**C**

$^{\circ}$ C	Celsius
cDNA	Complementary Deoxyribonucleic Acid
CD	Cluster of Differentiation
CDCP1	Cub Domain-Containing Protein 1
CFDA	Carboxy Fluorescein DiAcetate succinimidyl ester
CO <sub>2</sub>	Carbon dioxide
COL	Collagen
COPD	Chronic Obstructive Pulmonary Disease
CSC	Cell Surface Capturing
CTGF	Connective Tissue Growth Factor

**D**

DAPI	4',6-diamino-2-phenylindole
DMEM	Dulbecco's Modified Eagle Medium
DMSO	Dimethyl sulfoxide
dNTP	Desoxyribonucleotides
DNA	Deoxyribonucleic Acid
DPLD	Diffuse Parenchymal Lung Disease

DTT	Dithiothreitol
<b>E</b>	
ECM	Extracellular Matrix
ECL	Entry-level peroxidase substrate for enhanced chemiluminescence
EDTA	Ethylenediaminetetraacetic acid
EF	Elastic Fibers
EGFR	Epidermal Growth Factor Receptor
EMA	European Medicines Agency
EMT	Epithelial-to-Mesenchymal Transition
ER	Endoplasmic Reticulum
ERK	Extracellular signal–Regulated Kinase
<b>F</b>	
FACS	Fluorescence-Activated Cell Scanning
FAK	Focal Adhesion Kinase
FBS	Fetal Bovine Serum
FDA	Food and Drug Administration
FGF	Fibroblast Growth Factor
FVC	Forced Vital Capacity
FYN	FYN oncogene related to SRC, FGR, YES
<b>G</b>	
GRB2	Growth factor receptor-bound protein 2
GTP	Guanosine triphosphate
<b>H</b>	
h	hour
H <sub>2</sub> O	water
HEPES	N-2-Hydroxyethylpiperazine-N'-2-Ethanesulfonic Acid
HGF	Hepatocyte Growth Factor
HPRT	Hypoxanthine Phosphoribosyl Transferase
HRCT	High-Resolution Computer Tomography



μ	Micro
μl	Microliter
μM	Micromolar
MAPK	Mitogen-Activated Protein Kinase
MDD	Multidisciplinary Discussion
MEK	MAPK/Extracellular signal-regulated kinase Kinase
MEM	Minimal Essential Medium
MFI	Median Fluorescence Intensity
min	Minutes
mg	Milligram
mL	Milliliter
mm	Millimeter
MMP	Matrix Metalloproteinase
mRNA	messenger Ribonucleic Acid
mTOR	Mammalian Target of Rapamycin
MUC5B	Mucin 5B
MyF	Myofibroblasts
<b>N</b>	
NaCl	Sodium Chloride
Na <sub>2</sub> HPO <sub>4</sub>	Disodium Hydrogen Phosphate
NaOH	Sodium Hydroxide
ng	Nanogram
nM	Nanomolar
nm	Nanometer
NP-40	Nonidet P-40
<b>P</b>	
PAR	Protease-activated receptor
PBS	Phosphate Buffered Saline
PCR	Polymerase Chain Reaction
PDGF	Platelet-Derived Growth Factor
PDGFR $\alpha$	Platelet-Derived Growth Factor Receptor-alpha
PDGFR $\beta$	Platelet-Derived Growth Factor Receptor-beta

PE-conjugated	Phycoerythrin-conjugated
PFA	Paraformaldehyde
PGE2	Prostaglandin E2
PGI2	Prostaglandin I2 (Prostacyclin)
pH	Power of Hydrogen
phLFs	Primary human lung fibroblasts
PI3K	Phosphatidylinositol-3 kinase
PIP2	Phosphatidylinositol-4,5-biphosphate
PIP3	Phosphatidylinositol-3,4,5-triphosphate
PKC $\delta$	Protein Kinase C-delta
PVDF	Polyvinylidene difluorid

## Q

qRT-PCR	Quantitative Real-Time Polymerase Chain Reaction
---------	--

## R

RAS	Rat Sarcoma
RIPA	Radioimmunoprecipitation assay
RNA	Ribonucleic Acid
RPM	Rounds per minute
RT	Room Temperature
RTK	Receptor Tyrosine Kinase

## S

SB431542	Inhibitor of Alk 5 receptor
SD	Standard Deviation
SDS	Sodium Dodecyl Sulfate
SDS-PAGE	Sodium Dodecyl Sulfate – Polyacrylamide Gel Electrophoresis
SEM	Standard Error of the Mean
SFTPC gene	Surfactant Protein C gene
Shc	Src homology and collagen protein
Shh	Sonic hedgehog
SIMA135	Subtractive Immunization Associated 135 kDa
siRNA	Small Interfering RNA

SIS3	Specific inhibitor of Smad3
Smad	Mothers Against Decapentaplegic
SNP	Single Nucleotide Polymorphism
SOS	Son of sevenless
SPC	Surfactant Protein C
SRC	v-src sarcoma (Schmidt–Ruppin A-2) viral oncogene homolog

**T**

TBS	Tris-buffered saline
TEMED	Tetramethylethylenediamine
TERT	Telomerase Reverse Transcriptase
TERTC	Telomerase RNA Component
TGF $\beta$	Transforming Growth Factor Beta
THBS1	Thrombospondin 1
TNF $\alpha$	Tumor Necrosis Factor alpha
TRASK	Transmembrane and Associated with Src kinases

**U**

UIP	Usual Interstitial Pneumonia
-----	------------------------------

**V**

V	Volt
VEGF	Vascular Endothelial Growth Factor

**W**

WB	Western Blot
w/v	Weight per volume
WNT	Wingless/Integrase-1

**Y**

YES	v-yes Yamaguchi sarcoma viral oncogene homolog
-----	--

## SUMMARY

Idiopathic pulmonary fibrosis (IPF) is a chronic, irreversible, and life-threatening disease with a median survival of 3-5 years after diagnosis. The number of patients suffering from IPF is rapidly increasing, and therapeutic options are very limited. IPF is characterized by altered cellular composition and homeostasis in lung parenchyma, leading to excessive deposition of extracellular matrix (ECM), and ultimately, organ failure. Fibroblasts are the main cell types producing ECM in the lung. In general, fibroblasts play an important role in various cellular responses, including cell proliferation and migration, and therefore are essential for the processes of normal wound healing. The injury of the lung epithelium leads to the recruitment of inflammatory cells and the release of profibrotic growth factors, such as TGF $\beta$ , resulting in fibroblast to myofibroblast differentiation. Myofibroblasts represent a highly proliferating, migrating and increased ECM producing phenotype essentially participating in tissue remodeling of the fibrotic lung.

Little information, however, exists regarding changes in the fibroblast surface proteome under growth factor stimulation, since the fibroblasts surface proteome is not well characterized to date. Therefore, we have initially performed a cell-surface proteome profiling of primary human lung fibroblasts (phLFs) and further analyzed the impact of TGF $\beta$  on it [Heinzelmann et al., 2016]. Here, we identified Platelet derived growth factor receptor-alpha (PDGFR $\alpha$ ) and Cub domain containing protein 1 (CDCP1) among the top downregulated proteins. Thus, in my thesis I aimed to investigate in detail their functional role in lung fibroblasts and their impact on IPF.

In the first part of this thesis, the effect of TGF $\beta$  on the total mRNA and protein expression as well as on cell surface localization of PDGFR $\alpha$  and CDCP1 in primary human lung fibroblasts (phLFs) was determined. We confirmed PDGFR $\alpha$  and CDCP1 surface localization and downregulation of expression levels by TGF $\beta$ . In the second part, functional roles of both surface proteins in phLFs were addressed. With a focus on PDGF signaling first, PDGF ligand-receptor interactions were analyzed showing that ligand PDGF-AB predominantly activates PDGFR $\alpha$ , whereas PDGF-DD activates PDGFR $\beta$  downstream signaling as demonstrated by increased Akt phosphorylation. Surprisingly, the expression of PDGFR $\beta$  receptor was increased in the absence of PDGFR $\alpha$  via siRNA-mediated knockdown. Moreover, the role of PDGF signaling in cell invasion was addressed showing that PDGF-AB-induced signaling increased invasion properties of human lung fibroblasts and this effect is mediated in a PDGFR $\alpha$ -dependent manner. Importantly, Nintedanib decreased TGF $\beta$ -increased  $\alpha$ SMA and collagen V total protein expression, however, this effect was largely attenuated in PDGFR $\alpha$ -depleted cells.

Analysis of CDCP1 regulation revealed that TGF $\beta$  downregulated CDCP1 expression in a time-dependent manner and this effect was potentially mediated via increased ubiquitin-independent proteasomal degradation of CDCP1, but not canonical or non-canonical TGF $\beta$  pathway. Interestingly, CDCP1 also affected downstream TGF $\beta$  signaling as demonstrated by increased Smad3 phosphorylation in CDCP1-

depleted cells treated with TGF $\beta$ . Moreover, CDCP1 depletion enhanced TGF $\beta$ -mediated cell adhesion capacity of human lung fibroblasts. CDCP1 knockdown led to an increase in total protein expression levels of  $\alpha$ SMA, collagen III, and collagen V in pHLFs, which was independent of TGF $\beta$ . Importantly,  $\alpha$ SMA-positive interstitial myofibroblasts located in fibroblastic foci of IPF lung sections displayed a low expression of CDCP1, whereas non-differentiated interstitial lung fibroblasts in sections of donor lungs were highly CDCP1-positive, and clearly  $\alpha$ SMA-negative.

In sum, I showed in my study that TGF $\beta$  regulates the expression of fibroblasts surface proteins, as shown here for PDGFR $\alpha$  and CDCP1, which in turn modulates their function in lung fibroblasts and lung disease.

## **1 INTRODUCTION**

### **1.1 Idiopathic pulmonary fibrosis (IPF)**

Idiopathic pulmonary fibrosis (IPF) is defined as a chronic, progressive, and life-threatening lung disease with a median survival rate of 3-5 years from the time of diagnosis [Selman et al., 2001; Schwartz et al., 1994; King et al., 2001a]. IPF belongs to the category of interstitial lung diseases (ILD), also named diffuse parenchymal lung diseases (DPLD), and is further classified within this category to the subgroup of idiopathic interstitial pneumonias (IIP) with histopathological features of usual interstitial pneumonia (UIP) [Visscher and Myers, 2006; American Thoracic Society and European Respiratory Society, 2002; Raghu et al., 2011]. Generally, the prevalence of IPF varies between 2 and 29 cases per 100.000 persons [Annesi-Maesano et al., 2013]. Interestingly, the prevalence of IPF in the USA population is estimated between 42.7 and 63 cases per 100.000 persons, whereas in Europe numbers vary between 1.25 and 23.4 cases per 100.000 persons [Nalysnyk et al., 2012; Ley and Collard, 2013; Fernández Pérez et al., 2010].

#### **1.1.1 Clinical presentation of IPF**

IPF is associated with the older population since most patients are between 60-70 years old at the time of diagnosis [Patterson et al., 2017]. There is no correlation between the ethnic group or social environment and IPF manifestation, however, IPF often affects men more than women, as indicated by its prevalence (20.2 men per 100.000 persons compared to 13.2 women per 100.000 persons) and the majority of patients have a smoking history [Annesi-Maesano et al., 2013]. The initial clinical symptoms of IPF are not well described to date; however, dry cough lasting at least for 8 weeks has been reported in IPF patients [Hope-Gill et al., 2003; Chung and Pavord, 2008; Ryerson et al., 2011]. Dry cough is particularly presented in patients who have never smoked or patients with an advanced stage of the disease [Nakamura and Suda, 2015]. Moreover, dyspnea (shortness of breath) is another prominent symptom in IPF patients especially those in advanced stages of the disease [Swigris et al., 2005; King et al., 2001b]. Various studies have shown an evident correlation between the severity level of dyspnea and life quality/ survival rate in IPF patients [King et al., 2001b; Nishiyama et al., 2005]. Furthermore, clubbing fingers have been reported in 30-50 % of IPF patients, however their exact cause remains unknown [Nakamura and Suda, 2015]. IPF patients may also present clinical signs of weight loss, fatigue, or low-grade fever [Swigris et al., 2005; Atkins et al., 2016].

#### **1.1.2 Diagnosis of IPF**

The natural origin of IPF has been described as a rapid decline in forced vital capacity (FVC, the maximal volume of gas exhaled from the full inhalation by exhaling as forcefully as possible) associated with poor

prognosis of IPF patients [Gross and Hunninghake, 2001; Tukiainen et al., 1983; Carrington et al., 1978]. For each patient, the origin of the disease is individual and unforeseeable at the time of diagnosis. Some patients display slow manifestation and progression, whereas others experience acute exacerbation relatively early from the time of diagnosis (Figure 1.1) [Mejía et al., 2009; Wells et al., 2003; Lettieri et al., 2006; King et al., 2011].

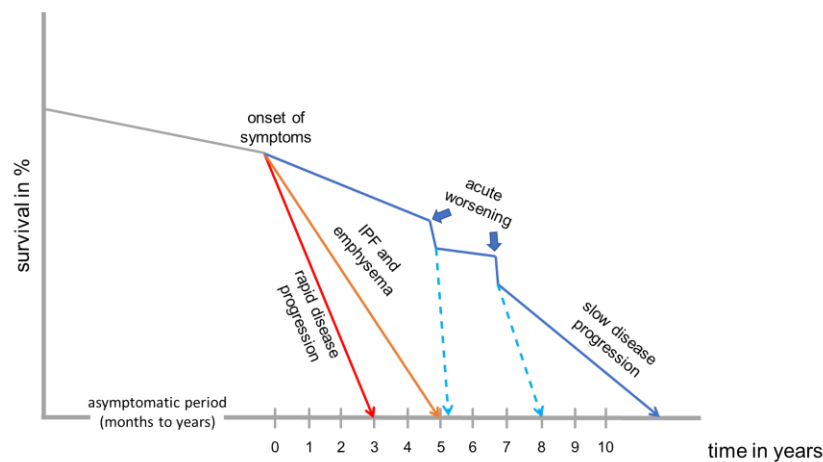


**Figure 1.1: Schematic illustration of potential clinical development and progression of IPF.** The manifestation as well as progression of IPF is very individual for each patient. Majority of patients experience slow disease progression with stable worsening. Some patients experience acute worsening during this period, which mainly occurs because of secondary complications or due to unknown reasons. On the other hand, patients experience rapid disease progression relatively early from the time of diagnosis. Illustration was adapted and modified from King et al., 2011 [King et al., 2011].

In general, IPF is hard to diagnose as it resembles symptoms similar to other pulmonary diseases. In order to avoid misdiagnosis, detailed medical history identifying possible environmental exposures, other extrapulmonary symptoms, and inherited disease predispositions must be considered [Martinez et al., 2017; Iwai et al., 1994; Hubbard et al., 1996; Miyake et al., 2005; Armanios et al., 2007; Tsakiri et al., 2007]. There are also several comorbid diseases, such as pulmonary hypertension, lung cancer and chronic obstructive pulmonary disease (COPD) associated with IPF, which also makes IPF diagnosis more difficult [Collard et al., 2012; Fernández Pérez et al., 2010; Mejía et al., 2009; Nadrous et al., 2005]. The diagnosis of IPF is most often determined by abnormal lung function confirmed via spirometry, or whole-body plethysmography (uncovering an evidence of restricted and/or impaired gas exchange) followed by high-resolution computed tomography (HRCT) of the chest [Raghu et al., 2011; Behr et al., 2013]. If HRCT scans show a distinct pattern of usual interstitial pneumonia (UIP), IPF can be diagnosed. However, if UIP patterns remain inconclusive, surgical lung biopsy or bronchoscopy is recommended [Behr, 2013; Raghu et al., 2011]. A huge interest lies in identifying diagnostic biomarkers in body fluids. Although there are no

validated biomarkers for predicting the prognosis and disease status of IPF yet, some potential candidates have been identified, such as MMP-7 and MUC5B [Bauer et al., 2017; Helling et al., 2017a; Hambly et al., 2015; Guiot et al., 2017]. Furthermore, the role of circulating autoimmune antigens in IPF as indicators of IPF have been previously described [Dreisin et al., 1978]. In line with this, the protein MZB1 was recently identified in a proteome profiling of a large cohort of ILD and scleroderma tissue samples as an upregulated protein localizing to plasma B cells [Schiller et al., 2017]. Importantly, there is an increased interest in combining a comprehensive analysis of clinical and omics-generated data using bioinformatic approaches which will help to uncover novel biomarkers in ILDs [Greiffo et al., 2017].

### 1.1.3 Treatment strategies of IPF

Treatment of IPF can be divided into *non-pharmacological and pharmacological* strategies. Regarding *non-pharmacological strategies*, the 2011 ATS/ERS/JRS/ALAT committee guidelines approved long-term oxygen therapy, and lung transplantation [Raghu et al., 2011]. Lung transplantation is, to date, the only option to prolong and improve patients' life quality. However there are only few patients who qualify for lung transplantation and the number of donor lungs is very low compared to the increased number of IPF patients [Glanville and Estenne, 2003].

Over the last decade, *pharmacological strategies* focused on targeting various molecules and pathways playing a role in IPF. Specifically, targeting signaling pathways activated by receptor tyrosine kinases has been of high interest for several years as their aberrant activity plays a central role in the manifestation and progression of fibrosis [Vittal et al., 2005; Garneau-Tsodikova and Thannickal, 2008; Beyer and Distler, 2013]. The first clinical trial assessing the efficiency of tyrosine kinase inhibitors for treatment of lung fibrosis was completed in 2010; *Imatinib mesylate (Gleevec)*, a tyrosine kinase inhibitor targeting platelet-derived growth factor receptors (PDGFRs), discoidin domain receptors (DDRs), c-kit, and c-Abl [Daniels et al., 2010], however results showed no improvement of lung function and survival of IPF patients enrolled in this study [Daniels et al., 2010].

*Pirfenidone* and *Nintedanib* have recently been approved by the European Medicines Agency (EMA, 2011/2014) and the US Food and Drug Administration (FDA, 2015/2014) for the treatment of IPF patients, both showing a decrease in disease progression (Azuma et al. 2005; Elmufdi et al. 2015; Noble et al. 2011; Tzouvelekis, Bonella, and Spagnolo 2015). A one-year treatment of IPF patients with *Pirfenidone* slows decline in the force vital capacity (FVC) [Noble et al., 2016], but brings several adverse effects, such as gastrointestinal reflux or photosensitivity rash were reported [Valeyre et al., 2014]. The exact molecular mechanism of action is not well known, however it has been demonstrated that *Pirfenidone* downregulates TGF $\beta$ -mediated fibroblast proliferation, migration and synthesis of lung collagens [Noble et al., 2011; Hisatomi et al., 2012]. *Nintedanib (BIBF1120)* is a triple receptor tyrosine kinase inhibitor targeting platelet-

derived growth factor (PDGF), vascular endothelial growth factor (VEGF), and basic fibroblast growth factor (FGF) receptor described to be safe in use, and with diarrhea as the most common adverse effect known [Richeldi et al., 2014a]. Results from multinational double-blinded, phase III clinical trials (INPULSIS-1 and INPULSIS-2) reported decrease in the FVC; however, data were significant only in the INPULSIS-1 trial [Antoniou, 2012; Richeldi et al., 2014a; Rafii et al., 2013; Richeldi et al., 2014b]. Although positive results from above-mentioned clinical trials gives hope to IPF patients, the inhibition of tyrosine kinase receptors remains highly unspecific and affects several (un)known targets [Noskovičová et al., 2015]. There are still open questions regarding the use of *Pirfenidone* or *Nintedanib* in the clinics, such as unpredictable adverse effects and long-term perspective of the treatment. A deeper understanding of IPF pathogenesis will arise new opportunities to develop novel, and more effective and safe drugs for the treatment of IPF patients.

#### **1.1.4 Histopathologic features of IPF**

According to the American Thoracic Society (ATS) consensus statement, IPF is associated with histopathological features of usual interstitial pneumonia (UIP) [Raghu et al., 2011]. The main histopathological features of UIP in surgical lung biopsies are described by heterogenous features due to irregularly distributed fibrotic scarring, honeycomb changes in a basal and subpleural area of the lung, and interstitial inflammation [American Thoracic Society and European Respiratory Society, 2002]. Tissue fibrosis prevails over inflammation and is accompanied with compact collagen deposition, often combined with smooth muscle cell hyperplasia [Raghu et al., 2011].

The Fleischner society glossary described honeycombing as "*destroyed and fibrotic lung tissue which contains numerous cystic airspaces with thick fibrous walls, representing the late stage of various lung diseases, with complete loss of acinar architecture*" [Hansell et al., 2008]. Furthermore, accumulation of hyperproliferative fibroblasts and myofibroblasts characterized by expression of  $\alpha$ -smooth muscle actin ( $\alpha$ SMA) in regions called interstitial fibroblastic foci represent a key histological feature of UIP (Figure 1.2) [Katzenstein and Myers, 1998]. Fibroblast foci are considered as small, distinct lesions localized between alveolar and interstitial regions of the lung and their formation is linked with the sites of ongoing lung injury [King et al., 2001a; Nicholson et al., 2002; Flaherty et al., 2003]. Importantly, increased numbers of fibroblast foci have been associated with disease activity and a rapid disease progression [Enomoto et al., 2006; Nicholson et al., 2002].

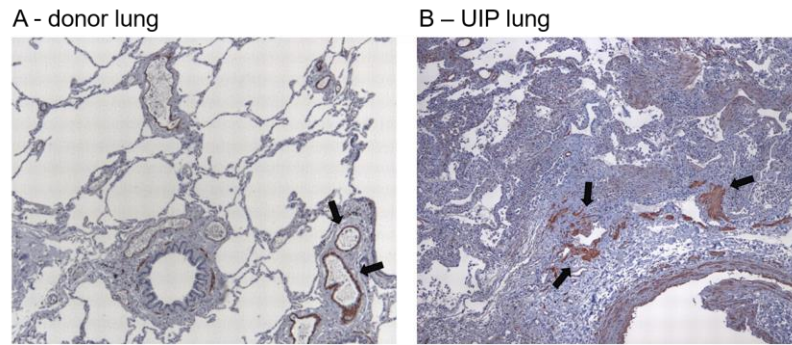


**Figure 1.2: Histopathological features of UIP.** Tissue stainings of  $\alpha$ -smooth muscle actin ( $\alpha$ SMA) in (A) a healthy donor lung and (B) UIP lung (brown, black arrowheads). Notice prominent  $\alpha$ SMA stainings in myofibroblasts accumulated in fibroblastic foci of UIP lung (panel B, black arrowheads). Modified from Eickelberg and Laurent, 2010 [Eickelberg and Laurent, 2010].

### 1.1.5 Pathogenesis of IPF

According to the latest concept of IPF manifestation and progression, IPF is a disease resulting from impaired, non-resolving wound healing together with progressive accumulation of extracellular matrix (ECM) components, decreased fibroblasts-myofibroblasts apoptosis, persistent epithelial cell apoptosis and abnormal reepithelization [Daccord and Maher, 2016]. Inflammation is still considered as a main driver of IPF development as there is increasing evidence that inflammatory cells strongly contribute to the tissue injuries and repair [Coward et al., 2010].

The onset of IPF is thought to be the result of initial alveolar type I cells (ATI) injury leading to alveolar epithelial cells (AEC) apoptosis followed by disruption of the AEC layer [Sakai and Tager, 2013]. Recent findings suggest that persistent microinjuries to the lung epithelium may be triggered by a combination of environmental factors such as tobacco smoke, gastroesophageal reflux, and viruses together with genetic predisposition or age-related factors [Zoz et al., 2011; Selman and Pardo, 2006; Macneal and Schwartz, 2012]. Regarding genetic predispositions, in the study of familial form of IPF, Noguee *et al.* identified a mutation in the gene encoding SPC (*SFTPC*) which led to fibrosis most likely due to the deficient expression and secretion of SPC protein, ER stress and cell apoptosis [Thomas et al., 2002; Mulugeta et al., 2007; Noguee et al., 2001]. Another study showed that mutations in age-related genes, such as telomerase reverse transcriptase (*TERT*) and telomerase RNA component (*TERC*) gene, may play a critical role in the development of IPF as observed in patients with familial and sporadic forms of IPF [Alder et al., 2008; Tsakiri et al., 2007; Cronkhite et al., 2008]. In general, telomeres shorten when cells divide, which finally leads to cell death or arrest of the cell cycle, thus resulting in the restricted capacity of tissue regeneration [Armanios, 2009]. This indicates a critical role of telomere shortening in age-related diseases. Additionally, it has been suggested that telomere shortening promotes the apoptosis of alveolar type II (ATII) cells, and thus promotes IPF manifestation [Alder et al., 2008; Waisberg et al., 2010]. MUC5B is a secreted mucin

with high expression levels in the normal respiratory tract, which is responsible for the clearance of upper airways from the potential bacterial infection preventing thus potential pathogen infiltration to the respiratory system [Roy et al., 2014]. An important study of Seibold and colleagues identified a single nucleotide polymorphism (SNP) located in the promoter region of the *MUC5B* gene (rs35705950) in patients with familial as well as sporadic IPF [Seibold et al., 2011]. Moreover, a recent study of Helling *et al.* identified a critical enhancer element in the promoter region of *MUC5B* gene which contains the rs35705950 variant of *MUC5B* gene [Helling et al., 2017b]. In addition, authors found that the enhancer element carries a highly conserved binding motif for transcription factor FOXA2, which may, together with RNA polymerase II, have an important role in regulating *MUC5B* transcription [Helling et al., 2017b]. The consequence of alteration in *MUC5B* gene increases the risk of developing IPF via chronic hypersecretion and accumulation of mucus in the peripheral airspace resulting in impaired mucus transport and its adhesion to bronchoalveolar space which promotes chronic inflammation and tissue injury [Seibold et al., 2011; Boucher, 2011]. Additionally, epigenetic modifications of genes associated with IPF, such as chemokine *IP-10*, *Thy-1 (CD90)*, and *ACTA* ( $\alpha$ SMA gene) were shown to play a role in the development of IPF [Coward et al., 2010; Sanders et al., 2008; Hu et al., 2010]. Sanders *et al.* showed in a comparative analysis of genome-wide DNA methylation combined with gene expression patterns from healthy and IPF lungs that expression of some IPF-related genes is inversely associated to DNA methylation of these genes [Sanders et al., 2012].

Due to the initial epithelial injury, it is next proposed that activated AECs start secreting increased amounts of profibrotic cytokines, chemokines, and proteases which subsequently leads to the recruitment and activation of inflammatory cells and fibroblasts to the site of injury [Todd et al., 2012]. In addition, the injury of AECs results in the activation of a coagulation cascade where fibrinogen is converted to fibrin to form a provisional matrix [Chambers and Scotton, 2012]. Here, chemokines and serum-derived mediators recruit fibroblasts, circulating cells and trigger epithelial-to-mesenchymal transition (EMT) of AECs. Subsequently, fibroblasts become activated by profibrotic cytokines, such as TGF $\beta$  and PDGF, which leads to their differentiation into highly contractile myofibroblasts, and which are thought to be the primary effector cells in IPF [Hinz et al., 2007a; Hinz, 2016]. Activated myofibroblasts produce and secrete excessive amounts of extracellular matrix (ECM) components and thus highly contribute to the progressive tissue remodeling and ultimately organ failure [Coward et al., 2010; White, 2015].

## **1.2 Lung fibroblasts**

Fibroblasts are a cell population of mesenchymal origin representing the most abundant cell type of connective tissue [Kendall and Feghali-Bostwick, 2014]. Generally, fibroblasts can be phenotypically recognized by their typical spindle-shaped morphology [Ravikanth et al., 2011]. In the lung, fibroblasts are

found in proximal airways and also in distal lung parenchyma, but cells differ in their morphology and proliferation capacity dependent on the area of isolation, as described in lung biopsies from asthma patients [Kotaru et al., 2006].

### **1.2.1 Fibroblasts in wound healing**

Due to their high proliferative and migratory capacities [Suganuma et al., 1995; Moodley et al., 2003], fibroblasts play an essential role in wound healing processes [Li and Wang, 2011; Bainbridge P, 2013]. In the early stages of tissue injury, fibroblasts migrate towards the wound and subsequently differentiate into highly contractile myofibroblasts with increased production and secretion capacities of ECM proteins, such as elastin, collagens, and fibronectin [Thannickal et al., 2004; Martin, 1997]. Thus, they can build and maintain temporary scaffold necessary for normal tissue repair and wound closure. Once the wound is closed, provisional tissue scaffold dissolves and myofibroblasts disappear through apoptosis [Li and Wang, 2011; Hinz et al., 2007a]. Although the exact mechanism of myofibroblasts apoptosis is not completely uncovered, this process is necessary for maintaining normal and healthy tissue architecture after injury [Desmoulière et al., 1995].

The main phenotypical differences between fibroblasts and myofibroblasts include large microfilaments, enlarged focal adhesions, abundant intracellular adherent molecules and gap junctions, increased ECM production and secretion and increased expression of alpha smooth muscle actin ( $\alpha$ SMA), highly contributing to its contractile properties (Figure 1.3) [Kendall and Feghali-Bostwick, 2014; Hinz, 2007; Hinz et al., 2007a; Tomasek et al., 2002; Hinz et al., 2003; Dugina et al., 2001; Hinz et al., 2007b, 2001a; Serini et al., 1998]. Generally, the abundance of myofibroblasts in normal healthy lung is expected to be low, however their appearance become more prominent once wound healing processes are dysregulated as it is the case in IPF [Hinz, 2012].

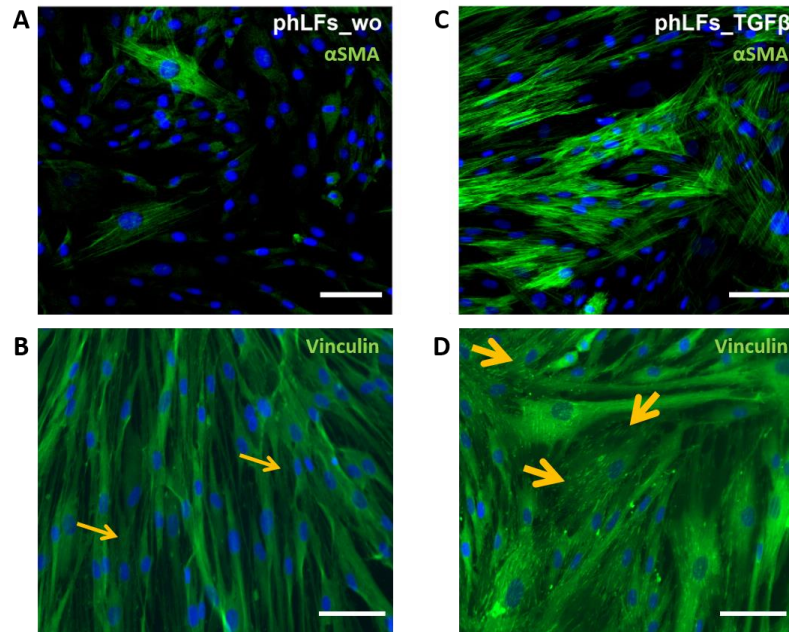


**Figure 1.3: Phenotypical differences between fibroblasts and myofibroblasts.** Under normal conditions, resident fibroblasts (left images) maintain a classical spindle-shape morphology with hardly detectable expression of  $\alpha$ SMA (A) and small, immature focal adhesions at cell edges (B, regular arrowheads). On the other hand, activated myofibroblasts (right images) display a highly contractile phenotype as shown by prominent  $\alpha$ SMA expression (C) and super mature focal adhesions (D, bold arrowheads) (unpublished data).

### 1.2.2 Activated fibroblasts in IPF

Fibroblasts and myofibroblasts in IPF exhibit a pathologic phenotype of uncontrolled proliferation, migration, and survival. Moreover, increased resistance to programmed cell death has been observed in primary human lung fibroblasts isolated from IPF tissues [White et al., 2003; Nho et al., 2013; Maher et al., 2010]. In IPF, fibroblasts accumulate in fibroblastic foci (chapter 1.1.4), where they initially acquire contractile features by displaying stress fibers composed of cytoplasmic actin with very low traction forces [Hinz et al., 2001b]. Subsequently, changes in the ECM compositions as well as extracellular stimuli such as growth factors act on fibroblasts leading to their phenotypic changes into  $\alpha$ SMA-expressing myofibroblasts. Incorporation of  $\alpha$ SMA into stress fibers enlarges the contractile properties of fibroblasts, which is one of the hallmarks of initiated tissue remodeling [Hinz et al., 2001b]. Additionally, activated myofibroblasts are characterized by excessive production, secretion, and deposition of ECM components, such as collagens and fibronectin and thereby essentially contribute to fibrotic tissue remodeling [Klingberg et al., 2013].

Several studies, mostly by animal studies, have focused on identifying the origin and progenitors of myofibroblast. Resident fibroblasts, circulating bone-marrow derived fibrocytes, smooth muscle cells,

pericytes, epithelial and endothelial cells undergoing endothelial- or epithelial-mesenchymal transition, and mesenchymal stromal cells are discussed as potential sources (Figure 1.4) [Porter and Turner, 2009; Dranoff and Wells, 2010; De Wever et al., 2008; Hinz, 2007; Coen et al., 2011; Herzog and Bucala, 2010; Keeley et al., 2011; Humphreys et al., 2010; Lin et al., 2008; Lee and Nelson, 2012; Chapman, 2011; Mishra et al., 2009].

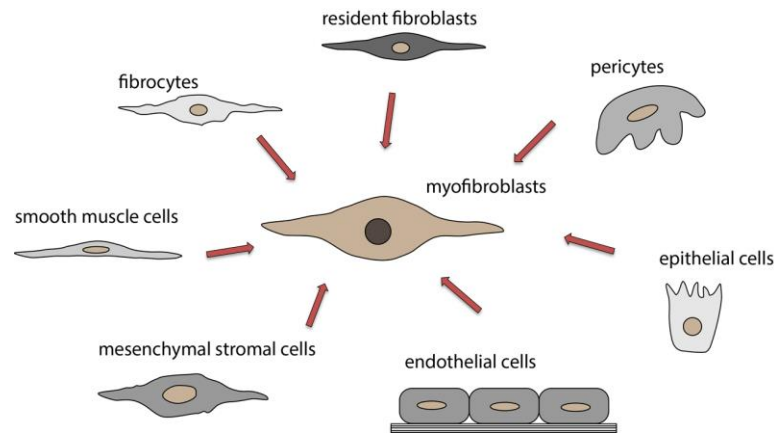


**Figure 1.4: Myofibroblast precursor cells.** In IPF, myofibroblasts can differentiate from various precursor cells including resident fibroblasts, pericytes, epithelial cells, endothelial cells, mesenchymal stromal cells, smooth muscle cells, and fibrocytes. Figure was adapted and modified from Fernandez and Eickelberg, 2012 [Fernandez and Eickelberg, 2012b].

### 1.2.3 Molecular mechanisms regulating fibroblasts activation

A large spectrum of profibrotic and antifibrotic factors act on fibroblasts by paracrine and autocrine mechanisms, driving fibroblast activation in fibrosis (Figure 1.5) (B Hinz et al., 2001b; Kendall & Feghali-Bostwick, 2014; Tomasek et al., 2002; White, 2015; Wolters, Collard, & Jones, 2014). Transforming growth factor-beta (TGF $\beta$ ) and platelet-derived growth factor (PDGF) are the most intensively studied profibrotic pathways regulating fibroblast to myofibroblast transdifferentiation in IPF [Scotton and Chambers, 2007; Khalil et al., 1993a; Allen and Spiteri, 2002]. Also, members of Wnt/ $\beta$ -catenin pathway were recently reported to prompt profibrotic responses from epithelial cells toward fibroblasts in IPF [Königshoff et al., 2009]. On the other hand, prostaglandin E2 (PGE2) and prostacyclin (PGI2) pathways were shown to mediate anti-fibrotic signals from epithelial cells towards fibroblasts by inhibiting proliferation, collagen production, and myofibroblasts differentiation in lung fibroblasts [Goldstein and Polgar, 1982; Kolodsick et al., 2003; McAnulty et al., 1997].

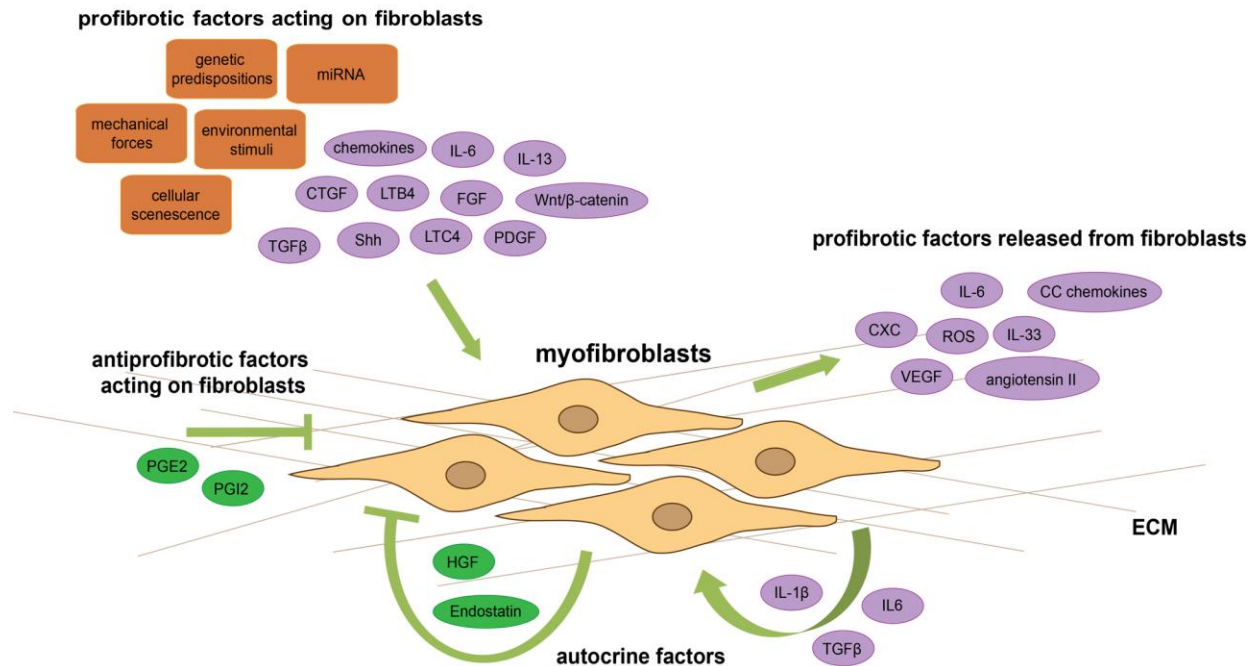


**Figure 1.5: A schematic overview of profibrotic stimuli promoting myofibroblasts transdifferentiation in IPF.** Various profibrotic factors act on fibroblasts leading to their transdifferentiation into myofibroblasts. Activated myofibroblasts also release several profibrotic cytokines by which they contribute to inflammation and ongoing fibrosis. Autocrine factors produced by fibroblasts act on fibroblasts and thus promote their profibrotic phenotype. Figure was adapted and modified from Kendall and Feghali-Bostwick, 2014 [Kendall and Feghali-Bostwick, 2014].

#### 1.2.4 Transforming growth factor-beta (TGF $\beta$ ) signaling

TGF $\beta$  is one of the most extensively studied profibrotic growth factors which plays a crucial role in the development and progression of IPF [Fernandez and Eickelberg, 2012a; Kendall and Feghali-Bostwick, 2014; Klingberg et al., 2013]. TGF $\beta$  signaling promotes chemotaxis and proliferation of fibroblasts, EMT and protects myofibroblasts from apoptosis in IPF [Maher and Adamali, 2012]. In the lung, alveolar macrophages, neutrophils, activated alveolar epithelial cells, endothelial cells, fibroblasts, and myofibroblasts are the main sources of TGF $\beta$  secretion [Merrilees and Sodek; Kumar et al., 1996; Grotendorst et al., 1989; Khalil et al., 1993b; Kelley et al., 1991]. To date, there have been three different TGF $\beta$  isoforms described - TGF $\beta$ 1, TGF $\beta$ 2, and TGF $\beta$ 3, of which only TGF $\beta$ 1 is found to be upregulated in IPF [Khalil et al., 1996; Yong et al., 2001]. TGF $\beta$  ligands are synthesized as latent precursors forming a complex with their latency-associated peptide (LAP), and a latent TGF $\beta$ -binding protein (LTBP), together creating a large latent complex (LLC). The activation of latent TGF $\beta$  requires the liberation of LLC complex from the ECM followed by further proteolytical cleavage of LAP [Hinz, 2015]. Several extracellular factors, such as integrins, matrix metalloproteinase 2 and 9 (MMP2 and MMP9) and thrombospondin 1 (THBS1)

have been described to activate latent TGF $\beta$  [Annes et al., 2003; Henderson et al., 2013; Schultz-Cherry et al., 1994].

Once activated, TGF $\beta$  signals via binding to two heterodimeric receptors, namely TGF $\beta$  type I (TGF $\beta$ RI) and type II (TGF $\beta$ RII) belonging to the family of serine/threonine kinase receptors [Itoh et al., 2000; Derynck and Feng, 1997; Moustakas et al., 2001]. First, TGF $\beta$  binds to the extracellular domain of TGF $\beta$ RII which in turn recruits TGF $\beta$ RI resulting in dimerization of both receptors forming a heterodimeric receptor complex, leading to phosphorylation and subsequent activation of the TGF $\beta$ RI-mediated intracellular signaling cascade [Feng and Derynck, 1996]. Downstream TGF $\beta$  signaling is mediated via two signaling pathways: *Smad-dependent (canonical) pathway* and *Smad-independent (non-canonical) pathway* [Derynck and Zhang, 2003].

#### **1.2.4.1 Smad-dependent signaling**

In the *Smad-dependent signaling pathway* (Figure 1.6), activation of TGF $\beta$ RI leads to the phosphorylation of cytoplasmic signaling molecules Smad2 and Smad3 known also as receptor-specific (R-Smad) proteins [Itoh et al., 2000]. R-Smads couple with coregulator Smad4 which leads to the translocation of Smad2/3-Smad4 complex into the cell nucleus where they act as transcription factors binding either directly or in a complex with other DNA-binding proteins to the promoter region of TGF $\beta$ -signaling target genes [Shi and Massagué, 2003]. Interestingly, Smad3 can directly bind to CAGAC DNA sequence as observed by several groups, whereas Smad2 requires DNA-binding protein from the Fast family to bind DNA [Shi et al., 1998; Zawel et al., 1998; Attisano et al., 2001]. In addition, inhibitory Smads (I-Smads), such as Smad6 and Smad7 regulate balanced phosphorylation and nuclear translocation of R-Smad/Smad4 complex into the nucleus [Kawabata et al., 1997; Nakao et al., 1997]. It has been shown that under normal conditions, Smad signaling regulates expression of ECM-related genes, such as *Col1A1*, *Col3A1*, and *Col5A1* [Verrecchia et al., 2001]. In IPF, aberrantly activated Smad signaling results in increased expression levels of collagens and also other ECM proteins, such as fibronectin, elastin, and integrins by fibroblasts [Pechkovsky et al., 2012; Kuang et al., 2007; Ignatz and Massagué, 1986; Honda et al., 2010]. Additionally, transcription of ACTA2 (encoding for  $\alpha$ SMA) is regulated by canonical Smad2/3 signaling via binding of Smad3 to the Smad-binding element 1 at the  $\alpha$ SMA promoter [Hu et al., 2003; Uemura et al., 2005].

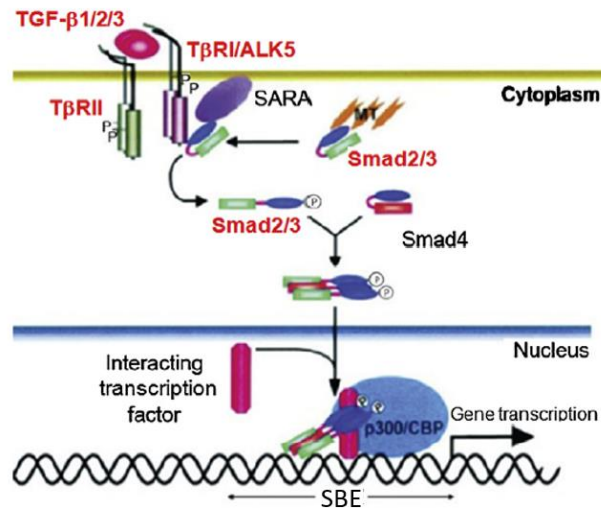


**Figure 1.6: A schematic illustration of Smad-dependent signaling pathway.** Smad-dependent signal transduction is initiated by binding of TGF $\beta$  ligand to TGF $\beta$ RII receptor, which results in the phosphorylation, and thus activation of TGF $\beta$ RI receptor. Activated TGF $\beta$ RI receptor then phosphorylates downstream signaling molecules Smad2 and Smad3 (R-Smads), which form complexes with the coregulator Smad4. Finally, Smad2/3-Smad4 complexes are translocated into the nucleus, where they act as transcription factors of TGF $\beta$ -related genes. The scheme is adapted from Jiang et al. [Jiang et al., 2015].

#### 1.2.4.2 Smad-independent signaling

Although TGF $\beta$  mostly signals via Smad pathway, activation of TGF $\beta$ RI also promotes signal transduction via *Smad-independent pathways* (Figure 1.7). These different downstream pathways include Erk-mediated non-Smad pathway, JNK/p38 pathway, PI3K/Akt pathway, and the small Rho-like GTPase pathway [Shi-Wen et al., 2009; Mucsi et al., 1996; Frey and Mulder, 1997; Engel et al., 1999; Hocevar et al., 1999; Derynck and Zhang, 2003; Sandbo et al., 2011]. Activation of these pathways leads to changes in the cell shape and regulation of gene programs that mediate fibroblasts differentiation and survival [Sandbo and Dulin, 2011; Horowitz et al., 2004]. Of interest, TGF $\beta$  receptors belong to the family of serine/threonine kinases; however, they can also undergo phosphorylation on their tyrosine residues [Lawler et al., 1997]. Thus, upon TGF $\beta$  ligand binding, both TGF $\beta$  receptors as well as signaling adaptor protein Shc become phosphorylated which in turn recruits adaptor proteins Grb2 and Sos to bind, resulting in activation of downstream MAPK kinase cascade via Raf, Mek, and Erk. Activated MAPK-Erk pathway further regulates disassembly of cell adherent junctions resulting in the increased migration and invasion of cancer cells during processes of TGF $\beta$ -induced EMT [Ravichandran, 2001; Davies et al., 2005]. Additionally, it has been reported that Erk substrates, such as AP-1 transcription factor can interact and function in the combination with Smads as regulators of transcription of various genes, such as Timp-1 and MMP-1 [Hall et al., 2003]. JNK/p38 pathway is one of the best characterized non-Smad signaling pathway. It is initiated

by binding of adaptor protein TRAF6 to intracellular domains of activated TGF $\beta$  receptors, subsequently resulting in K63-linked polyubiquitination of TRAF6. Unlike K48-linked polyubiquitination by which proteins are subjected for a proteasomal degradation [Grice and Nathan, 2016], K63-linked polyubiquitination mediates activation of protein substrates [Haglund and Dikic, 2005]. Thus, activated TRAF6 recruits, and further phosphorylates TAK1 by which downstream JNK/p38 pathway becomes activated [Wang et al., 2001]. Of note, TRAF6-TAK1-JNK/p38 pathway also regulates TGF $\beta$ -mediated cellular responses such as apoptosis and EMT via interaction between JNK/p38 and Smads in the cell nucleus [Yamashita et al., 2008].

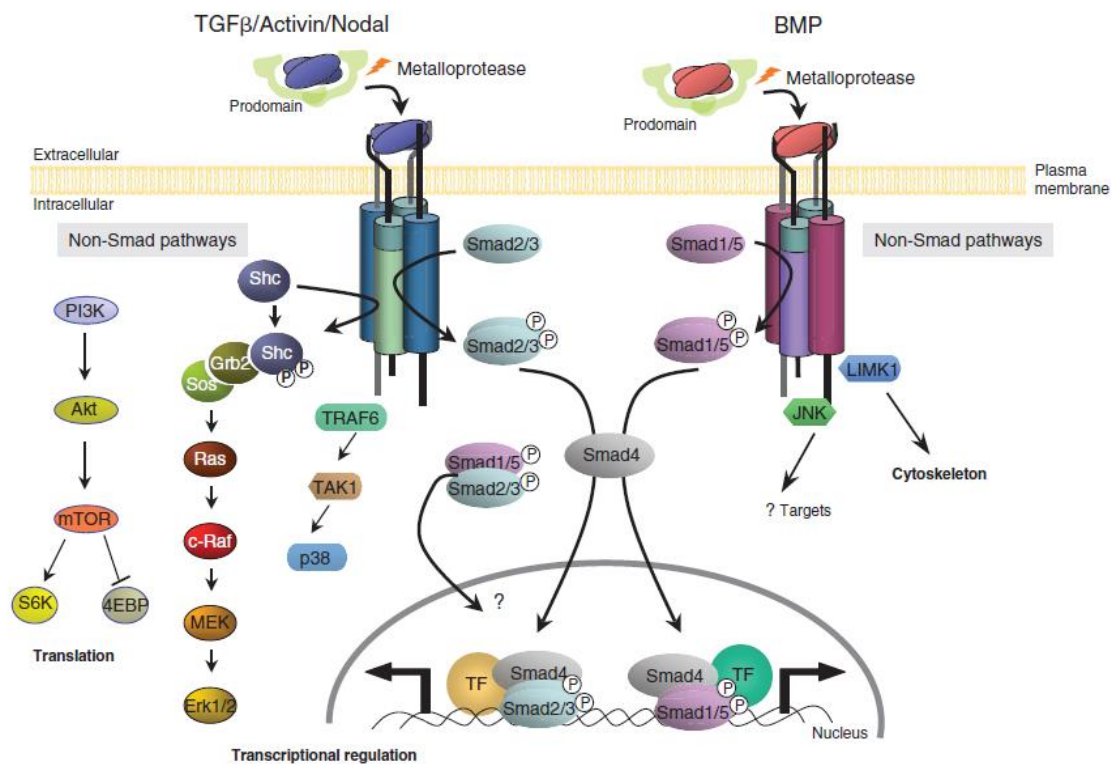


**Figure 1.7: A schematic illustration of Smad-independent signaling pathway.** It is well established that TGF $\beta$  also activates multiple Smad-independent pathways through either phosphorylation or direct interaction of TGF $\beta$  receptors with non-Smad signal transducers. This includes signaling molecules of various branches of MAP kinase (MAPK) pathway, Rho-like GTPase signaling pathway, and phosphatidylinositol-3-kinase (PI3K)/ AKT pathway. The scheme is adapted from Wharton and Derynck [Wharton and Derynck, 2009].

### 1.3 Fibroblasts surface proteins

Fibroblasts, as any other cell type, gets in contact within the organ microenvironment via its surface molecules. This includes physical interaction with the ECM or cell-cell communication by cytokine-

receptor interaction, further mediating and affecting its cellular function [Rozario and DeSimone, 2010]. The few studies existing characterized surface proteome of fibroblasts [Slany et al., 2014; Predic et al., 2002]. However, identification of specific fibroblast surface markers remains challenging as fibroblasts, myofibroblasts, and other contractile cell types such as smooth muscle cells (SMCs) showed similar expression patterns of surface proteins [Hinz, 2007].

In IPF, binding of several growth factors to fibroblast receptors and their functional consequences have mainly been described, as e.g. for TGF $\beta$  signaling and the phenotypic switch towards the highly proliferating and migratory myofibroblast [Fernandez and Eickelberg; Sakai and Tager, 2013]. Little information, however, exists how cytokines alter expression and localization of surface proteins, and thereby changing the binding and further interaction capacities of the cell.

In a recently published comprehensive study investigating changes of the fibroblasts surface proteome after TGF $\beta$  stimulation, we identified platelet-derived growth factor receptor-alpha (PDGFR $\alpha$ ) and Cub domain-containing protein 1 (CDCP1) as one of the top candidates regulated by TGF $\beta$  [Heinzelmann et al., 2016]. These two proteins have been the focus of my thesis and will be introduced in more detail in the following.

### **1.3.1 Platelet-derived growth factor receptor-alpha (PDGFR $\alpha$ )**

Platelet-derived growth factors (PDGFs) and their receptors (PDGFRs) represent a family of profibrotic growth factors intensively studied in the lung field since aberrant PDGF signaling has been implicated in IPF pathogenesis [Vaillant et al., 1996; Bonner, 2004b; Kelly et al., 2003]. In general, PDGF signaling plays an important role in processes of normal wound healing by regulating migration and ECM deposition of fibroblasts [Alvarez et al., 2006]. However, during fibrogenesis, injured epithelial cells and recruited macrophages secrete excessive amounts of PDGF ligands which contribute to the impaired biological responses of activated myofibroblasts, such as resistance to apoptosis, and excessive proliferation, and migration to the site of the injury [Bonner, 2004b].

To date, five heterodimeric PDGF ligand isoforms have been described; namely PDGF-AA, PDGF-AB, PDGF-BB, PDGF-CC and PDGF-DD [Li et al., 2000; Boström et al., 2002; Kimani et al., 2009]. Those ligands showed distinct binding affinities towards three PDGF receptor dimers – PDGFR $\alpha\alpha$ , PDGFR $\alpha\beta$ , and PDGFR $\beta\beta$  (Figure 1.8). According to *in vitro* studies PDGF-AA, PDGF-AB, PDGF-BB, and PDGF-CC bind PDGFR $\alpha$ , whereas PDGF-BB and PDGF-DD to PDGFR $\beta$  [Noskovičová et al., 2015]. On the other hand, PDGF-AB, PDGF-BB, PDGF-CC, and PDGF-DD display binding affinities toward heterodimeric PDGFR $\alpha\beta$  [Gilbertson et al., 2001; Cao et al., 2002; LaRochelle et al., 2001].

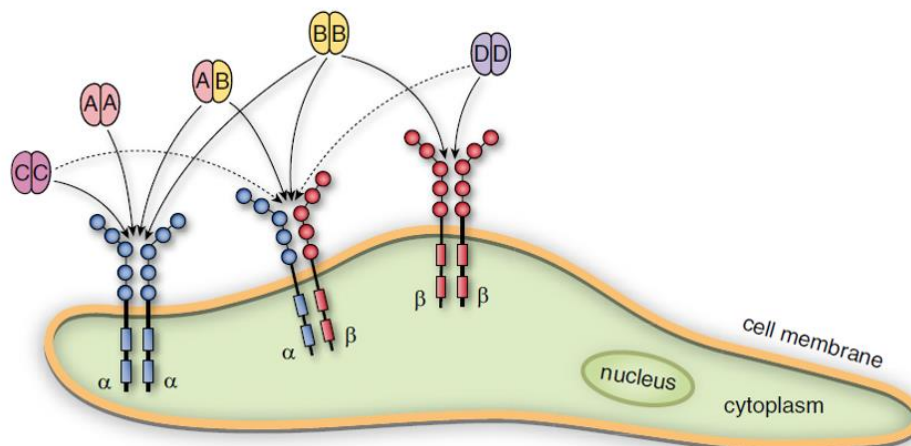


**Figure 1.8: A schematic overview of PDGF receptors and PDGF/PDGFR binding patterns.** PDGFRs are transmembrane tyrosine kinase receptors spanning the cell surface of most cell types. Three dimeric receptor forms exist, namely homodimeric PDGFR $\alpha\alpha$  and PDGFR $\beta\beta$ , and one heterodimeric PDGF $\alpha\beta$  receptor. Five different PDGF ligand isoforms possess specific binding affinities towards those receptors as indicated. The black solid arrows display *in vitro* documented binding interactions whereas dotted arrows show potential binding affinities. Adapted from [Noskovičová et al., 2015].

PDGFR $\alpha$  and PDGF $\beta$  belong to the family of receptor tyrosine kinases (RTKs) [Claesson-Welsh et al., 1989; Matsui et al., 1989]. Inactive PDGFRs are first presented as monomeric receptor units on the cell surface. Once PDGF ligands bind to its respective receptors, conformational changes within the receptors occur which leads to receptor dimerization and thus autophosphorylation of the tyrosine residues in their intracellular domain [Noskovičová et al., 2015]. This leads to further downstream signaling via two main pathways: the phosphatidylinositol 3'-kinase/Akt/mammalian target of rapamycin (PI3K/Akt/mTOR) pathway and the MAPK cascade signaling pathway.

In PI3K/Akt/mTOR pathway, activated PDGF receptor first recruits PI3K which is accompanied by phosphorylation of PIP2 into PIP3. This activates phosphoinositide-dependent kinase-1 which in turn activates Akt. Activated Akt stimulates signal transduction of various signaling molecules including mTOR controlling cellular growth, proliferation, and cell survival [Noskovičová et al., 2015]. On the other hand, MAPK dependent signaling pathway is initiated by phosphorylation of Shc protein and adaptor growth factor receptor-bound protein 2 (Grb2) which directly bind to autophosphorylated PDGF receptors via their SH2 domains. Subsequently, the SH3 domain of Grb2 couples with SOS, a nucleotide exchange factor of Ras leading to hydrolytic conversion of RAS-guanosine diphosphate (RAS-GDP) to RAS-guanosine triphosphate (GTP). Activated Ras then transduces the signal by Raf-1 and MAPK cascade members MEK and ERK. Thus this pathway takes part in specific cell responses such as cell growth, proliferation,

differentiation and migration [Noskovičová et al., 2015]. Moreover, several studies have reported crosstalk between PDGF-and other signaling pathways such as EGFR, leading to PDGF-B-stimulated cell migration of mouse embryonic cells [Mendelson et al., 2010].

Aberrant PDGF signaling plays a critical role in IPF pathogenesis, that is why research in the past has focused on targeting PDGF signaling in the lung by inhibiting PDGF ligands, receptors or PDGF receptor-kinase activity [Noskovičová et al., 2015].

### **1.3.2 Cub domain containing protein 1**

Cub domain containing protein 1 (CDCP1) is a cell surface glycoprotein which is also known as Subtractive Immunization Associated 135 kDa (SIMA135), gp40, or Transmembrane and associated with Src kinases (Trask) [Brown et al., 2004a; Hooper et al., 2003; Bhatt et al., 2005]. The expression of CDCP1 has been described in various cell types, including lung epithelial cells, hepatocytes, and hematopoietic progenitor cells and different organs such as breast, kidney, and colon [Hooper et al., 2003; Bühring et al., 2004; Siva et al., 2008; Emerling et al., 2013; Wright et al., 2016; Scherl-Mostageer et al., 2001].

Aberrant CDCP1 expression has been associated with development and progression of various cancers including lung, breast, and colon cancer [Bühring et al., 2004; Scherl-Mostageer et al., 2001], as e.g. elevated expression levels of CDCP1 significantly contribute lung adenocarcinoma, and therefore represent a potential therapeutic target for cancer treatment [Chiu et al., 2015; Wortmann et al., 2009]. It has been shown that phosphorylated CDCP1 interacts with specific molecules such as Src, Yes, Fyn, and PKC $\delta$ , and thus promotes resistance to apoptosis by increased invasion and metastatic properties of cancer cells [Uekita et al., 2007, 2008b; Bhatt et al., 2005]. Additionally, activated CDCP1 couples with  $\beta$ 1 integrin subunit, which in turn induces intracellular FAK/PI3K-mediated Akt signaling pathway, by which cancer cells gain their migratory properties [Casar et al., 2014]. Interestingly, some studies suggested that CDCP1 may also act as a marker of leukemia, since normal peripheral blood cells lack CDCP1 [Bühring et al., 2004]. Dysregulated expression of CDCP1 in various cancers might be the result of epigenetic modifications. In breast cancer samples Ikeda and colleagues demonstrated an opposite correlation between mRNA levels and methylation status of CpG motifs in the transcription initiation site of the *CDCP1* gene [Perry et al., 2007; Ikeda et al., 2009]. Consistently, inverse correlation between CDCP1 mRNA levels and CpG methylation was found in hematopoietic cell lines [Kimura et al., 2006]. To our knowledge, no information exists about CDCP1 expression in fibroblasts or its role in IPF.

## 2 OBJECTIVES

Little information exists about the lung fibroblast surface proteome in general as well as its changes under normal and growth factor stimulation since specific fibroblasts surface markers have not been identified to date. The working group of Prof. Eickelberg therefore performed an unbiased proteome analysis of primary human lung fibroblasts in the presence/absence of TGF $\beta$ . By this, they wanted to determine markers significantly enriched on the cell surface, and identify proteins potentially regulated by TGF $\beta$  signaling and thereby contributing to the profibrotic phenotype. The surface fraction of fibroblasts was analyzed by mass spectrometry in collaboration with Dr. Stefanie Hauck and Dr. Juliane Merl-Pham (Research Unit Protein Science, Helmholtz Zentrum München) [Heinzelmann et al., 2016]. They identified 750 proteins by a 2-peptide hit, among which 213 surface proteins were significantly regulated by TGF $\beta$ , thereof 70 proteins up- and 143 downregulated. These proteins were ranked by their fold change values and among the 15 top up and down regulated surface proteins by TGF $\beta$  markers randomly chosen for data validation. Down- and upregulation of ROR1, PDGFR $\alpha$  and SEMA7A by TGF $\beta$ , respectively, was confirmed via immunoblot and additionally FACS analysis for PDGFR $\alpha$ .

In the first part of my project we continued working on PDGFR $\alpha$ , whereas in parallel I performed an intensive literature research to identify novel candidates to be regulated by but not associated yet with TGF $\beta$  or fibrosis. This led to the detailed characterization of CDCP1 in the second part of this work in hand.

I first aimed to confirm the effect of TGF $\beta$  on the expression of PDGFR $\alpha$  and CDCP1 in detail by analyzing RNA and protein levels and visualizing the effect on proteins' surface localization. CDCP1 expression and function has only been little characterized in general and mainly in epithelial cells. PDGFR $\alpha$  and PDGF signaling on the other hand, have been associated with pulmonary fibrosis [Abdollahi et al., 2005]. But the precise mechanisms of PDGF signaling in the context of TGF $\beta$  in human lung fibroblasts had not been clarified when I started this project.

Thus, the second aim of this thesis was to examine PDGF signaling in dependency of PDGFR $\alpha$  expression in human lung fibroblasts, as well as the impact of TGF $\beta$  on it, and to describe for the very first time functional properties of transmembrane glycoprotein CDCP1 in lung fibroblasts under basal conditions and TGF $\beta$  stimulation. I thereby aimed to investigate whether a potential cross-talk between PDGFR $\alpha$  and TGF $\beta$  pathway exists and whether this contributes to fibroblast differentiation to a profibrotic phenotype. Furthermore, I aimed to investigate whether activated and non-activated cells express CDCP1, and how does TGF $\beta$  regulate CDCP1 expression in lung fibroblasts. Finally, I aimed to uncover whether the presence or absence of both, PDGFR $\alpha$  and CDCP1, modify functional role of activated fibroblasts as main producers of ECM components in lung fibrosis.

### 3 MATERIALS AND METHODS

#### 3.1 Materials

##### 3.1.1 Chemicals and reagents

**Table 3.1: Chemical and reagents**

<i>Product</i>	<i>Company</i>
0.25% Trypsin-EDTA solution	Sigma-Aldrich; Taufkirchen, Germany
2-Phospho-L-ascorbic acid trisodium salt	Sigma-Aldrich; Taufkirchen, Germany
87% Glycerol	AppliChem; Darmstadt, Germany
Ammonium peroxodisulfate (APS)	AppliChem; Darmstadt, Germany
Antibody diluent	Zytomed Systems; Berlin, Germany
Bovine serum albumin (BSA)	Sigma-Aldrich; Taufkirchen, Germany
Bright-Glo™ Luciferase Assay System	Promega, Mannheim, Germany
Complete® Mini without EDTA (Protease-inhibitor)	Roche Diagnostics; Mannheim, Germany
Collagen G from bovine calf skin	Merck Millipore; Berlin, Germany
DAPI (4', 6-diamino-2-phenylindole)	Sigma-Aldrich; Taufkirchen, Germany
Desoxyribonucleotides mix (dNTPs)	Fermentas, Thermo Fisher Scientific; Schwerte, Germany
Dimethyl sulfoxide (DMSO)	Carl Roth; Karlsruhe, Germany
Dithiothreitol (DTT)	AppliChem; Darmstadt, Germany
ECL Plus Western Blotting Substrate	Pierce, Thermo Fisher Scientific; ; Schwerte, Germany
Ethanol (p.a.)	AppliChem; Darmstadt, Germany
Fetal bovine serum (FBS) "GOLD ", heat inactivated	PAA, GE Healthcare; Freiburg, Germany
Fluorescence mounting medium	Dako; Hamburg, Germany
Glo Lysis Buffer, 1x	Promega, Mannheim, Germany
Human TruStain FcX™	BioLegend; San Diego, USA
Isopropanol (p.a.)	AppliChem; Darmstadt, Germany
Light Cycler 480 SybrGreen 1 Master Mix	Roche Diagnostics; Mannheim, Germany
Lipofectamine LTX with PLUS reagent	Invitrogen, Life Technologies; Carlsbad, USA
Lipofectamine RNAiMAX	Invitrogen, Life Technologies; Carlsbad, USA
Methanol (p.a.)	AppliChem; Darmstadt, Germany
Non-fat dried milk powder	AppliChem; Darmstadt, Germany
Nonidet P-40	AppliChem; Darmstadt, Germany
Paraformaldehyde (PFA)	AppliChem; Darmstadt, Germany
Penicillin-Streptomycin (100 U/ml)	Gibco, Life Technologies; Carlsbad, USA
Phalloidin	Invitrogen, Life Technologies; Carlsbad, USA

PhospSTOP (Phosphatase-inhibitor)	Roche Diagnostics; Mannheim, Germany
Protein marker V	Peqlab; Erlangen, Germany
Random hexamers	Applied Biosystems, Life Technologies; Carlsbad, USA
Recombinant human PDGF-AA protein	Invitrogen, Life Technologies; Carlsbad, USA
Recombinant human PDGF-AB protein	Invitrogen, Life Technologies; Carlsbad, USA
Recombinant human PDGF-CC protein	R&D Systems; Minneapolis, USA
Recombinant human PDGF-DD protein	R&D Systems; Minneapolis, USA
Recombinant human TGF $\beta$ 1 protein	R&D Systems; Minneapolis, USA
Restore Plus Western Blot Stripping Buffer	Pierce, Thermo Fisher Scientific; Schwerte, Germany
Sircol, Alkali Reagent	Biocolor; Northern Ireland, U.K.
Sircol, Acid Neutralizing Reagent	Biocolor; Northern Ireland, U.K.
Sircol, Acid-Salt Wash Reagent (Concentrate)	Biocolor; Northern Ireland, U.K.
Sircol, Collagen Isolation & Concentration Reagent	Biocolor; Northern Ireland, U.K.
Sircol, Dye Reagent	Biocolor; Northern Ireland, U.K.
Sircol, Bovine Collagen Reference Standard	Biocolor; Northern Ireland, U.K.
SuperSignal West Dura Chemiluminescent Duration Substrate	Pierce, Thermo Fisher Scientific; Schwerte, Germany
SuperSignal West Femto Chemiluminescent Duration Substrate	Pierce, Thermo Fisher Scientific; Schwerte, Germany
TEMED	AppliChem; Darmstadt, Germany
Tween 20	AppliChem; Darmstadt, Germany
Tryptan Blue Solution (0.4%)	Sigma-Aldrich; Taufkirchen, Germany
UltraPure DNase/RNase-Free Distilled Water	Invitrogen, Life Technologies; Carlsbad, USA
Vybrant® CFDA SE intracellular dye	ThermoFisher Scientific; Rockford, USA

### 3.1.2 Consumables

**Table 3.2: Consumables**

<i>Product</i>	<i>Company</i>
$\mu$ -Plate 24 Well	Ibidi; Planegg/Martinsried, Germany
96-well imaging plates, Falcon®	Corning, Thermo Fisher Scientific; Schwerte, Germany
white 96-well microplates	Berthold Technologies; Bad Wildbad, Germany
Amicon Ultra 3K-0.5 mL centrifugal filters	Merck Millipore; Darmstadt, Germany
Cell culture dishes	Corning, Thermo Fisher Scientific; Schwerte, Germany
Cell culture multi-well plates	TPP Techno Plastic Producers; Trasadingen, Switzerland

Cell scrapers	Corning, Thermo Fisher Scientific; Schwerte, Germany,
Cotton Swabs, PP applicator 150 x 2.5 mm, for Sircol assay	Laboratory Analysis LTD; Topsham, UK
Combitips advanced®	Eppendorf ; Hamburg, Germany
Cryovials 1.5 ml	Greiner Bio- One; Frickenhausen, Germany
FACS tubes	BD Bioscience; Heidelberg, Germany
Falcon Tube (15 ml, 50 ml)	BD Bioscience; Heidelberg, Germany
Filter Tips	Biozym Scientific; Hessisch Oldendorf, Germany
Glas Pasteur pipettes	VWR International; Darmstadt, Germany
Hyperfilm ECL Film	Amersham, GE Healthcare; Freiburg, Germany
Protein LoBind Tubes (1.5 ml)	Eppendorf; Hamburg, Germany
Measuring pipettes, sterile, single use (5 ml, 10 ml, 25 ml, 50 ml)	VWR International; Darmstadt, Germany
Microscope slides	Thermo Fisher Scientific; Darmstadt, Germany
Nylon filters, pore size 70 µm	BD Bioscience; Heidelberg, Germany
PCR plates, 96-well plate	Kisker Biotech; Steinfurt, Germany
PVDF membrane	Merck Millipore; Darmstadt, Germany
Reaction tubes (0.5 ml, 1.5 ml, 2 ml)	Eppendorf; Hamburg, Germany
Reagent reservoirs, 50 mL	Corning; New York, USA
Sealing foils for PCR plates	Kisker Biotech; Steinfurt, Germany
Tips	Eppendorf; Hamburg, Germany
Whatman blotting paper, 3 mm	GE Healthcare; Freiburg, Germany

### 3.1.3 Cell culture media

**Table 3.3: Media**

<i>Type</i>	<i>Company</i>
DMEM/F12 (1:1)	Gibco, Life Technologies; Carlsbad, USA
Opti-MEM I Reduced Serum Medium	Gibco, Life Technologies; Carlsbad, USA

### 3.1.4 Small interfering RNA (siRNA)

**Table 3.4: Human siRNAs**

<i>siRNA</i>	<i>Company</i>	<i>Product number</i>
scrambled <i>Silencer</i> ® Negative control No. 1	Ambion, Life Technologies; Carlsbad, USA	AM4611
<i>Silencer</i> ® Select PDGFR $\alpha$ siRNA	Ambion, Life Technologies; Carlsbad, USA	s10235
<i>Silencer</i> ® Select PDGFR $\beta$ siRNA	Ambion, Life Technologies; Carlsbad, USA	s10240
<i>Silencer</i> ® Select CDCP1 siRNA	Ambion, Life Technologies; Carlsbad, USA	s35060

### 3.1.5 DNA constructs

**Table 3.5: DNA plasmids**

<i>Type</i>	<i>Company</i>
pGL4-10, control vector	Promega; Mannheim, Germany
pGL3-CAGA(9)-luc	[Dennler et al., 1998]

### 3.1.6 Inhibitors and antagonists

**Table 3.6: Inhibitors and antagonists**

<i>Product</i>	<i>Function</i>	<i>Stock concentration</i>	<i>Working concentration</i>	<i>Solvent</i>	<i>Company</i>
Nintedanib (BIBF 1120)	Inhibitor of VEGF1/2/3, FGFR1/2/3, PDGFR	1 mM	1 $\mu$ M	DMSO	Selleckchem; Munich, Germany
Imatinib Mesylate (STI571)	Inhibitor of v-Abl, c-Kit and PDGFR	10 mM	-	DMSO	Selleckchem; Munich, Germany
SB431542	Inhibitor of ALK5 receptor	10 mM	10 $\mu$ M	DMSO	Tocris Bioscience; Bristol, U.K.
Sis3	Inhibitor of pSmad3	3 mM	6 $\mu$ M	DMSO	Tocris Bioscience; Bristol, U.K.
UO126	Inhibitor of pErk	10 mM	10 $\mu$ M	DMSO	Tocris Bioscience; Bristol, U.K.
SCH79797	Inhibitor of PAR1	10 mM	0.05 – 1 $\mu$ M	DMSO	Tocris Bioscience; Bristol, U.K.
FSLLRY-NH2	Peptide antagonist of PAR2	10 mM	0.1 – 10 $\mu$ M	MilliQ H <sub>2</sub> O	Tocris Bioscience; Bristol, U.K.
GM6001 (Ilomastat, Galardin)	Broad spectrum MMPs inhibitor (MMP1-3, MMP7-9, MMP12, MMP14, and MMP26)	5 mM	0.1 – 10 $\mu$ M	DMSO	Selleckchem; Munich, Germany
Bortezomib	Inhibitor of proteasome	2.6 mM	1 – 10 nM	PBS	Milleium, Takeda; MA, USA
Bafilomycin A1	Inhibitor of the late phase of autophagy	10 $\mu$ M	1 – 10 nM	DMSO	Sigma-Aldrich; Taufkirchen, Germany

### 3.1.7 Antibodies

**Table 3.7: Primary antibodies for Western blot**

<i>Antibody</i>	<i>Host</i>	<i>Dilution</i>	<i>Molecular size</i>	<i>Company</i>
PDGFR $\alpha$ (sc-338)	rabbit	1:500	170 kDa	Santa Cruz Biotechnology; Dallas, USA

PDGFR $\beta$ (sc-432)	rabbit	1:500	170 kDa	Santa Cruz Biotechnology; Dallas, USA
Akt (9272S)	rabbit	1:1000	60 kDa	Cell Signaling; Danvers, USA
Phospho-Akt (Ser473) (D9E) XP (4060S)	rabbit	1:1000	60 kDa	Cell Signaling; Danvers, USA
Anti - Smad3 (ab28379)	rabbit	1:1000	58 kDa	Abcam; Cambridge, UK
Phospho anti - Smad3 (S423+S425) (ab52903)	rabbit	1:1000	58 kDa	Abcam; Cambridge, UK
Collagen type I (600-401-103-0.5)	rabbit	1:5000	230 kDa	Rockland; Gilbertsville, USA
Collagen type III (600-401-105-0.1)	rabbit	1:5000	250 kDa	Rockland; Gilbertsville, USA
Collagen type V (Col5A1) (sc-20648)	rabbit	1:1000	260 kDa	Santa Cruz Biotechnology; Dallas, USA
Fibronectin (sc-9068)	rabbit	1:500	220 kDa	Santa Cruz Biotechnology; Dallas, USA
anti-actin, $\alpha$ -smooth muscle ( $\alpha$ SMA) (A5228)	mouse	1:1000	42 kDa	Sigma; St. Louis, USA
CDCP1 (4115)	rabbit	1:1000	135 kDa	Cell Signaling; Danvers, USA
Erk1/2 (phospho44/42) (9101)	rabbit	1:1000	44, 42 kDa	Cell Signaling; Danvers, USA
Anti-Erk1 (554100)	mouse	1:1000	44 kDa	BD; Franklin Lakes, USA
Anti-Erk2 (610103)	rabbit	1:1000	42 kDa	BD; Franklin Lakes, USA
Lys48-specific ubiquitin, clone Apu2 (05-1307)	rabbit	1:1000	250-16 kDa	Merck Millipore; Danvers, USA
LC3B (D11) XP (3868)	rabbit	1:1000	14, 16 kDa	Cell Signaling; Danvers, USA
Actin (anti-beta, Peroxidase (clone AC-15) (A3854)	HRP-conjugated	1:40 000	42 kDa	Sigma-Aldrich; Taufkirchen, Germany

**Table 3.8: Secondary antibodies for Western blot**

<i>Antibody</i>	<i>Host</i>	<i>Dilution</i>	<i>Company</i>
HRP Linked Whole AB Rabbit IgG (NA934V)	donkey	1:20 000	GE Healthcare; Freiburg, Germany
HRP Linked Whole AB Mouse IgG (NA931V)	sheep	1:20 000	GE Healthcare; Freiburg, Germany

**Table 3.9: Fluorochrome-conjugated antibodies for FACS analysis**

<i>Antibody</i>	<i>Host</i>	<i>Dilution</i>	<i>Company</i>
PDGFR $\alpha$ _ (CD140a)-PE (323505)	mouse	1:5	BioLegend; San Diego, USA
PDGFR $\beta$ _ (CD140b)-PE (323605)	mouse	1:20	BioLegend; San Diego, USA
PDGFR $\beta$ _ (CD140b)-APC (323608)	mouse	1:10	BioLegend; San Diego, USA
APC anti-human CD318 (CDCP1) (324008)	mouse	1:10	BioLegend; San Diego, USA

**Table 3.10: Isotype controls for FACS analysis**

<i>Isotype Ctrl</i>	<i>Host</i>	<i>Dilution</i>	<i>Company</i>
PE Mouse IgG1 (400113)	n.d.	1:20 / 1:10	BioLegend; San Diego, USA
APC Mouse IgG1 (400121)	n.d.	1:3	BioLegend; San Diego, USA
APC Mouse IgG2b (400320)	n.d.	1:5	BioLegend; San Diego, USA

**Table 3.11: Primary antibodies for immunofluorescence stainings**

<i>Isotype Ctrl</i>	<i>Host</i>	<i>Dilution</i>	<i>Company</i>
CDCP1/CD318 (PA5-17245)	rabbit	1:100	ThermoFisher Scientific; Rockford, USA
anti-human CD90 (Thy-1) (14-9090-82)	mouse	1:100	eBioscience; San Diego, USA
anti-actin, $\alpha$ -smooth muscle ( $\alpha$ SMA) (A5228)	mouse	1:5000	Sigma; St. Louis, USA

**Table 3.12: Secondary antibodies for immunofluorescence stainings**

<i>Isotype Ctrl</i>	<i>Host</i>	<i>Dilution</i>	<i>Company</i>
Alexa Fluor 568 Goat Anti-Rabbit IgG (H+L) (A11011)	goat	1:250	ThermoFisher Scientific; Rockford, USA
Goat anti-Mouse IgG (H+L) Cross-Adsorbed Secondary Antibody, Alexa Fluor 488 (A11001)	goat	1:250	ThermoFisher Scientific; Rockford, USA

**Table 3.13: Antibodies for immunoprecipitation**

<i>Antibody</i>	<i>Host</i>	<i>Dilution</i>	<i>Company</i>
CDCP1 (4115)	rabbit	1:1000	Cell Signaling; Danvers, USA

### 3.1.8 Human primers

**Table 3.14: Sequences of human primers**

<i>Target gene</i>	<i>Sequence 5' - 3'</i>
ACTA2 ( $\alpha$ SMA)	fw: CGAGATCTCACTGACTACCTCATGA rv: AGAGCTACATAACACAGTTTCTCCTTGA
CDCP1	fw: TTCAGCATTGCAAACCGCTC rv: ATCAGGGTTGCTGAGCCTTC
HPRT	fw: AAG GAC CCC ACG AAG TGT TG rv: GGC TTT GTA TTT TGC TTT TCC A

### 3.1.9 Kits

**Table 3.15: Kits**

<i>Product</i>	<i>Company</i>
Pierce BCA Protein Assay Kit	Biochrom; Berlin, Germany
Dual luciferase reporter system	Promega; Mannheim, Germany
PeqGold RNA kit	Peqlab; Erlangen, Germany
Sircol collagen assay kit	Biocolor; Northern Ireland, U.K.

### 3.1.10 Laboratory equipment

**Table 3.16: Laboratory equipment**

<i>Laboratory equipment</i>	<i>Company</i>
-80°C freezer U570 HEF	New Brunswick; Hamburg, Germany
-20°C freezer MediLine LGex 410	Liebherr; Biberach, Germany
2100 Antigen Retriever	Aptum Biologics; Southampton, U.K.
Analytical scale XS20S Dual Range	Mettler Toledo; Gießen, Germany
Autoclave DX-45	Systec; Wettengel, Germany
Autoclave VX-120	Systec; Wettengel, Germany
AxioImager M2	Zeiss; Jena, Germany
Axiovert 40C microscope	Zeiss; Jena, Germany
Cell culture work bench Herasafe KS180	Thermo Fisher Scientific; Darmstadt, Germany
Centrifuge MiniSpin plus	Eppendorf; Hamburg, Germany
Centrifuge Rotina 420R	Hettich; Tuttlingen, Germany
Centrifuge with cooling, Micro200R	Hettich; Tuttlingen, Germany
CO <sub>2</sub> cell Incubator BBD6620	Thermo Fisher Scientific; Darmstadt, Germany
Confocal microscope LSM 710	Zeiss; Jena, Germany
Corning® LSE™ Mini Microcentrifuge, 120V	Corning; Wiesbaden, Germany
Demineralized water	Thermo Fisher Scientific; Darmstadt, Germany
Dry ice container Forma 8600 Series, 8701	Thermo Fisher Scientific; Darmstadt, Germany
Dynabeads™ Protein A	Thermo Fisher Scientific; Darmstadt, Germany
DynaMag™ - 2 Magnet	Thermo Fisher Scientific; Darmstadt, Germany
Electronic pipet filler	Eppendorf; Hamburg, Germany
Film developer Curix 60	AGFA; Morsel, Belgium
Fridge MediLine LKv 3912	Liebherr; Biberach, Germany
Fisher Science Education™ 4-Way Microtube Racks	Thermo Fisher Scientific; Darmstadt, Germany
Gel imagine system ChemiDoc XRS+	Biorad; Hercules, USA
Ice machine ZBE 110-35	Ziegra; Hannover, Germany
Light Cycler LC480II	Roche Diagnostic; Mannheim, Germany
Liquid nitrogen cell tank BioSafe 420SC	Cryotherm; Kirchen/Sieg, Germany
BD LSR II Flow Cytometer	BD; Franklin Lakes, USA
Magnetic stirrer KMO 2 basic	IKA; Staufen, Germany
Mastercycler Nexus	Eppendorf; Hamburg, Germany
Microm HMS740 Robot-Stainer	Thermo Fisher Scientific; Darmstadt, Germany
Multipette stream	Eppendorf; Hamburg, Germany
Nalgene® Freezing Container (Mr. Frosty)	Omnilab; Munich, Germany
NanoDrop 1000	PeqLab; Erlangen, Germany

pH meter InoLab pH 720	WTW; Weilheim, Germany
Pipettes Research Plus	Eppendorf; Hamburg, Germany
Plate centrifuge 5430	Eppendorf; Hamburg, Germany
Plate reader TriStar LB941	Berthold Technologies; Bad Wildbach, Germany
Plate reader Sunrise	Tecan; Crailsheim, Germany
VWR® Tube Rotator and Rotisseries	VWR International; Darmstadt, Germany
Roll mixer	VWR International; Darmstadt, Germany
Power Supply Power Pac HC	Biorad; Hercules, USA
Scale XS400 2S	Mettler Toledo; Gießen, Germany
Shaker Duomax 1030	Heidolph; Schwabach, Germany
Thermomixer compact	Eppendorf; Hamburg, Germany
Ultra-pure water supply MilliQ Advantage A10	Merck Millipore; Darmstadt, Germany
Vortex Mixer	IKA; Staufen, Germany
Vacuum pump NO22AN.18 with switch 2410	KNF; Freiburg, Germany
Water bath Aqua Line AL 12	Lauda; Lauda-Königshofen, Germany

### 3.1.11 Software

**Table 3.17: Software**

<i>Product</i>	<i>Company</i>
BD FACSDIVA™	BD Biosciences; Heidelberg, Germany
FlowJo Software, Version 9.6.4	TreeStar Inc; Ashland, OR, USA
GraphPad Prism 5	GraphPad Software; La Jolla, USA
Imaris Scientific 3D/4D Image Processing and Analysis Software, Version 8.1.2	Bitplane; Zurich, Switzerland
Image Lab Software, Version 5.2.1	Biorad; Hercules, USA
LightCycler® 480 SW 1.5	Roche Diagnostics; Mannheim, Germany
Magelan Software	Tecan; Crailsheim, Germany
Tristar MicroWin 2000	Berthold Technologies; Bad Wildbach, Germany
ZEN 2010 – Digital Imaging for Lightmicroscopy Software	Zeiss; Oberkochen, Germany

## 3.2 Methods

### 3.2.1 Isolation of primary human lung fibroblasts

Primary human lung fibroblasts (phLFs) were isolated from lung tissues derived from lung explants or tumor-free areas of lung resections provided by the CPC-M Bioarchive, Munich, Germany. This project was approved by the local ethics committee of the LMU Munich (333-10, removal request 454-12). For the

isolation procedure, the lung tissue explants were placed in a 10 cm dish containing prewarmed DMEM-F12 media supplemented with 20% FBS and 100 U/ml of penicillin/streptomycin. Subsequently, tissue explants were subdivided into 1-2 mm<sup>2</sup> pieces using scissors or scalpel, and thereafter transferred in a 50 ml falcon tube for further enzymatic digestion with 5 mg of Collagenase I (Biochrom) for 1 h at 37°C. Afterwards, the digested tissue pieces were filtered through 70 µm Nylon filters, and further washed with 10 ml sterile 1x PBS for 5 min at 450g at 4°C. The supernatant was carefully aspirated and cell pellets resuspended in 10 ml DMEM-F12 media supplemented with 20 % FBS plus 100 U/ml of penicillin/streptomycin. Cells were subsequently plated on 10 cm cell culture dishes and cultured under standard cell culture conditions at 37°C and 5% CO<sub>2</sub>.

### **3.2.2 Cryopreservation of primary human lung fibroblasts**

For cryopreservation, phLFs were detached with 0.25 % Trypsin-EDTA and Cell suspension was transferred in a 50 ml falcon tube followed by centrifugation for 5 min at 450g at 4°C. Next, media was carefully aspirated and cell pellet immediately resuspended in freezing media (DMEM-F12, 70 % FBS, 100 U/ml of penicillin/streptomycin, and 10 % DMSO). Cell suspensions were transferred into cryovials, and stored in Mr. Frosty (Omnilab) overnight at -80°C. Next day, cryovials were transferred to liquid nitrogen for long-term storage at -195°C.

### **3.2.3 Thawing frozen cells**

Cryovials with frozen cell suspensions were placed in a 37°C water bath for approximately 90 s until cell suspension defrosted followed by immediate dilution of the cell suspension with 1 ml prewarmed 20% DMEM-F12 media supplemented with 100 U/ml of penicillin/streptomycin. Defrosted cell suspension was transferred in a 50 ml falcon tube and carefully supplemented with 8 ml of cell culture media. Cells were then centrifuged for 5 min at 450 g at 37 °C, and the cell pellet was resuspended with fresh cell culture medium (20 % FBS, DMEM-F12, 100 U/ml of penicillin/streptomycin). Cells were plated in a 10 cm cell culture dish and cultured under standard cell culture conditions at 37°C and 5% CO<sub>2</sub>.

### **3.2.4 Cell culture experiments**

#### **3.2.4.1 Growth factor stimulation**

PhLFs were seeded on a 6-well plate ( $2.6 \times 10^4$  cells/cm<sup>2</sup>) or a 10 cm cell culture dish ( $1.2 \times 10^4$  cells/cm<sup>2</sup>) in 20 % DMEM-F12 cell culture media supplemented with 100 U/ml of penicillin/streptomycin. Cells were serum starved the next day in 0.5 % DMEM-F12 media supplemented with 100 U/ml of penicillin/streptomycin for 24 h, and subsequently stimulated in starvation media with 1 ng/ml or 2 ng/ml

of human recombinant TGF $\beta$ 1 either for 40 min or every 24 h for a total 48h treatment. Additionally, pHLFs were stimulated with 10, 50, or 100 ng/ml recombinant human PDGF-AA, PDGF-AB, PDGF-CC, and PDGF-DD ligands for various time points starting from 40 min up to 24 h.

### 3.2.4.2 siRNA-mediated reverse transfection

All human siRNAs used in this study (Table 3.4) were purchased from Thermo Fisher Scientific as lyophilized products. Prior transfection, siRNAs were first dissolved in 50  $\mu$ l sterile, DNase/RNase-free water in order to obtain 100  $\mu$ M stock solutions. For the experimental procedures, the stock solutions were further diluted in 1:5 ratios to obtain 2  $\mu$ M working solutions, and stored at  $-20^{\circ}\text{C}$  degrees until further use.

For the procedure, transfection mix containing solution A and B was prepared as described in Table 3.18.

**Table 3.18: Complete transfection mix per one well of a 6-well plate or one 10 cm dish**

Solution	Reagent	Volume (2 nM siRNA)	Volume (10 nM siRNA)	Volume (10 nM siRNA)
		6-well plate	6-well plate	10 cm dish
A	OptiMem media	247.5 $\mu$ l	237.5 $\mu$ l	760 $\mu$ l
	siRNA	2.5 $\mu$ l	12.5 $\mu$ l	40 $\mu$ l
B	OptiMem media	244 $\mu$ l	244 $\mu$ l	780.8 $\mu$ l
	Lipofectamine <sup>®</sup> RNAiMax	6 $\mu$ l	6 $\mu$ l	19.2 $\mu$ l

Solutions A and B were first separately incubated for 5 min at RT, and then incubated together for 20 – 30 min at RT in order to form siRNA-lipid complexes. Subsequently, transfection carried out in a 6-well plate was performed as follows: 500  $\mu$ l of complete transfection mix was transferred to each well and mixed with 2.5 ml of cell suspension containing  $2.6 \times 10^4$  cells/cm<sup>2</sup>. On the other hand, transfection carried out in a 10 cm dishes was performed by transferring 1.6 ml of complete transfection mix to each 10 cm dish and mixed with 8 ml of cell suspension containing  $1.2 \times 10^4$  cells/cm<sup>2</sup>. Importantly, pHLFs were seeded in 20% DMEM-F12 cell culture media without penicillin/streptomycin. To test siRNA efficiency in pHLFs, cells remained transfected for 24 h, 48 h, and 72 h. For the main experiment, 24 h after adding transfection mix, cells were starved in 0.5% DMEM-F12 starvation media supplemented with 100 U/ml of penicillin/streptomycin overnight and treated with growth factors as described in section 3.2.4.1.

### 3.2.4.3 Plasmid DNA transfection

Per one well of a 48-well plate,  $3.2 \times 10^4$  cells/cm<sup>2</sup> were reversely transfected for 24 h with 10 nM siRNA against CDCP1 and control scrambled siRNA as described above (section 3.2.4.2). Subsequently, cells were

washed once with 1x PBS and refreshed with 200  $\mu$ l 20% DMEM-F12 cell culture media supplemented with 100 U/ml of penicillin/streptomycin. Plasmid transfection was performed with 250 ng/ml of the SMAD signaling luciferase reporter plasmid pGL3-CAGA(9)-luc [Dennler et al., 1998] and control pGL4-10 construct (Table 3.5). For plasmid transfection, 25  $\mu$ l of solution A and B per one well were prepared as described in Table 3.19 and Table 3.20. Both solutions were separately incubated for 5 min at RT and afterwards incubated together for additional 20 – 30 min at RT. Subsequently, 50  $\mu$ l of complete transfection mix per one well of a 48-well plate was transferred to respective wells, and plasmid transfection was performed for additional 6 h. Afterwards, cells were serum starved overnight in 0.5 % DMEM-F12 media containing antibiotics followed by stimulation with 1 ng/ml TGF $\beta$  for 1 h, 26 h, and 48 h. Finally, cells were washed once with 1x PBS and plates were stored at – 80°C until luciferase assay was performed.

**Table 3.19: Plasmid calculations**

Plasmid	Concentration	Volume 250 ng/well
pGL4-10	2.0 mg/ml	0.125 $\mu$ l
pGL3-CAGA(9)-luc	1.4 mg/ml	0.18 $\mu$ l

**Table 3.20: Complete transfection solution per one well of a 48-well plate**

Plasmid	Solution	Reagent	Volume
pGL4-10	Solution A	OptiMem media	25 $\mu$ l
		Plasmid	0.125 $\mu$ l
		PLUS reagent	0.25 $\mu$ l
	Solution B	OptiMem media	25 $\mu$ l
		Lipofectamine LTX	0.6 $\mu$ l
pGL3-CAGA(9)-luc	Solution A	OptiMem media	25 $\mu$ l
		Plasmid	0.18 $\mu$ l
		PLUS reagent	0.25 $\mu$ l
	Solution B	OptiMem media	25 $\mu$ l
		Lipofectamine LTX	0.6 $\mu$ l

#### 3.2.4.4 Luciferase reporter assay

Fortyeight hours after plasmid transfection (section 3.2.4.3), pHLFs were lysed with 65  $\mu$ l per well of Glo Lysis Buffer (Promega) for 30 min at RT while incubating at an orbital shaker. Thereafter, 25  $\mu$ l of cell lysate was transferred in a white 96-well microplate and luciferase activity was quantified by incubation of cell lysates with 100  $\mu$ l Bright-Glo<sup>TM</sup> luciferase assay substrate in a plate reading luminometer with an

automatic injection system (Berthold). All measurements were carried out in quadruplicates and all treatment conditions were normalized to control scrambled siRNA measurement.

#### **3.2.4.5 Cell treatment with inhibitors**

Cells were plated in a density of  $2.6 \times 10^4$  cells/cm<sup>2</sup> in DMEM-F12 media containing 20 % FBS and 100 U/ml of penicillin/streptomycin. Next day, cells were starved with DMEM-F12 media containing 0.5 % FBS plus 100 U/ml of penicillin/streptomycin 24 h prior the treatment. Thereafter, cells were stimulated with individual inhibitors or antagonists enlisted in Table 3.6. Nintedanib stimulation was performed by treating cells either with 1  $\mu$ M Nintedanib for 30 min followed by cell stimulation with 10 ng/ml PDGF-AB, PDGF-DD, or 1 ng/ml TGF $\beta$ 1 for 40 min, or in parallel with 1 or 2 ng/ml TGF $\beta$  every 24 h for a total of 48 h. Else, cells were treated with single inhibitors in the presence of 1 ng/ml TGF $\beta$  every 24 h for a total of 48 h treatment.

#### **3.2.4.6 Cell treatment with 2-phospho-L-ascorbic acid**

Cells were treated as described in section 3.2.4.5 with media further supplemented with 0.1 mM 2-phospho-L-ascorbic acid.

#### **3.2.4.7 Cell adhesion assay**

Treated phFLs cells as described in section 3.2.4.2 were harvested and  $1.1 \times 10^4$  cells/cm<sup>2</sup> plated in a 48-well plate in quadruplicates. Cells were resuspended in 0.5% starvation DMEM-F12 media and allowed to attach for 10 min at 37°C under humidified cell culture conditions. Afterwards, non-adherent cells were removed by washing the wells with 1x PBS. Adherent cells were fixed with 4% PFA for 15 min at RT, washed twice with 1x PBS, and incubated with DAPI (nuclear staining) and Phalloidin (cytoskeletal staining) for 1 h at RT. Cells were again washed three times with 1x PBS, and finally stored in 1x PBS at 4°C. For the analysis, each well was individually scanned with an LSM710 confocal microscope and images were acquired by an 8x8 tile scan covering the middle area of each well. Data were quantified by Imaris software version 8.1.2. (Bitplane).

#### **3.2.4.8 Cell invasion assay**

##### **3.2.4.8.1 Preparation of collagen G Gels**

Collagen G Gels were prepared according to the manufacturer's instructions (Biochrom AG). Briefly, solution A was prepared by mixing 0.7 M NaOH together with 1 M HEPES buffer (Sigma Aldrich) in a 1:1 ratio. Thereafter, 10x PBS supplemented with 20 % FCS was added to the solution A in a 1:1 ratio, forming a solution B with pH 7.90 - 8.05. For a final gelation step, solution B was thoroughly mixed with collagen

G in a ratio 1:4. Importantly, all solutions were kept and prepared on ice during the whole procedure. For the invasion assay, 40  $\mu$ l of collagen G solution was poured in each well of a 96-well image plate, and polymerization of the final collagen G gels was achieved by incubation at 37°C for 1 h. The quality of collagen G gels was examined with an Axiovert 40C microscope (Carl Zeiss).

### **3.2.4.8.2 3D collagen-based invasion assay**

Cells were plated in a density of  $5.8 \times 10^4$  cells/cm<sup>2</sup> on the top of polymerized collagen G matrix (section 3.2.4.8.1). Cells were plated in DMEM-F12 media supplemented with 5% FBS and 100 U/ml of penicillin/streptomycin, and starved overnight in media containing 0.5% FBS. Subsequently, cells were stimulated with 10 ng/ml PDGF-AA, PDGF-AB, and PDGF-DD ligands (five technical replicates per stimulation) and left for invasion into collagen gels for 48 h under standard cell culture conditions (at 37°C and 5% CO<sub>2</sub>). The collagen matrices were carefully washed once with 1x PBS, fixed with 4% PFA for 45 min at 37°C, and subsequently stained with DAPI (1:1500) and Phalloidin (1:300) in 1x PBS for 1 h at RT. Phalloidin staining was used to visualize the cell layer, and to estimate cell confluency. DAPI was used to visualize cell nuclei. Finally, cells were washed twice with 1x PBS and an LSM710 confocal microscope was used to image each well containing pLFs embedded in a 3D collagen gels. The exact settings and parameters for image acquisition as well as final data quantification were previously described in Burgstaller *et al.*, 2013 [Burgstaller *et al.*, 2013].

## **3.2.5 Protein analysis**

### **3.2.5.1 Protein extraction from primary fibroblasts**

Cells attached on a 6-well plate were washed with 1x PBS and subsequently scratched with a cell scraper in 80  $\mu$ l of a RIPA protein lysis and extraction buffer (50 mM Tris-HCl, pH 7.5, 150 mM NaCl, 1% NP-40, 0.5% Sodium – deoxycholate, and 0.1% SDS) supplemented with 1x Roche complete mini protease inhibitor cocktail and PhosphoStop phosphatase inhibitor (per one well of a 6-well plate). Cell lysates were transferred in a 1.5 ml reaction tube, placed on ice and incubated in complete RIPA buffer for 30 min. Subsequently, cell lysates were centrifuged for 15 min at 15.000 RPM at 4°C to separate total protein content (supernatant) from cell debris (pellet). Cell supernatants were stored at -80°C. Protein concentration was determined using the Pierce BCA Protein Assay Kit according to the manufacturer's instructions.

### **3.2.5.2 Protein concentration from cell supernatants**

Cell supernatants were thawed on ice and Amicon Ultra-0.5 Centrifugal Filter Devices (Millipore) were used to concentrate cell supernatants according to the manufacturer's instructions. Briefly, 500  $\mu$ l per sample was transferred into an Amicon Ultra 3k Centrifugal Filter Unit inserted into microcentrifuge tube and

samples were centrifuged for 30 min at 14.000 g at 4°C. To recover the concentrated proteins, Amicon Ultra 3k Centrifugal Filter Unit was inverted and placed in a new clean microcentrifuge tube followed by centrifugation for 2 min at 1000 g at 4°C. Finally, the ultrafiltrate was stored in the centrifuge tube at -80°C for further analysis.

### 3.2.5.3 SDS-PAGE and immunoblotting

4% stacking and 7.5 % or 10 % separation gels were prepared as described in the Table 3.21 and Table 3.22. For protein separation via SDS-PAGE electrophoresis, samples from total protein lysates were prepared by mixing 25 µg of total protein lysates with 2x or 6x Laemmli loading buffer in Millipore-H<sub>2</sub>O for equal volumes. Samples from concentrated cell supernatants were prepared by mixing 60 µl of cell supernatants together with 10 µl of 6x Laemmli loading buffer. Finally, samples were incubated for 5-10 min at 95°C.

**Table 3.21: Composition of 4 % SDS-PAGE Stacking gel**

Reagent	Volume
Millipore-H <sub>2</sub> O	1.50 ml
0.5 M Tris-HCl pH 6.8	630 µl
10 % SDS	30 µl
Acrylamide/Bisacrylamide	330 µl
TEMED	2 µl
10 % APS	13 µl

**Table 3.22: Composition of 7.5 % and 10 % SDS-PAGE Separation gels**

Reagent	7.5 %	10 %
	Volume	Volume
Millipore-H <sub>2</sub> O	4.36 ml	3.61 ml
1.5 M Tris-HCl pH 8.8	2.25 ml	2.25 ml
10 % SDS	90 µl	90 µl
Acrylamide/Bisacrylamide	2.25 ml	3 ml
TEMED	7.2 µl	7.2 µl
10 % APS	45 µl	45 µl

Proteins were further separated on 7.5 % or 10 % SDS-polyacrylamide gels at 120 V per gel for approximately 1.5 h. For immunoblotting, protein samples were transferred to a methanol-activated polyvinylidenedifluoride (PVDF, Millipore, 0.45 µm) membrane at 240 mA per gel for 90 min. Membranes were blocked with 5 % non-fat dry milk prepared in 1x TBST (0.1% Tween®20 / 10x TBS) for 30 min at

RT, followed by incubation with primary antibodies overnight at 4 °C while rotating. Membranes were washed three times with 1x TBST for 10 min and subsequently incubated with respective HRP-conjugated secondary antibodies for 1 h at RT while rotating. Afterwards, membranes were again washed three times with 1x TBST for 10 min and proteins were visualized by using western blot chemiluminescent substrates (SuperSignal® West Dura and Femto Substrate, Thermo Fisher). Signals were analyzed with the film developer Curix60 (AGFA) and finally documented on x-ray films. For densitometry quantification, x-ray films were first scanned using ChemiDoc Imaging System (Bio-Rad) and protein quantity was measured using Image Lab Software (Bio-Rad).

#### **3.2.5.4 Immunoprecipitation**

$1.4 \times 10^4$  cells/cm<sup>2</sup> were treated as described in section 3.2.4.5, washed with 1x PBS and subsequently scratched with cell scraper in 2-3 ml of 1x PBS. Cell pellets were afterwards stored in a 1.5 ml reaction tube at -80°C for further analysis.

First, Dynabeads™ Protein A (Thermo Fisher Scientific) magnetic beads were equilibrated as follows: beads were gently vortexed, transferred in 1.5 ml Protein LoBind Tubes (Eppendorf) and subsequently washed three times with 500 µl of ice-cold RIPA protein lysis and extraction buffer supplemented with 1x Roche complete mini protease inhibitor cocktail and PhosphoStop phosphatase inhibitor. Each time, 500 µl of complete RIPA buffer was added to beads followed by inverting a tube for approximately 10x. Lysis buffer was then discarded by placing a reaction tube on a DynaMag™ -2 magnet (Thermo Fisher Scientific), where magnetic beads remained on the wall of a tube and thus lysis buffer could be carefully pipetted away. Magnetic beads were finally resuspended in a 500 µl of lysis buffer.

For immunoprecipitation, cell pellets were lysed in 500 µl of RIPA protein lysis and extraction buffer supplemented with 1x Roche complete mini protease inhibitor cocktail and PhosphoStop phosphatase inhibitor. Cell pellets were placed on ice and incubated in complete RIPA buffer for 30 min followed by centrifugation for 15 min at 15.000 RPM at 4°C to separate total protein content (supernatant) from intracellular cell debris (pellet). A preclearing step of the cell lysate was performed by incubating with 75 µl of equilibrated magnetic Dynabeads™ Protein A for 1 h at 4°C while rotating. Subsequently, suspension was centrifuged for 1 min at 800g at 4°C and placed on a DynaMag™ -2 magnet with magnetic beads remained on the wall of reaction tubes. Thus, 100 µl of whole protein lysate was pipetted away and stored at -80°C as an input (20 % of whole cell lysate). Remaining protein lysates were subsequently transferred in new 1.5 ml Protein LoBind Tubes and precleared beads also stored at -80°C for further analysis. Afterwards, 0.4 µg of antibody directed against CDCP1 or respective rabbit IgG control were added to protein lysates and incubated for 1 h on ice. Finally, 45 µl of equilibrated magnetic beads were added to each reaction tube followed by incubation of the mix overnight at 4°C using VWR® Tube Rotator. Next

day, the whole suspension was centrifuged for 1 min at 800g at 4°C and supernatant collected by placing the tubes on a DynaMag™ -2 magnet. Supernatant was stored at -80°C for further analysis. Magnetic beads containing immunoprecipitated CDCP1 were washed three times in 500 µl of ice-cold NP-40 wash buffer, each time for 5 min at 4°C under continuous inverting. Reaction tubes were then placed on a DynaMag™ -2 magnet, to completely remove the wash buffer. Finally, immunoprecipitants were resuspended in 35 µl of 2x Laemmli buffer, incubated for 10 min at 95°C and analyzed via immunoblot as described in section 3.2.5.3.

### **3.2.5.5 Sircol collagen assay**

Cells were treated as described in section 3.2.4.6 and 1 ml of cell supernatant from treatments were stored in 1.5 ml Protein LoBind Tubes (Eppendorf) at -80°C. Importantly, the whole Sircol collagen assay was carried out on ice.

Collagen Standards were prepared according to manufacturer's instructions (Bicolor). Cell supernatants were thawed on ice, and proteins from cell supernatants were concentrated as described in chapter 3.2.5.2. Subsequently, 200 µl of ice cold Isolation and Concentration Reagent was added to 1 ml of cell supernatant (test sample, duplicates), 1 ml of standard dilution (Collagen Standard, duplicates), and to 1 ml of starvation medium containing 0.1 mM ascorbate (Blank, duplicates). Reaction tubes were well mixed by inverting approximately 10x and subsequently placed into a container half filled with an ice-water mix for overnight incubation at 4°C. Next day, reaction tubes containing collagen precipitates were centrifuged for 30 min at 14,000 RPM at 4°C and supernatants afterwards carefully discarded by inverting each reaction tube. Transparent pellets of hydrated collagen remained on the bottom of reaction tubes. Next, 1 ml of Sircol Dye Reagent was added to each reaction tube which was mixed well by inverting, followed by incubation of each reaction tube for 30 min at 400 RPM at RT in a Thermomixer under gentle shaking. Afterwards, reaction tubes were centrifuged for 30 min at 14,000 RPM and supernatant was removed by inverting each reaction tube. Inverted tubes were dried on tissues and cotton buds were used to remove unbound dye from inside walls of reaction tubes while dye-bound collagen precipitates remained on the bottom of each tube. Afterwards, 750 µl of ice-cold Acid-Salt Wash reagent was added to the pellet and the reaction mix centrifuged for 30 min at 14,000 RPM at RT. Wash solution was again carefully removed as described above and the washing step repeated one more time. Finally, 250 µl of Alkali Reagent was added to each reaction tube and pellets containing precipitated dye-bound collagens were dissolved by vortexing. Once all bound dye was dissolved, 200 µl of each sample was transferred in duplicates to a 96-well plate and the absorbance of each samples measured at 550 nm using Sunrise Plate Reader (Tecan).

### 3.2.5.6 Immunofluorescence staining of primary human lung fibroblast

PhLFs were seeded in a 96-well image plate (BD Falcon) or a 24-well image plate (Ibidi) and cultured till a confluency of 80 %. Cells were washed once with 1x PBS and subsequently fixed either with 4% PFA in PBS for 15 min at RT or with 100% ice-cold methanol for 90s on ice. Methanol fixation was at the same time used for cellular permeabilization to access intracellular antigens. After fixation step, cells were washed twice with 1x PBS followed by incubation with 5% BSA in 1x PBS for 30 min at RT. Subsequently, cells were stained with primary antibody against CDCP1, CD90 (Thy-1), and  $\alpha$ SMA for 1 h at RT. Afterwards, cells were washed three times with 1x PBS for 5 min at RT, and incubated with fluorescently-labeled secondary antibody AlexaFluor 568 and AlexaFluor 488 in parallel with DAPI (nuclei visualization) for 45 min at RT in darkness. Subsequently, cells were washed three times with 1x PBS, and antibody stainings were fixed again either with 4% PFA in PBS for 15 min at RT or 100% ice-cold methanol for 90s on ice. Finally, cells were washed once with 1x PBS and kept in 1x PBS until further analysis using an LSM710 laser scanning microscope (Carl Zeiss). Images were acquired using the ZEN 2010 software (Carl Zeiss).

### 3.2.5.7 Immunofluorescence staining of spherically-shaped primary human lung fibroblasts

PhLFs were seeded in a density of  $1.2 \times 10^4$  cells/cm<sup>2</sup> on cell culture dishes and cultured until 95% confluency. Subsequently, cells were washed with 1x PBS, trypsinized with 0.25% Trypsin-EDTA (Gibco), and finally neutralized with 20% DMEM-F12 cell culture media. Afterwards,  $0.2 \times 10^6$  cells were transferred in sterile 2 ml reaction tubes, centrifuged for 5 min at 450g at 4°C, and remaining media was aspirated. Cell pellets were washed with 1x PBS, centrifuged again for 5 min at 450g at 4°C, and PBS was aspirated. Next, cells were resuspended in 4% PFA in PBS for 15 min at RT, centrifuged for 5 min at 450g at 4°C and washed twice with 1x PBS again through centrifugation step. Subsequently, cell pellets were incubated with 5% BSA in 1x PBS for 30 min at RT, and blocking agent was removed through centrifugation for 5 min at 450g at 4°C. Cells were then incubated with antibodies as described under section 3.2.5.6. Cells were kept in 1x PBS until further analysis using an LSM710 laser scanning microscope (Carl Zeiss). Images were acquired using the ZEN 2010 software (Carl Zeiss).

### 3.2.5.8 Live-cell staining

For live-cell staining prior fixation,  $0.2 \times 10^6$  cells were transferred in sterile 2 ml reaction tubes and cell suspension was incubated with Vybrant CFDA Cell Tracker dye (AlexaFluor 488, 1:2000, Molecular Probes) for 15 min at 37°C under humidified condition with 5% CO<sub>2</sub>. Thus, initially colorless Vybrant CFDA Cell Tracker dye passively diffused into live cells and underwent enzymatic conversion by which cell cytosol remained labeled with green color. Immediately afterwards, cell suspension was centrifuged for 5 min at 450g at 4°C, and cell pellets were resuspended and incubated in a fresh 20% DMEM-F12 cell

culture media for 30 min at 37°C under humidified condition with 5% CO<sub>2</sub>. Cell suspension was then centrifuged for 5 min at 450g at 4°C, cell pellets resuspended and washed twice with 1x PBS under centrifugation. Subsequently, cell pellets were fixed, but not permeabilized, with prewarmed 4% PFA in PBS for 15 min at RT, washed twice with 1x PBS as described above, and immunofluorescence staining of spherically shaped phLFs performed with a CDCP1-specific antibody as described in section 3.2.5.7. Cells remained in 1x PBS until further analysis using an LSM710 laser scanning microscope (Carl Zeiss). Images were acquired using the ZEN 2010 software (Carl Zeiss).

### 3.2.5.9 Immunofluorescence staining of paraffin-embedded tissue sections

The paraffin-embedded lung tissue sections from healthy donors and IPF patients were first placed at 60°C overnight followed by tissue deparaffinization and hydration using a Microm HMS 740 Robot-Stainer (Thermo Fisher Scientific). Here, tissue slides were automatically transferred and incubated with different chemicals as described in the Table 3.23.

**Table 3.23: Deparaffinization protocol**

Description	Reagent	Cycles	Time
Deparaffinization step	Xylene	2x	5 min
Hydration step	100% ethanol	2x	2 min
	90% ethanol	1x	1 min
	80% ethanol	1x	1 min
	70% ethanol	1x	1 min
	dH <sub>2</sub> O	1x	30 sec

Afterwards, tissue sections were placed into R-Universal buffer (Aptum Biologics) followed by antigen retrieval in a decloacking chamber (2100 Retrieval, Aptum Biologics) for 20 min with 2 h of cooling down step to complete the program. Subsequently, slides were washed three times in Tris buffer (0.5 M Tris, 1.5 M NaCl, pH 6.8) for 10 min, then incubated in 5% BSA in PBS for 40 min at RT, and subsequently stained with primary antibody against CDCP1, and  $\alpha$ SMA overnight at 4°C under humid conditions. Next day, slides were washed three times in Tris buffer (0.5 M Tris, 1.5 M NaCl, pH 6.8) for 10 min, and subsequently incubated with fluorescently-labeled secondary antibody AlexaFluor 568 and AlexaFluor 488 for 1 h at RT under humid conditions. Following three additional washes, slides were counterstained with DAPI for 10 min at RT, washed again three times in Tris buffer (0.5 M Tris, 1.5 M NaCl, pH 6.8) for 10 min and subsequently let dried at RT. Finally, tissue slides were mounted with Fluorescent Mounting Medium (DAKO) and stored at 4°C until further analysis. Tissue slides were visualized using Axio Imager Microscope (Carl Zeiss) and images acquired using the ZEN 2010 software (Carl Zeiss).

### **3.2.5.10 Flow cytometry**

PhLFs were treated as described in sections 3.2.4.1 or in 3.2.4.2. Cells were then washed with 1x PBS, afterwards detached with 0.25% Trypsin-EDTA and subsequently neutralized with prewarmed 20% DMEM-F12 cell culture media. Next, cell suspension containing  $2.5 \times 10^5$  cells per test was centrifuged for 5 min at 450g at 4°C and cells were once washed with 1x PBS, and MACS buffer. Cells were resuspended and incubated in MACS buffer containing TruStain FcX™ for 10 min at RT. Subsequently, cells were transferred in a 96-well plate with round bottom, centrifuged for 5 min at 450g at 4°C, and afterwards cell pellets stained with PE-conjugated antibodies against PDGFR $\alpha$ , PDGFR $\beta$  (both Biolegend), APC-conjugated CDCP1 antibody (Biolegend), or corresponding isotype controls in the same concentration for 20 min at 4°C. Cells were afterwards washed three times with MACS buffer as described above, fixed with 4% PFA for 15 min at RT, washed once more with MACS buffer and finally 350  $\mu$ l of cell suspension was used for FACS analysis (LSRII, BD). Number of positive cells and median fluorescent intensity were determined using FlowJo software version 9.6.4.

### **3.2.6 RNA expression analysis**

#### **3.2.6.1 RNA isolation**

The peqGOLD Total RNA Kit was used to isolate total RNA from fibroblasts according to the manufacturer's instructions (Peqlab). Total RNA was eluted in 35  $\mu$ l of pre-warmed DNase/RNase-free dH<sub>2</sub>O. The concentration of isolated RNA was determined at a wavelength of 260 nm using NanoDrop 1000.

#### **3.2.6.2 cDNA synthesis by Reverse Transcription**

For cDNA synthesis, 1  $\mu$ g of isolated RNA was first diluted in 18  $\mu$ l of DNase/RNase-free dH<sub>2</sub>O and subsequently subjected for denaturation in an Eppendorf Mastercycler using the following settings: lid=45°C, 70°C for 10 min and 4°C for 5 min. Afterwards, components of the GeneAMP PCR kit (Applied Biosystems) were added to the mix according to Table 3.24, and reverse transcription was carried out in an Eppendorf Mastercycler with the following settings: lid=105°C, 20°C for 10 min, 42°C for 60 min and 99°C for 5 min. Finally, cDNA was diluted in 1:4 ratios with DNase/RNase-free dH<sub>2</sub>O and stored at – 20°C.

**Table 3.24: Mastermix for cDNA synthesis**

Reagent	Stock concentration	Final concentration (40 $\mu$ l)	Final volume ( $\mu$ l)
10x PCR Buffer II	10x	1x	4
MgCl <sub>2</sub> solution	25 mM	5 mM	8
PCR Nucleotide Mix (dNTP)	10 mM	1 mM	4
Random Hexamers	50 $\mu$ M	2.5 $\mu$ M	2
RNase Inhibitor	20 u/ $\mu$ l	1 u/ $\mu$ l	2
MuLV Reverse Transcriptase	50 u/ $\mu$ l	2.5 u/ $\mu$ l	2
Denaturated RNA	-	-	18
Total volume of the mastermix			40

### 3.2.6.3 Quantitative Real-Time Polymerase Chain Reaction (qRT-PCR)

10  $\mu$ l of reaction mix containing cDNA, primer mix, and SYBR green I Master Mix was prepared according to Table 3.25. qRT-PCR was carried out in a LightCycler<sup>®</sup> 480II (Roche) according to the standard PCR protocol summarized in the Table 3.26. Denaturation, annealing and elongation step were repeated in 45 cycles. All qPCR assays were performed in triplicates and relative mRNA expression was normalized to HPRT housekeeper gene expression. Relative transcript abundance of target gene is presented as  $-\Delta C_p$  values ( $-\Delta C_p = C_p^{(\text{target gene})} - C_p^{(\text{housekeeper gene})}$ ).

**Table 3.25: qPCR reaction mix per one assay**

Reagent	Stock concentration	Final concentration	Final volume ( $\mu$ l)
DNase/RNase-free H <sub>2</sub> O	-	-	1
SYBR green I Master Mix	2x	1x	5
Forward/Reverse Primer Mix	10 $\mu$ M each	0.5 $\mu$ M each	2
cDNA	6.25 ng/ $\mu$ l	12.5 ng/ $\mu$ l	2
Total volume of the reaction mix			10

**Table 3.26: Standard qRT-PCR protocol**

Cycle step	Temperature	Duration
Initial denaturation	95°C	5 min
Denaturation	95°C	5 s
Annealing	59°C	5 s
Elongation	72°C	20 s
Melting curve	60 – 95°C	1 min
Cooling down	4°C	on hold

## 4 RESULTS

### Chapter A: TGF $\beta$ regulates cell surface marker expression

The first aim of my thesis was to corroborate the potential effect of TGF $\beta$  on PDGFR $\alpha$  and CDCP1 expression levels and to determine their subcellular localization in pHLFs. To achieve this, cells were treated in the presence or absence of TGF $\beta$  and the expression changes and surface localization of both markers monitored via qRT-PCR, immunoblot, FACS and immunofluorescent microscopy.

#### 4.1 TGF $\beta$ decreases PDGFR $\alpha$ expression in pHLFs

Immunoblot analysis showed a significant downregulation ( $p < 0.01$ ) of PDGFR $\alpha$  protein expression after 48 h of TGF $\beta$  treatment (Figure 4.1 A, B). The efficacy of TGF $\beta$  treatment was confirmed by increased  $\alpha$ SMA protein expression (Figure 4.1 A, C).

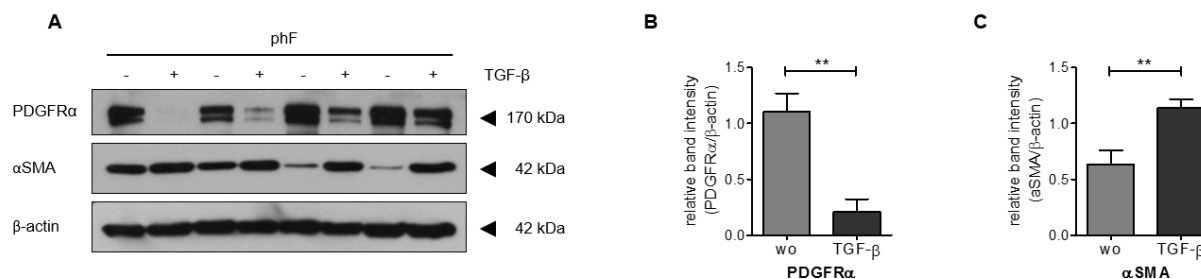


**Figure 4.1: TGF $\beta$  downregulates PDGFR $\alpha$  expression in pHLFs.** (A) Immunoblot analysis of PDGFR $\alpha$  and  $\alpha$ SMA expression in the whole cell lysates upon TGF $\beta$  treatment (1 ng/ml, 48 h). Shown is one representative blot with four biological replicates ( $n=4$ ). (B, C) Densitometric quantification of eight biological replicates ( $n=8$ ) was used to determine PDGFR $\alpha$ / $\beta$ -actin and  $\alpha$ SMA/ $\beta$ -actin ratio. Data shown as mean  $\pm$  SEM. Statistical analysis: Paired two-tailed t-test. \*\* $p$ -value  $< 0.01$ .

To further investigate whether downregulation of PDGFR $\alpha$  whole protein levels also impacts cell surface localization, FACS analysis was used to determine the percentage of PDGFR $\alpha$ -positive cells upon TGF $\beta$  treatment. Here, TGF $\beta$ -treated cells displayed a significant decrease in the percentage of PDGFR $\alpha$ -positive cells ( $7.4\% \pm 10.1$ ) when compared to non-treated cells ( $33.7\% \pm 11$ ). In contrast, the numbers of PDGFR $\beta$  positive cells significantly increased by TGF $\beta$  treatment ( $81.4\% \pm 8.1$ ) compared to non-treated cells ( $52.2\% \pm 13.8$ ) (Figure 4.2 A, B). Likewise, the same pattern was observed for the median fluorescence intensity

(MFI) values, which decreased for PDGFR $\alpha$  ( $71.0 \pm 30.0$  to  $16.0 \pm 14.0$ ) and increased for PDGFR $\beta$  ( $211.0 \pm 113.0$  to  $550.0 \pm 263.0$ ) among all cells (Figure 4.2 C).

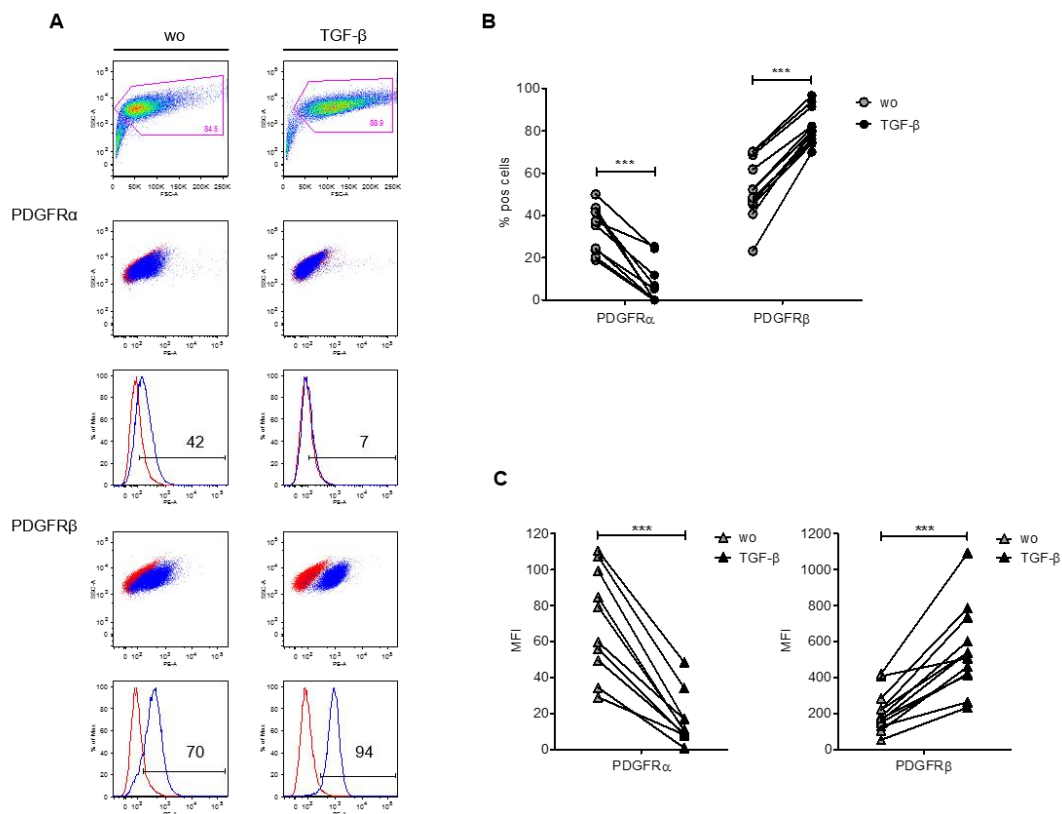


**Figure 4.2: TGF $\beta$  decreases PDGFR $\alpha$  expression on the surface of phLFs.** FACS analysis was used to determine the percentage of PDGFR $\alpha$  and PDGFR $\beta$  positive cells in the presence or absence of TGF $\beta$  (1 ng/ml, 48 h). (A) Histogram and dot blot with the isotype control labeled in red and the PDGFR $\alpha$ - or PDGFR $\beta$ -positive population in blue. (B) Quantification of PDGFR $\alpha$ - and PDGFR $\beta$ -positive cells from (A) as a summary of ten to twelve independent experiments with mean  $\pm$  SD (n=10-12). (C) The respective median fluorescence intensity (MFI) values ( $\Delta$ MFI) were calculated by the subtraction of the isotype MFI values. Shown is a summary of MFI values for PDGFR $\alpha$ , PDGFR $\beta$  and isotype control from ten to twelve independent experiments (n=10-12). Statistical analysis: Paired two-tailed t-test. \*\*\*p-value < 0.001.

#### 4.2 TGF $\beta$ downregulates CDCP1 expression in phLFs

CDCP1 has never been described in human lung fibroblasts to date. We therefore first examined its expression and localization in phLFs via immunofluorescence stainings. Here, I demonstrated for the very first time CDCP1's cells surface expression (Figure 4.3 A), as well as co-localization with CD90 (Thy-1), a commonly accepted cell surface marker for mesenchymal cells. This was observed on the surface of PFA-fixed cell monolayers (Figure 4.3 B) as well as on the surface of detached, and thus spherically shaped lung

fibroblasts (Figure 4.3 C). To further support this observation, trypsinized phLFs were labeled with Vybrant® CFDA SE intracellular dye, and the surface localization of CDCP1 imaged via 3-dimensional z-stack sections (Figure 4.3 D).

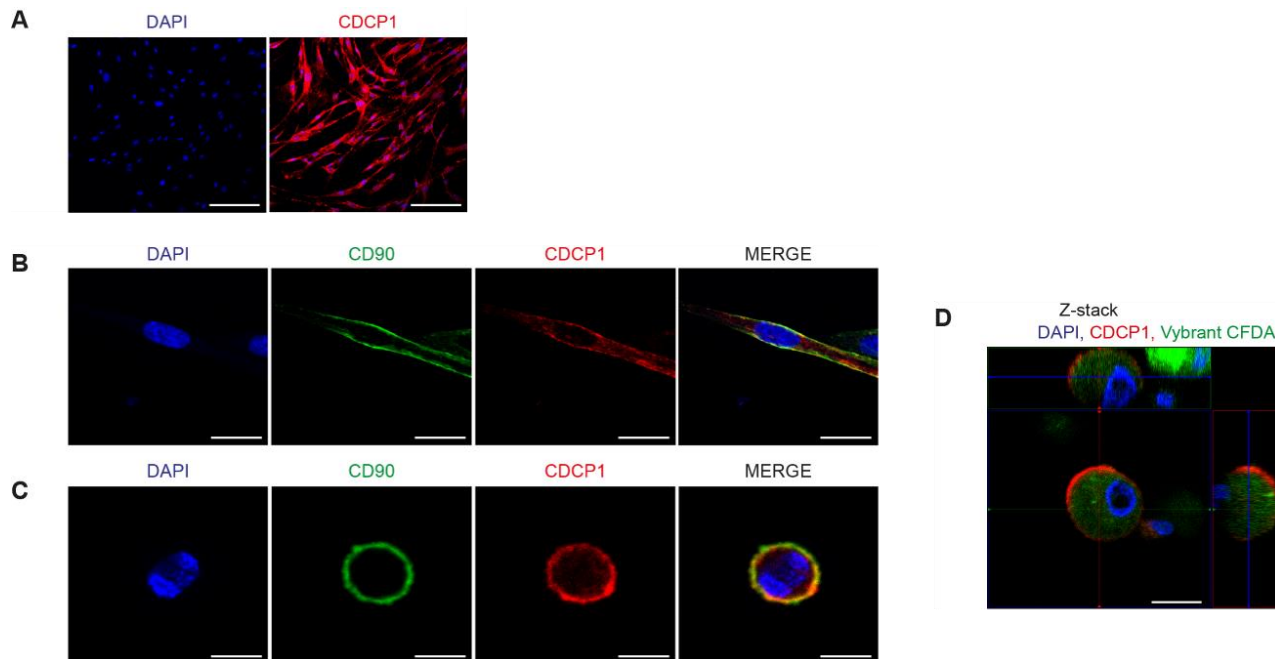


**Figure 4.3: CDCP1 co-stains with CD90 (Thy-1) on the surface of phLFs.** Representative stainings of monolayer phLFs (A) single stained with CDCP1 (red) or (B) double-stained with CDCP1 (red) and CD90 (green). (C) Representative stainings of spherically shaped phLFs double-stained with CDCP1 (red) and CD90 (green). (D) Orthoview of a confocal z-stack section demonstrating spherically shaped phLFs labeled intracellularly with Vybrant CFDA dye (green) and on the cell surface immunostained with CDCP1 (red). In each case, cell nuclei were counterstained with DAPI (blue). Images are presented as one representative staining of three technical replicates from three independent experiments (n=3). Scale bars: (A) 200  $\mu$ m, (B) 10  $\mu$ m, (C) 20  $\mu$ m, (D) 10  $\mu$ m.

Next, I analyzed the effect of TGF $\beta$  on CDCP1 expression in general and determined the timepoint of significant expression change. TGF $\beta$  significantly decreased CDCP1 on mRNA (2.9-fold) and protein (2.8-fold) levels as shown by qRT-PCR (Figure 4.4 C) and immunoblot (Figure 4.4 D, E) analysis, respectively. The efficacy of TGF $\beta$  treatment was confirmed by increased gene (Figure 4.4 C) and protein (Figure 4.4 A, B and D) expression of  $\alpha$ SMA. Further, downregulation of CDCP1 protein was first observed after 24 h and the strongest effect after 48 h (Figure 4.4 A, B). Furthermore, TGF $\beta$ -treated cells displayed a significant decrease in the percentage of CDCP1-positive cells ( $73.5\% \pm 14.8$ ) compared to non-treated cells ( $85.7\% \pm 10.0$ ) as shown by FACS analysis (Figure 4.4 E, F). Similarly, the median fluorescence intensity (MFI)

values significantly decreased for CDCP1 among all cells ( $1559.1 \pm 1172.0$  to  $585.9 \pm 351.2$ ) ( $p < 0.05$ ) in the presence of TGF $\beta$  for 48 h (Figure 4.4 F).

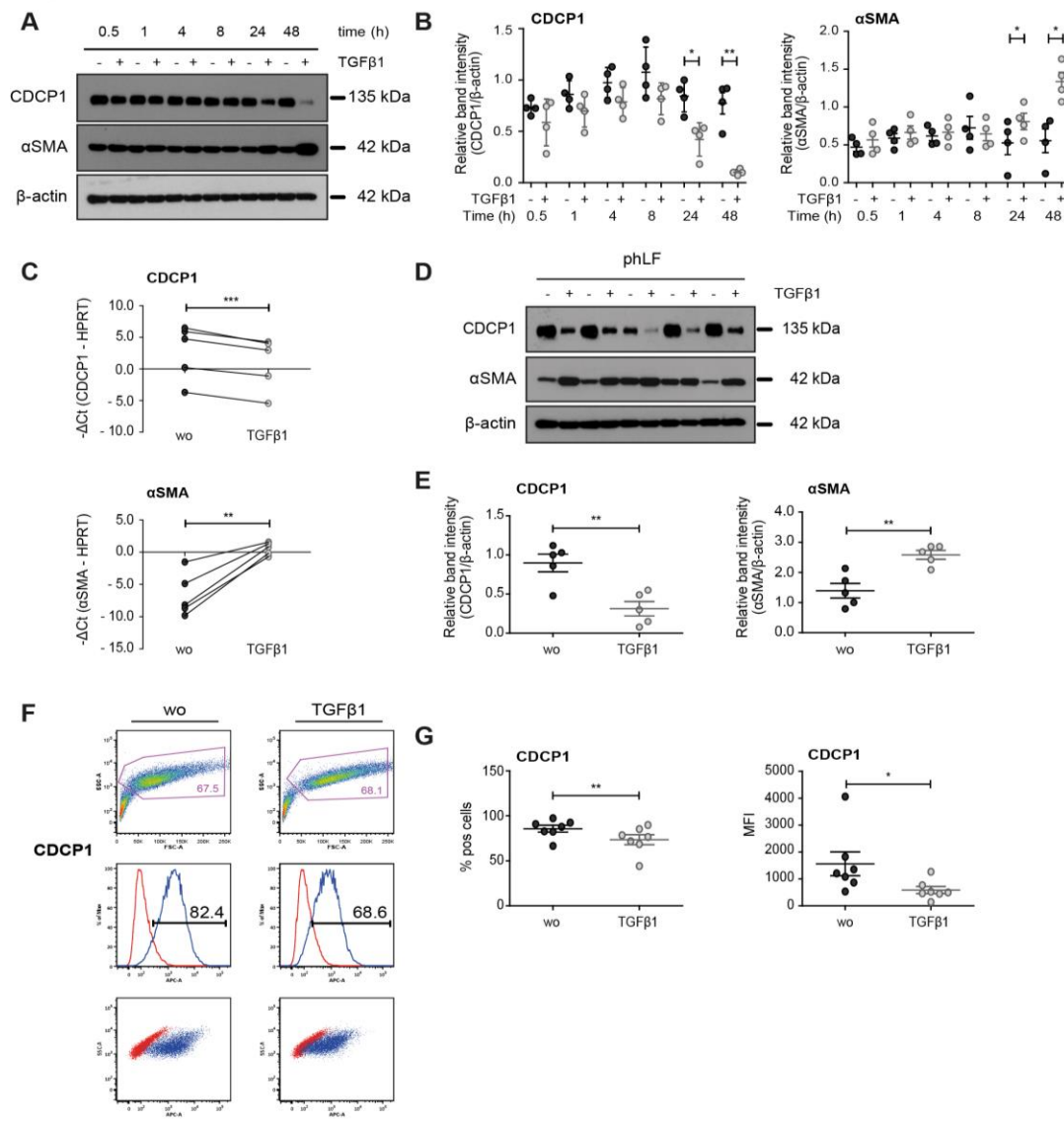


**Figure 4.4: CDCP1 is downregulated by TGF $\beta$  in phLFs.** (A) Immunoblot analysis of CDCP1 and  $\alpha$ SMA expression in the whole cell lysates treated with 1 ng/ml TGF $\beta$  at indicated time points. Shown is one representative blot out of four independently performed experiments ( $n=4$ ). (B) Densitometric quantification from (A) presented as mean  $\pm$  SEM. (C) qRT-PCR and (D) immunoblot analysis of CDCP1 and  $\alpha$ SMA expression from phLFs treated with TGF $\beta$  for 48 h. HPRT was used as a housekeeping gene. (E) Densitometric analysis of CDCP1 and  $\alpha$ SMA expression from (D) depicted as mean  $\pm$  SEM from five independent experiments ( $n=5$ ). (F) FACS analysis evaluating changes in the percentage of CDCP1 positive cells in the presence or absence of TGF $\beta$  for 48 h. Representative histograms and dot plots are shown. The isotype control is depicted in red and the CDCP-positive cell population in blue. (E) Percentage of CDCP1-positive cells (left graph) shown as a summary of seven independent experiments with mean  $\pm$  SEM ( $n=7$ ). The median fluorescence intensity (MFI) values (right graph) were calculated by subtraction of the MFI

values from isotype control. Data were obtained from seven independent experiments (n=7). Statistical analysis for each experiment: Paired two-tailed t-test. \*\*\*p-value<0.001, \*\*p-value < 0.01, \*p-value < 0.05.

## **Chapter B: Functional consequence of altered surface marker expression**

Fibroblasts are the most important cell types producing ECM in the lung. TGF $\beta$  induces fibroblast-myofibroblast transdifferentiation, which leads to  $\alpha$ SMA-expressing myofibroblasts with increased ECM secretion. Nevertheless, little is known about specific receptors controlling this process beside TGF $\beta$  receptors. PDGF receptors and their signaling are well-known to play a role in IPF. On the other hand, the role of CDCP1 in lung fibroblasts and IPF has never been described to date. Thus, in the second part of my thesis I aimed to investigate a functional consequence of altered PDGFR $\alpha$  and CDCP1 expression by TGF $\beta$  in lung fibroblasts and IPF, particularly in the context of myofibroblasts activation and ECM production.

### **4.3 Characterization of PDGF signaling in lung fibroblasts and analysis of potential cross-talk to TGF $\beta$ signaling**

#### **4.3.1 PDGF ligands promote downstream PDGF signaling in lung fibroblasts**

To study the effect of single PDGF ligands on PDGF signaling in phLFs, cells were stimulated with PDGF-AA, PDGF-AB, PDGF-CC, or PDGF-DD in a dose- and time-dependent manner, and phosphorylation levels of Akt (pAkt), a downstream mediator of PDGF signaling, assessed via immunoblot. Increased pAkt levels were already observed with 10 ng/ml for each ligand (Figure 4.5 A). The strongest increase was detected by PDGF-AB and PDGF-DD stimulation after 40 min (Figure 4.5 B), indicating that these two ligands mainly drive the signaling in phLFs

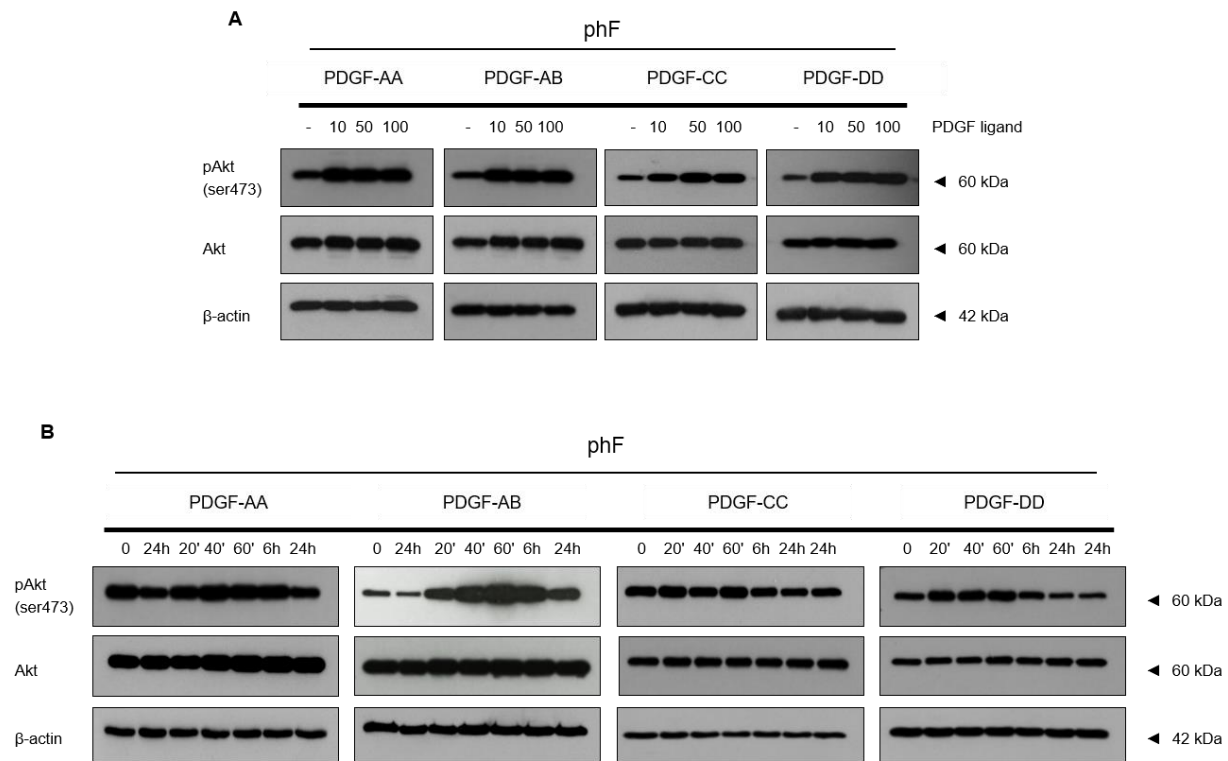


**Figure 4.5: PDGF signaling in human lung fibroblasts.** PhLFs were treated with PDGF ligands (A) in a concentration-dependent manner and (B) over time as indicated above and the phosphorylation and total levels of Akt in the whole protein lysates determined via immunoblot. (B) Of note, time points 0 and 24 h (for PDGF-AA and -AB interpreted in the first and second band; for PDGF-CC and -DD interpreted in the first and last band) were used to monitor pAkt levels under non-stimulated conditions. As this was a pilot test, the experiment was performed only once (n=1).

#### 4.3.2 PDGF-AB increases invasion properties of primary human lung fibroblasts

PDGF signaling has been described to be involved in cellular processes, such as invasion and proliferation [Heldin, 2013; Oehrle et al., 2015]. To investigate whether PDGF ligand-specific signaling, affects invasion properties of phLFs, we seeded phLFs on the top of a collagen G matrix, serum starved overnight, and subsequently left for invading into a matrix after incubation with 10 ng/ml of PDGF-AA, PDGF-AB, and PDGF-DD for 48 h (Figure 4.6 A).

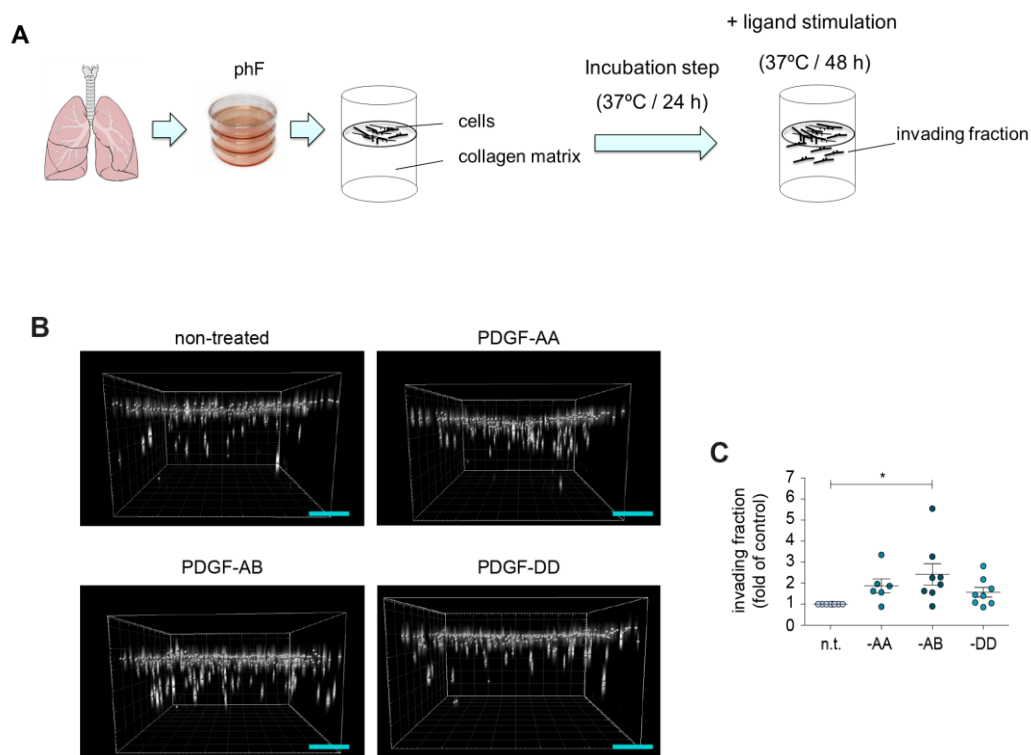


**Figure 4.6: PDGF-AB signaling plays a role in invasion properties of pHLFs.** (A) A schematic illustration of a 3D collagen invasion assay. (B) Spot analysis of invading pHLFs presented as snapshot image. The non-invasive population remained on the top of a collagen matrix whereas invading cells can be found within the collagen matrix. Scale bar: 10 μm. (C) Quantification and statistical analysis of six to eight independent experiments is presented as mean ± SEM (n=6-8). Statistical analysis: One-way ANOVA with Dunnett's multiple comparison test. \*p-value < 0.05 in comparison to non-treated control (n.t.).

All PDGF ligands led to an increase in cell invasion into the matrix (Figure 4.6 B, C) with a significant effect ( $p < 0.05$ ) observed for PDGF-AB (Figure 4.6 C). This indicates a role of PDGF-AB signaling in the invasion properties of lung fibroblasts in a ligand-receptor specific manner.

#### 4.3.3 PDGF-AB and PDGF-DD enhance PDGF signaling independently of TGFβ

To study whether TGFβ affects downstream PDGF signaling in pHLFs, we treated cells with TGFβ for 48 h followed by PDGF-AB and PDGF-DD ligand stimulation for 40 min and analyzed the changes in Akt phosphorylation via immunoblot. TGFβ alone led to a slight increase in pAkt levels compared to non-treated cells, whereas PDGF-AB and PDGF-DD led to a significant increase of pAkt ( $p < 0.05$  for PDGF-AB and  $p < 0.001$  for PDGF-DD). Interestingly, the effect by TGFβ was reversed when additionally stimulated with either PDGF-AB or PDGF-DD (Figure 4.7 A-C).

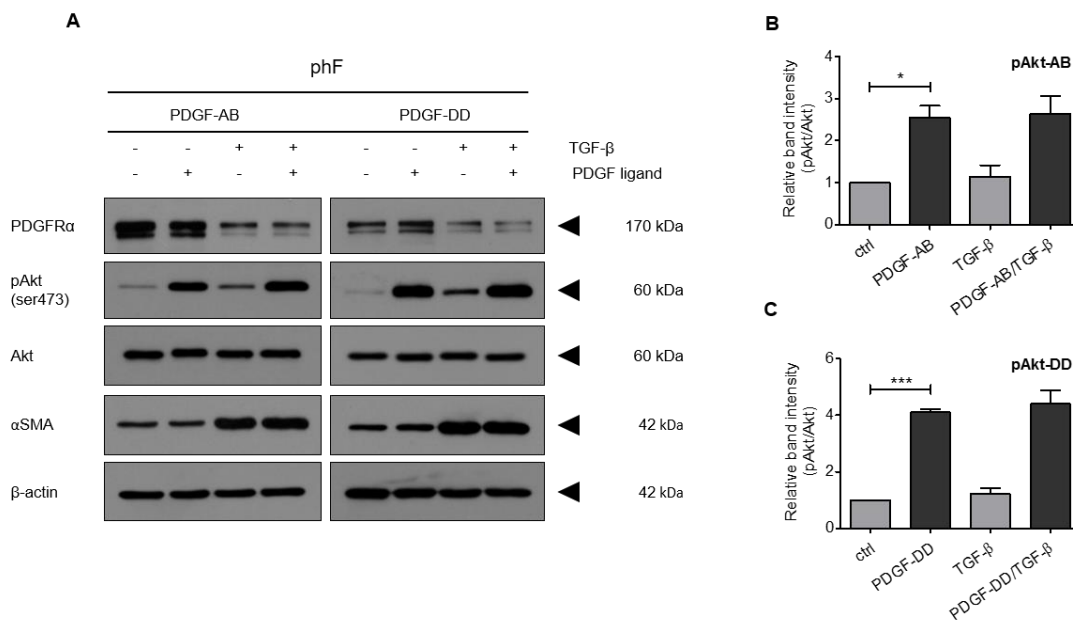


**Figure 4.7: PDGF-AB and PDGF-DD enhance PDGF signaling independently of TGF $\beta$ .** (A) Immunoblot analysis of whole cell lysates from pHLFs treated with 1 ng/ml TGF $\beta$  (48 h) followed by stimulation with 10 ng/ml PDGF-AB and PDGF-DD ligands (40 min). (B, C) Densitometric quantification of four independent biological replicates (n=4) was used to determine pAkt/Akt ratio. Data are shown as mean  $\pm$  SEM. Statistical analysis: Paired two-tailed t-test. \*\*\*p-value < 0.001, \*p-value < 0.05.

#### 4.3.4 PDGF signaling is increased in the absence of PDGFR $\alpha$

Furthermore, I wanted to explore if a specific ligand-receptor interaction mainly activates downstream Akt signaling in lung fibroblasts. To do so, I performed siRNA-mediated silencing of PDGFR $\alpha$ , PDGFR $\beta$ , or both receptors in combination and analyzed pAkt in the presence/absence of different PDGF ligands. Knockdown efficiency was controlled by FACS, qPCR and immunoblot. We first determined decreased receptor levels on the surface after knockdown by FACS analysis to exclude any receptor recycling back to the surface which could still lead to further signaling. Receptor-specific knockdown decreased the receptor surface levels accordingly (Figure 4.8 A, B). Interestingly, the knockdown of PDGFR $\alpha$  intend to increase the number of PDGFR $\beta$  positive cells (Figure 4.8 A, B). In addition, qPCR and immunoblot analysis revealed an effective knockdown of PDGFR $\alpha$  and PDGFR $\beta$  on total mRNA (Figure 4.8 C) and protein levels (Figure 4.8 D) after 48 h.

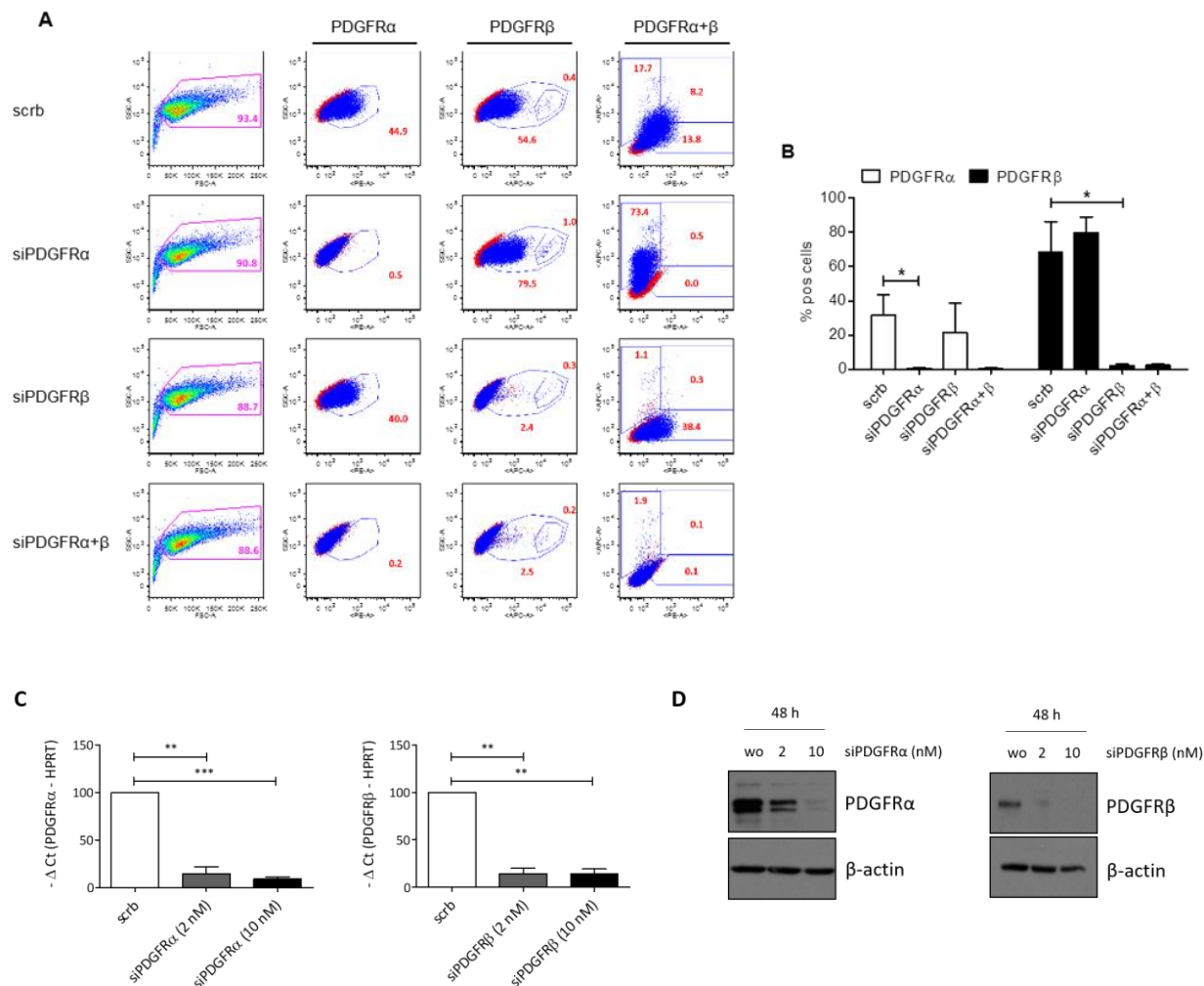


**Figure 4.8: Knockdown of PDGFR $\alpha$  and PDGFR $\beta$  decreases their expression in pHLFs.** (A) siRNA-mediated knockdown of PDGFR $\alpha$ , PDGFR $\beta$ , or both (10 nM, 48 h) followed by FACS analysis was used to confirm the surface localization of the receptors in pHLFs. Shown is a representative dot blot with the isotype control labeled in red and the PDGFR $\alpha$ - and PDGFR $\beta$ -positive population in blue. (B) Summary of FACS data from three independent biological experiments (n=3) with mean  $\pm$  SD. (C) qPCR and (D) immunoblot analysis of PDGFR $\alpha$  and - $\beta$  levels from pHLFs reversely transfected with 2 or 10 nM of scrambled and PDGFR $\alpha$  or PDGFR $\beta$ -specific siRNA for 48 h. (C) Data are presented as mean  $\pm$  SEM from three independent experiments (n=3). (D) Shown is one representative blot from three different experiments (n=3). Statistical analysis: Paired two-tailed t-test. \*p-value < 0.05, \*\*p-value < 0.01, \*\*\*p-value < 0.001. scrb = scrambled.

Next, we analyzed the ligand-receptor specific activation and compared this to TGF $\beta$  induced effects. As expected, PDGF-AB and PDGF-DD stimulation increased pAkt levels in scrambled conditions, which was also observed when cells were stimulated with TGF $\beta$  (Figure 4.9 A, B). On the other hand, knockdown of PDGFR $\alpha$  under basal, scrambled conditions led to a significant increase in pAkt levels, which was not observed after PDGFR $\beta$  knockdown (Figure 4.9 A). In line with the previous experiment, knockdown of

PDGFR $\alpha$  led to a significant increase ( $p < 0.05$ ) in total protein expression of PDGFR $\beta$  under basal (wo) as well as PDGF-AB, but not PDGF-DD stimulation (Figure 4.9 A, F). This indicates that a potential regulatory effect between the two receptors exists in phLFs.

In the presence of PDGF-AB ligand, PDGFR $\alpha$ -depleted cells displayed a decrease in pAkt levels, whereas PDGFR $\beta$ -depleted cells showed a decrease in pAkt in the presence of PDGF-DD ligand., These data indicate a binding preference of PDGF-AB towards PDGFR $\alpha$  and PDGF-DD towards PDGFR $\beta$  receptor (Figure 4.9 A). Interestingly, knockdown of PDGFR $\alpha$  enhanced pAkt levels when cells had been pre-stimulated with TGF $\beta$  (Figure 4.9 B, D).

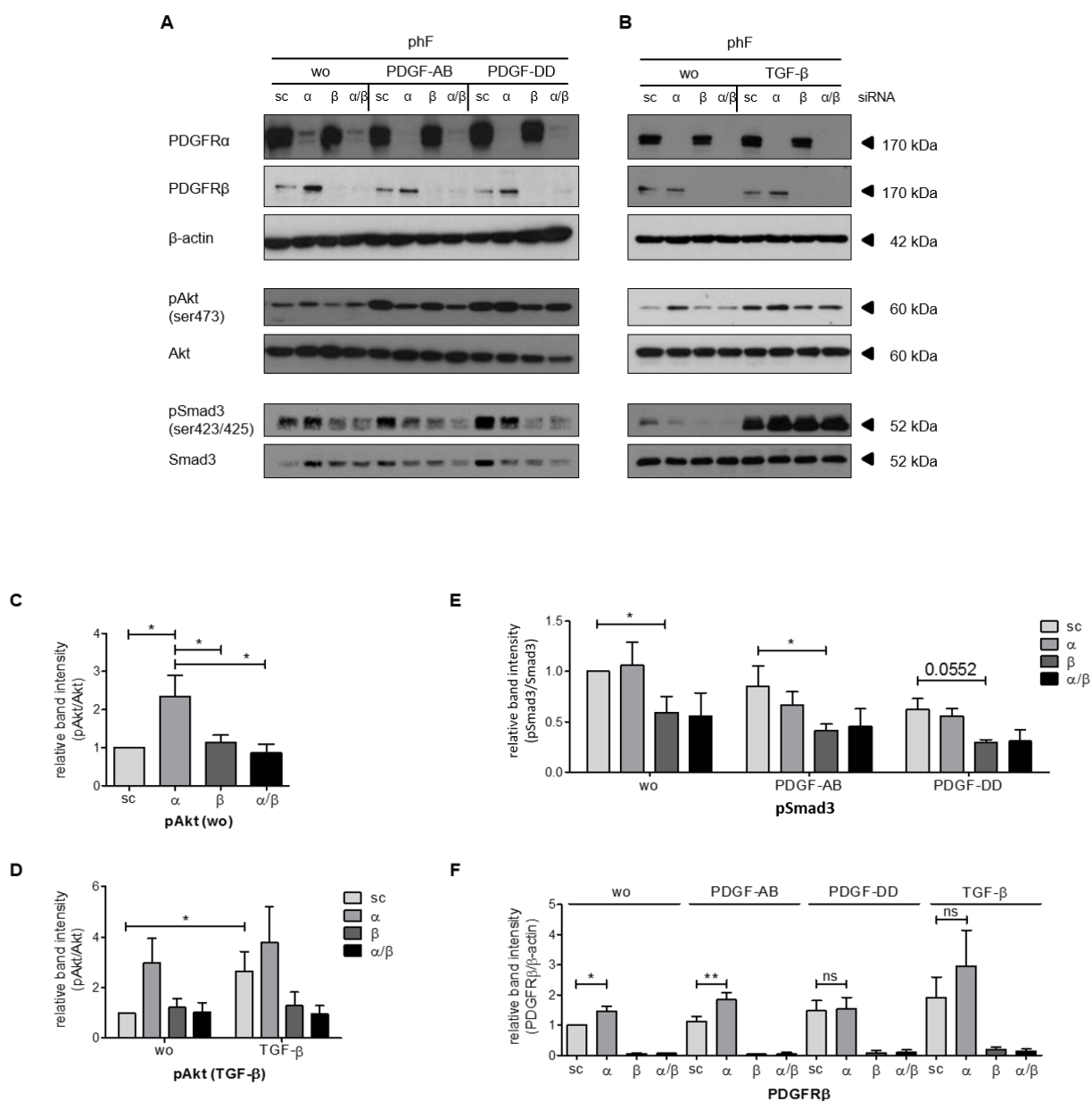


**Figure 4.9: PDGF ligands enhance PDGF signaling in the absence of PDGFR $\alpha$ .** Immunoblot analysis of PDGFRs, pAkt, and pSmad3 in whole protein lysates obtained from reversely transfected pHLFs with siRNAs against PDGFR $\alpha$ , PDGFR $\beta$ , or both for 48 h and subsequently stimulated with (A) 10 ng/ml of PDGF-AB and PDGF-DD or (B) 1 ng/ml TGF $\beta$  for 40 min. One representative blot out of six independent biological experiments is shown (n=6). (C-F) Densitometric quantification of pAkt/Akt, pSmad3/Smad3 and PDGFR $\beta$ / $\beta$ -actin ratio is shown as mean  $\pm$  SEM. (C) For statistical analysis of pAkt in non-treated cells (wo), six technical replicates of reloaded samples together with six independent biological experiments were used (n=6) and a paired two-tailed t-test was performed. (D) For statistical analysis of pAkt in the presence of TGF $\beta$ , a two-way ANOVA with Bonferroni post-test was used for six independent biological replicates (n=6). (E, F) For statistical analysis of pSmad3 and PDGFR $\beta$ , a paired two-tailed t-test was used (comparison of single columns). \*\*p-value < 0.01, \*p-value < 0.05, ns = not significant.

Additionally, I tested whether downstream PDGF signaling interferes with TGF $\beta$  pathway which was achieved by analyzing Smad3 phosphorylation (pSmad3), a downstream mediator of canonical TGF $\beta$  signaling. TGF $\beta$  alone enhanced pSmad3 as expected (Figure 4.9 B). Knockdown of PDGFR $\beta$  significantly decreased pSmad3 without ligand stimulation and in the presence of PDGF-AB (p<0.05) (Figure 4.9 A), with a similar trend observed for PDGF-DD stimulation.

Taken together, my data indicate that TGF $\beta$  seems to increase Akt phosphorylation levels in lung fibroblasts under basal conditions via a non-canonical TGF $\beta$  pathway (Figure 4.9 D). On the other hand, absence of PDGFR $\beta$  attenuated downstream TGF $\beta$  signaling under basal conditions as well as in the presence of ligands (Figure 4.9 E) indicating that a potential cross-talk between PDGF and TGF $\beta$  signaling exists.

#### 4.3.5 The activity of tyrosine kinase inhibitor is attenuated in the absence of PDGFR $\alpha$

We further wanted to analyze if inhibiting the PDGF receptors for ligand binding would lead to the opposite effect of downstream signaling observed. Two different potent tyrosine kinase inhibitors, Imatinib mesylate and Nintedanib, were used and the effective concentration first determined by stimulating pHLFs in a dose-dependent manner for 30 min followed by stimulation with PDGF-AB, PDGF-DD, and TGF $\beta$  for 40 min. Immunoblotting analysis showed that increased concentrations of both inhibitors decreased pAkt levels in a PDGF ligand independent way (Figure 4.10 A, B). Importantly, PDGFR $\alpha$  and PDGFR $\beta$  expression as well as Smad3 phosphorylation remained unaffected in the presence of both inhibitors (Figure 4.10 A-D).

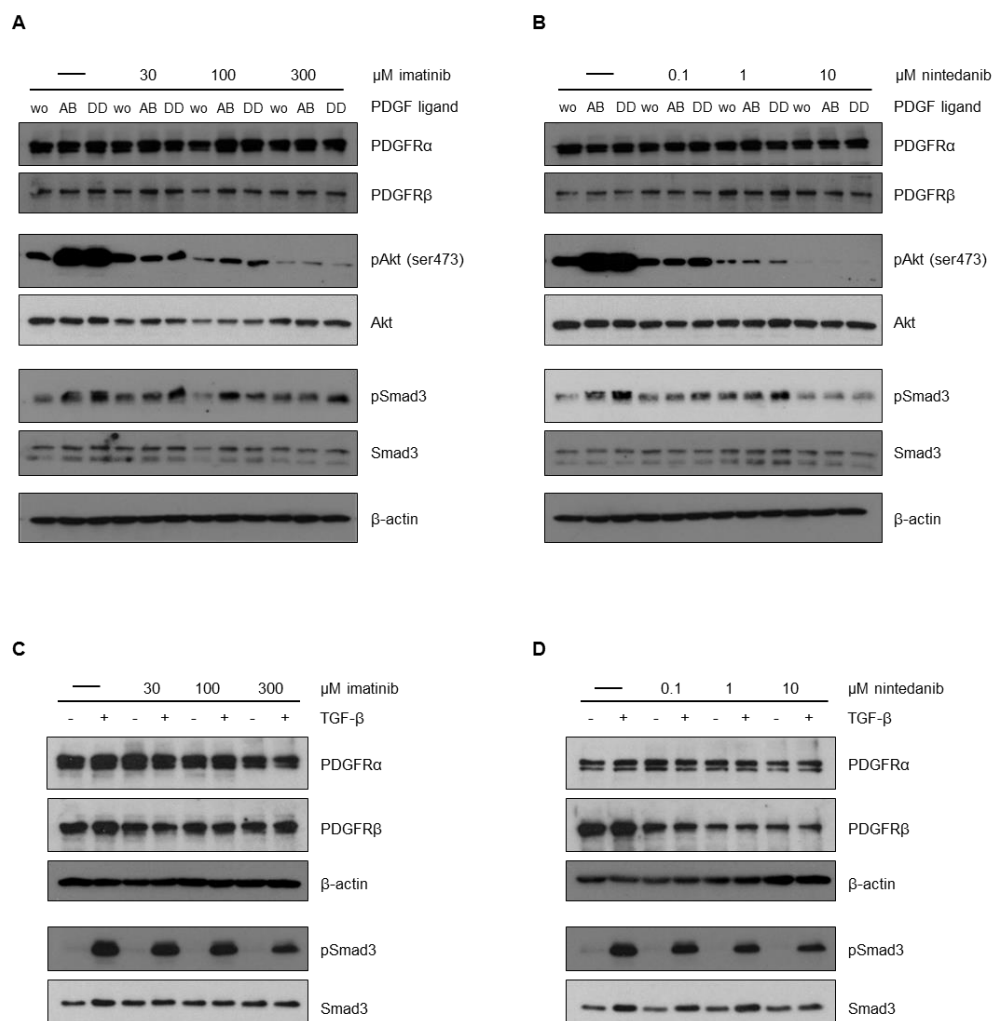


**Figure 4.10: Imatinib and Nintedanib block PDGF signaling in phLFs.** Immunoblot analysis of PDGFR $\alpha$  and - $\beta$  expression, and Akt and Smad3 phosphorylation in the whole protein lysates treated with increased doses of (A) Imatinib and (B) Nintedanib for 30 min followed by PDGF-AB and PDGF-DD (10 ng/ml) or TGF $\beta$  (1 ng/ml) stimulation for 40 min. Shown is one representative blot of three biological replicates (n=3).

Since a stronger effect on Akt phosphorylation was observed when treating cells with Nintedanib compared to Imatinib, we continued and further addressed the effect of Nintedanib on PDGF signaling in the presence or absence of PDGF receptors. To do so, phLFs were reverse transfected with siRNA against PDGFR $\alpha$ , PDGFR $\beta$ , or both receptors for 48 h, and afterwards treated with Nintedanib for 30 min followed by PDGF-AB or PDGF-DD and TGF $\beta$  stimulation for 40 min. Basal pAkt (scrambled) levels under normal or PDGF-AB or TGF $\beta$  conditions were decreased by Nintedanib. This effect was, however, less pronounced for PDGF-DD (Figure 4.11 A, B). Interestingly, Nintedanib did not attenuate the increase in Akt

phosphorylation of PDGFR $\alpha$ -depleted cells (Figure 4.11 A). This indicates that the inhibitory effect of Nintedanib is abrogated in the absence of PDGFR $\alpha$  receptor.

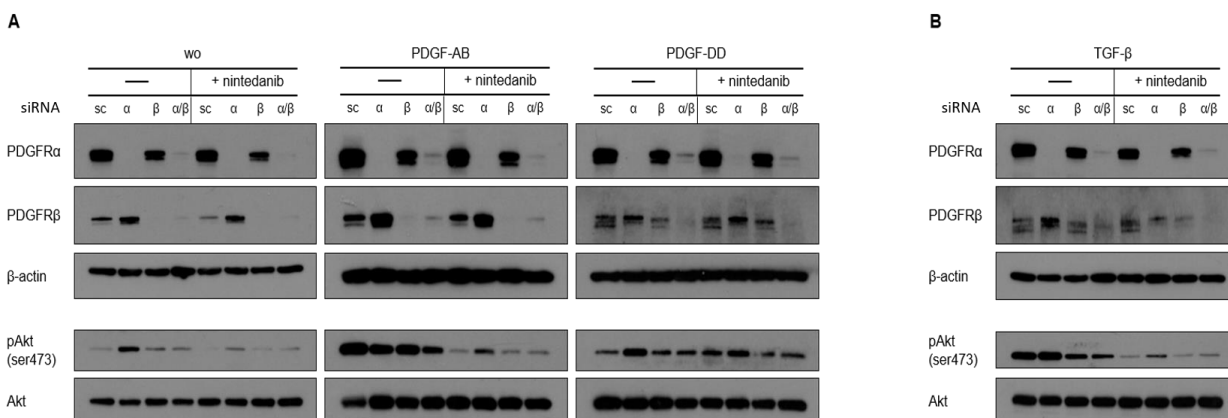


**Figure 4.11: The absence of PDGFR $\alpha$  receptor diminishes inhibitory effect of Nintedanib on PDGF signaling.** Knockdown of PDGFR $\alpha$ , PDGFR $\beta$ , or both (10 nM) was performed for 48 h. Cells were treated with 1  $\mu$ M Nintedanib for 30 min followed by (A) PDGF-AB or PDGF-DD (10 ng/ml), and (B) TGF $\beta$  (1 ng/ml) stimulation for 40 min. The effect of Nintedanib on PDGF signaling in the presence or absence of PDGFRs was analyzed by immunoblot. Shown is one representative blot of six biological replicates (n=6).

#### 4.3.6 Knockdown of PDGFR $\alpha$ together with TGF $\beta$ increases myofibroblasts differentiation and ECM production

To investigate the significance of PDGFR $\alpha$  in myofibroblasts differentiation and the effect of Nintedanib, we analyzed ECM expression and secretion in phLFs after reverse transfection with siRNA against PDGFR $\alpha$  for 48 h, and subsequent stimulation with TGF $\beta$  alone or in combination with Nintedanib for additional 48 h. Expression changes of  $\alpha$ SMA and the selected ECM components fibronectin, collagen I, collagen III, and collagen V were analyzed via immunoblot. Protein levels of fibronectin, collagen I, collagen V, and  $\alpha$ SMA were increased by TGF $\beta$ , however, no change was observed for collagen III (Figure 4.12 A). Interestingly, PDGFR $\alpha$ -depleted cells displayed an increase in  $\alpha$ SMA and collagen V expression, which was even more prominent in the presence of TGF $\beta$  (Figure 4.12 A). Also, increased secretion of collagen V by PDGFR $\alpha$ -depleted myofibroblasts was detected in the presence of TGF $\beta$  (Figure 4.12 B). Next, the impact of Nintedanib on ECM changes in PDGFR $\alpha$ -depleted myofibroblasts was addressed. Knockdown of PDGFR $\alpha$  led to a strong increase in  $\alpha$ SMA and collagen V expression in the presence of Nintedanib. In addition, the inhibitory effect of Nintedanib was lost in the presence of TGF $\beta$  for  $\alpha$ SMA and collagen V, as their expression levels were still detectable. This effect was even more prominent in the absence of PDGFR $\alpha$  (Figure 4.12 A).

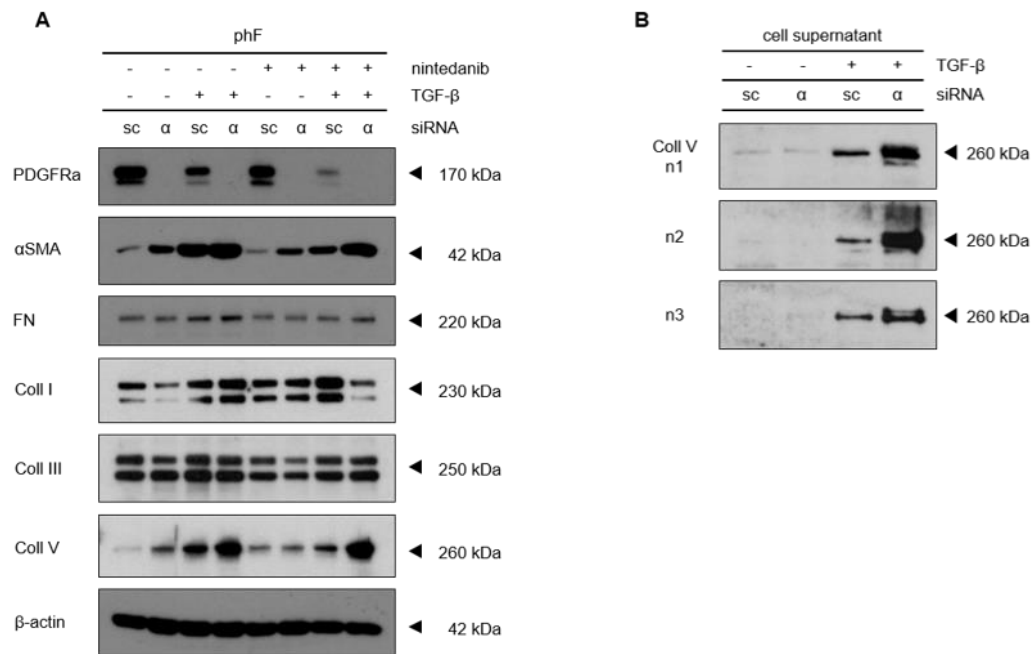


**Figure 4.12: Knockdown of PDGFR $\alpha$  enhances  $\alpha$ SMA and collagen V expression.** (A) Immunoblot analysis of PDGFR $\alpha$ ,  $\alpha$ SMA and selected ECM components in whole cell lysates from phLFs reversely transfected with 10 nM of siPDGFR $\alpha$  for 48 h, and in parallel stimulated with TGF $\beta$  (1 ng/ml) and Nintedanib (1  $\mu$ M) for additional 48 h. Shown is one representative Western blot of three biological replicates (n=3). (B) Immunoblot analysis of collagen V secretion in cell supernatants obtained from PDGFR $\alpha$ -depleted cells treated with or without 1 ng/ml TGF $\beta$  for 48 h. Shown are three immunoblots from three different biological experiments (n=3).

Taken together, my data indicate that PDGFR $\alpha$  negatively controls TGF $\beta$ -mediated myofibroblasts transdifferentiation, and enhanced ECM expression and that the inhibitory effect of Nintedanib is lost in the presence of TGF $\beta$ .

#### 4.4 Identifying the role of CDCP1 in myofibroblast differentiation of human lung fibroblasts

I next investigated whether CDCP1 controls different profibrotic or antifibrotic properties of lung fibroblasts.

##### 4.4.1 SiRNA-mediated silencing of CDCP1 affects its cell surface and total protein levels in phLFs

For functional studies, we performed siRNA-mediated silencing of CDCP1 in phLFs and analyzed knockdown stability on protein level for 24, 48 and 72 hours by immunoblotting and FACS. The percentage of CDCP1-positive cells significantly decreased ( $p < 0.001$ ) after 48 h (Figure 4.13 A, B). Likewise, the MFI

values from the knockdown cells significantly declined ( $p < 0.05$ ) for CDCP1 among all cells (Figure 4.13 B), indicating an efficient surface depletion of CDCP1. Moreover, immunoblot analysis revealed an effective CDCP1 protein depletion after 48 h and 72 h. Interestingly,  $\alpha$ SMA protein levels increased in CDCP1-depleted cells (Figure 4.13 C).

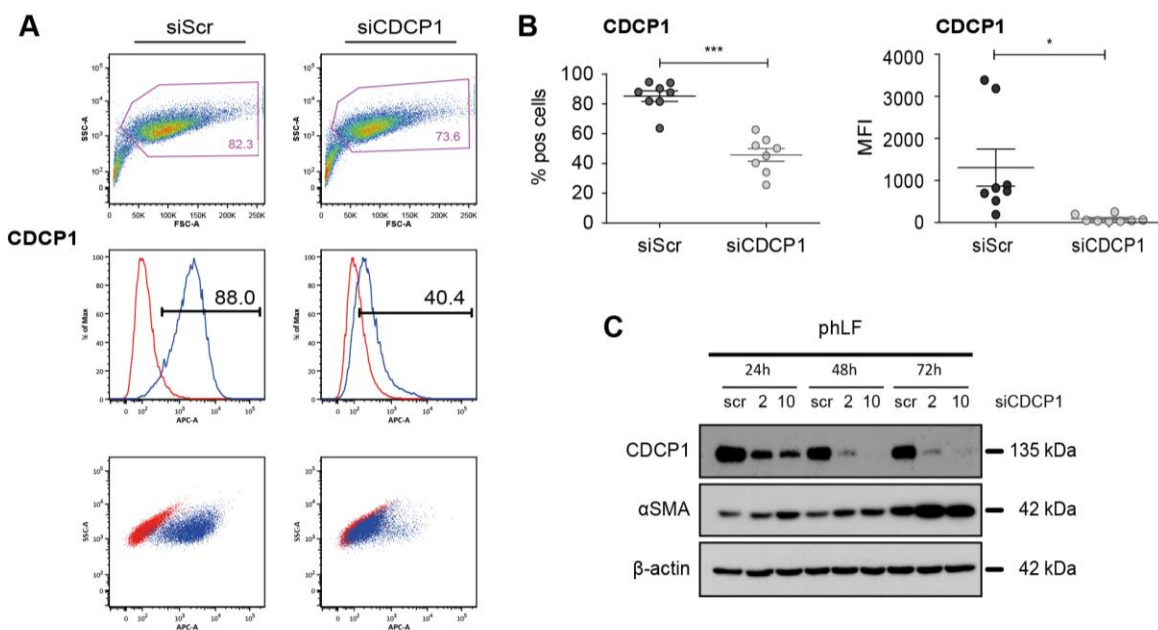


**Figure 4.13: Silencing of CDCP1 decreases its cell surface and total protein levels.** (A) The percentage of CDCP1-positive cells from phLFs incubated for 48 h with scrambled and CDCP1-specific siRNA was determined by FACS. Isotype control is labeled in red and CDCP1-positive cells in blue as shown in histogram and dot blot analysis. (B) Changes in the percentage of CDCP1-positive cells (left graph) and MFI values (right graph) after CDCP1 silencing for 48 h are presented as a summary of eight independent experiments with mean  $\pm$  SEM ( $n=8$ ). Statistical analysis: Paired two-tailed t-test. \*\*\* $p$ -value  $< 0.001$ , \* $p$ -value  $< 0.05$ . (C) Immunoblot analysis of CDCP1 and  $\alpha$ SMA levels from whole protein lysates reversely transfected with 2 or 10 nM of scrambled and CDCP1-specific siRNA for 24 h, 48 h, and 72 h. Shown is one representative blot from three different experiments ( $n=3$ ).

#### 4.4.2 CDCP1 inhibits cell adhesion of phLFs

CDCP1 plays an essential role in regulating cell adhesion of certain cancer cell lines to the ECM [Deryugina et al., 2009; Uekita et al., 2008b]. I therefore wanted to investigate if CDCP1 modulates cell adhesion of phLFs, and if this might be dependent on TGF $\beta$ . Therefore, phLFs were reversely transfected with siRNA against CDCP1, and subsequently treated with TGF $\beta$  for 48h. Absence of CDCP1 led to a slight increase in the adhesion capacity of lung fibroblasts when compared to control siRNA-transfected cells (Figure 4.14 A,

B), and this effect was even more pronounced when siRNA-mediated knockdown of CDCP1 was followed by TGF $\beta$  stimulation (Figure 4.14 A, B).

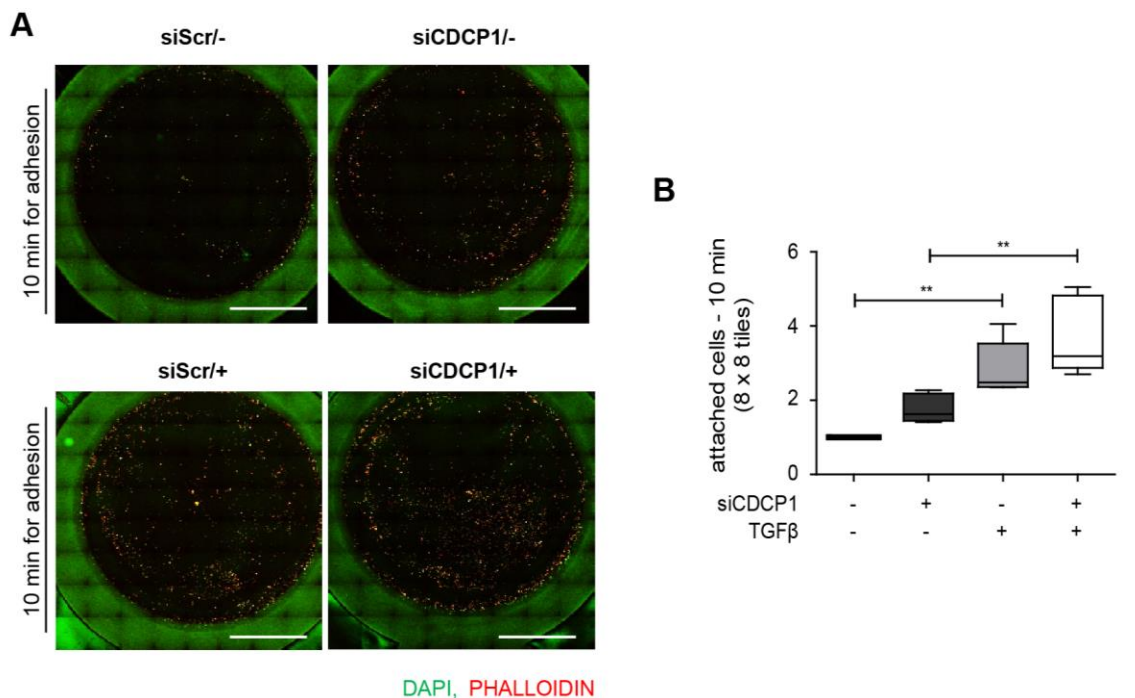


**Figure 4.14: CDCP1 silencing negatively impacts cell adhesion of pHLFs.** (A) PhLFs were reversely transfected with scrambled (siScr) or CDCP1 siRNA (siCDCP1) for 48 h followed by incubation with or without (-/+) 1 ng/ml TGF $\beta$  for 48 h. Thereafter, cells were placed in a 48-well plate and allowed to attach for 10 min. Attached cells were subsequently fixed with 4 % PFA, stained with DAPI (green) and Phalloidin (red), and a confocal LSM microscope was used to scan and thus image each well. Shown are representative images of one replicate out of four technical replicates from five different biological experiments (n=5). Scale bar: 10  $\mu$ m. (B) Summary of cell adhesion data from (A) presented as mean  $\pm$  SEM. Statistical analysis: One-way ANOVA with Bonferroni's Multiple Comparison Test. \*\*p-value < 0.01.

#### 4.4.3 Absence of CDCP1 enhances the expression of $\alpha$ SMA and ECM proteins

In section 4.4.1 we observed changes in  $\alpha$ SMA levels after knocking down CDCP1. We next wanted to investigate, if CDCP1 takes part in myofibroblast differentiation, a process known to be mainly activated by TGF $\beta$ , and characterized by an  $\alpha$ SMA expressing and increased ECM secreting phenotype. We therefore performed siRNA-mediated silencing of CDCP1 followed by cell stimulation with TGF $\beta$  for 48 h. Immunoblot was used to monitor the expression changes of  $\alpha$ SMA and the ECM proteins fibronectin, collagen type I, III and V. TGF $\beta$  alone led to an increase in  $\alpha$ SMA, collagen, and fibronectin protein levels (Figure 4.15 A, B). Interestingly, the knockdown of CDCP1 alone significantly enhanced (p<0.01) the

expression of collagen V. This effect was even more prominent for collagen V and collagen III when cells were additionally stimulated with TGF $\beta$  (Figure 4.15 A, B).

Also, CDCP1 enhanced  $\alpha$ SMA protein expression independently of TGF $\beta$  as shown via immunoblotting (Figure 4.15 A, B), and immunofluorescence stainings of methanol-fixed phLFs monolayers (Figure 4.15 C). Moreover, immunofluorescence stainings of healthy and IPF tissue sections revealed that  $\alpha$ SMA-positive interstitial myofibroblasts located in fibroblastic foci of IPF lung sections displayed a low expression of CDCP1 (Figure 4.15 D, lower panel), whereas non-differentiated interstitial lung fibroblasts in sections of healthy lungs were highly CDCP1-positive, and clearly  $\alpha$ SMA-negative (Figure 4.15 D, upper panel).

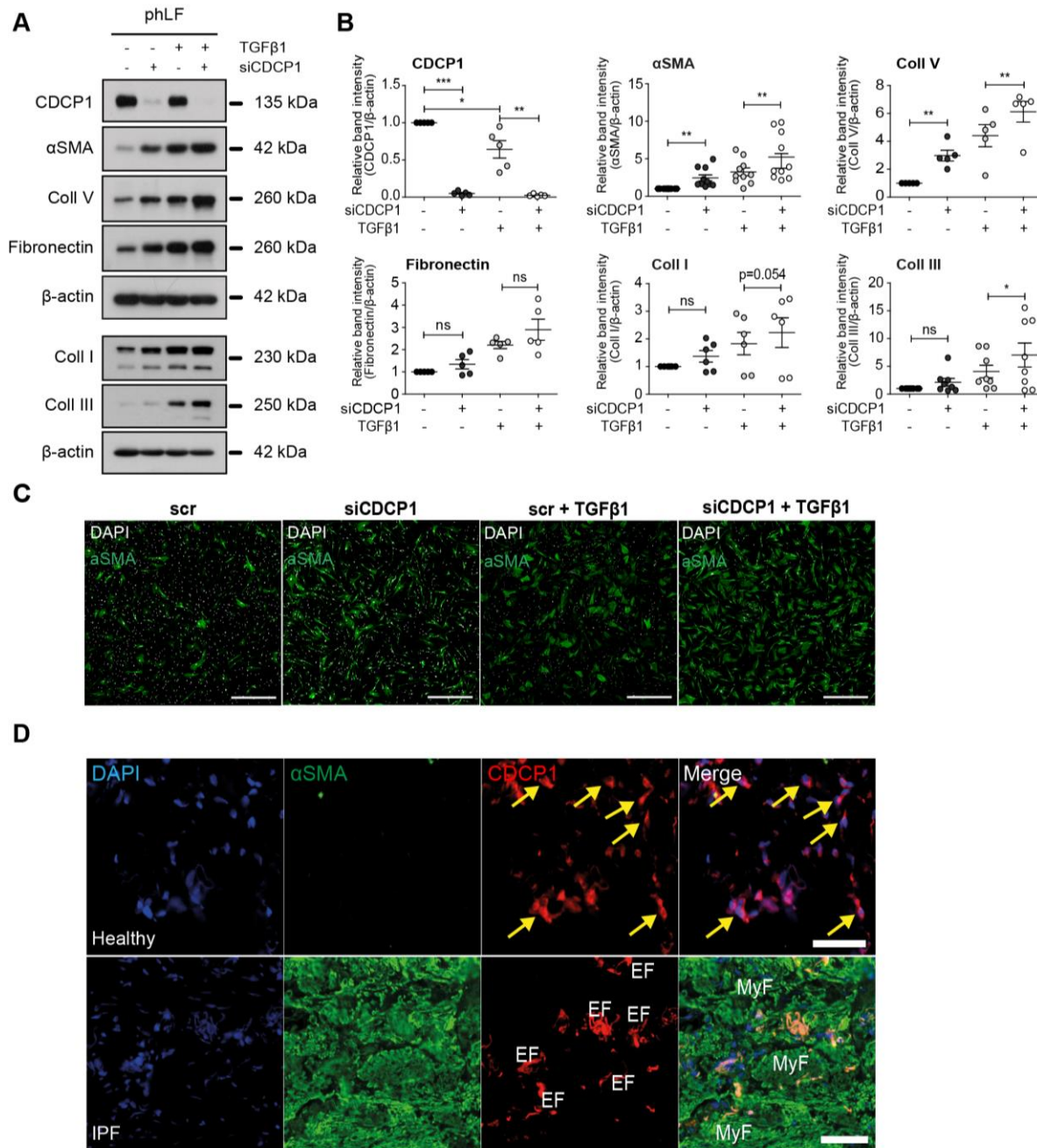


**Figure 4.15: CDCP1-depleted lung fibroblasts exhibit increased αSMA and ECM expression.** (A) Cells were transfected with control scrambled (-) or CDCP1-specific siRNA (+), and subsequently stimulated with 1 ng/ml TGFβ for 48 h. The changes in protein expression of CDCP1, αSMA, collagens, and fibronectin in total cell lysates were monitored via immunoblot. Shown is one representative immunoblot from five-ten independent biological experiments (n=5-10). (B) Densitometric quantification from (A) presented as mean ± SEM. Statistical analysis: Paired two-tailed t-test for a comparison of single columns. \*\*\*p-value < 0.001, \*\*p-value < 0.01, \*p-value < 0.05. (C) Representative stainings of methanol-fixed pHLFs monolayers, which were reversely transfected with scrambled (scr) and CDCP1-specific siRNAs (siCDCP1), and treated in the presence or absence of 1 ng/ml TGFβ for 48 h. Images were acquired by confocal microscopy scanning each well (8x8 tiles scanning area). Nuclei were counterstained

with DAPI (white). Representative images from three independent experiments are shown (n=3). Scale bar: 1000  $\mu$ m. (D) Immunofluorescent co-stainings of CDCP1 (red, yellow arrows) and  $\alpha$ SMA (green) in healthy (upper panel) and IPF (lower panel) paraffin tissues sections. Nuclei were counterstained with DAPI (blue). Shown is one representative section from four different donors (n=4) and four different IPF patients (n=4). Scale bar: 50  $\mu$ m. EF = elastic fibers, MyF = myofibroblasts.

#### 4.4.4 CDCP1 inhibits canonical TGF $\beta$ signaling in lung fibroblasts

Moreover, I tested whether CDCP1 impacts downstream TGF $\beta$  signaling in pHLFs. Thus, siRNA-mediated knockdown of CDCP1 for 48 h was performed followed by cell treatment with TGF $\beta$  for 1 h, 26 h, and 48 h. Changes in Smad3 phosphorylation were analyzed via immunoblot. TGF $\beta$  alone increased Smad3 phosphorylation levels as expected (Figure 4.16 A-D). Surprisingly, CDCP1-depleted cells exhibited an even stronger increase in Smad3 phosphorylation ( $p < 0.05$ ) in the presence of TGF $\beta$  (Figure 4.16 D).

To further corroborate our data, pHLFs were stimulated as described above and subsequently a luciferase reporter assay was performed using the Smad3-reporter pGL3-CAGA(9)-luc plasmid [Dennler et al., 1998] and a control pGL-4 plasmid. The knockdown of CDCP1 significantly enhanced ( $p < 0.05$ ) the TGF $\beta$ -mediated Smad3 promoter activity after 26 h and 48 h (Figure 4.16 E, F).

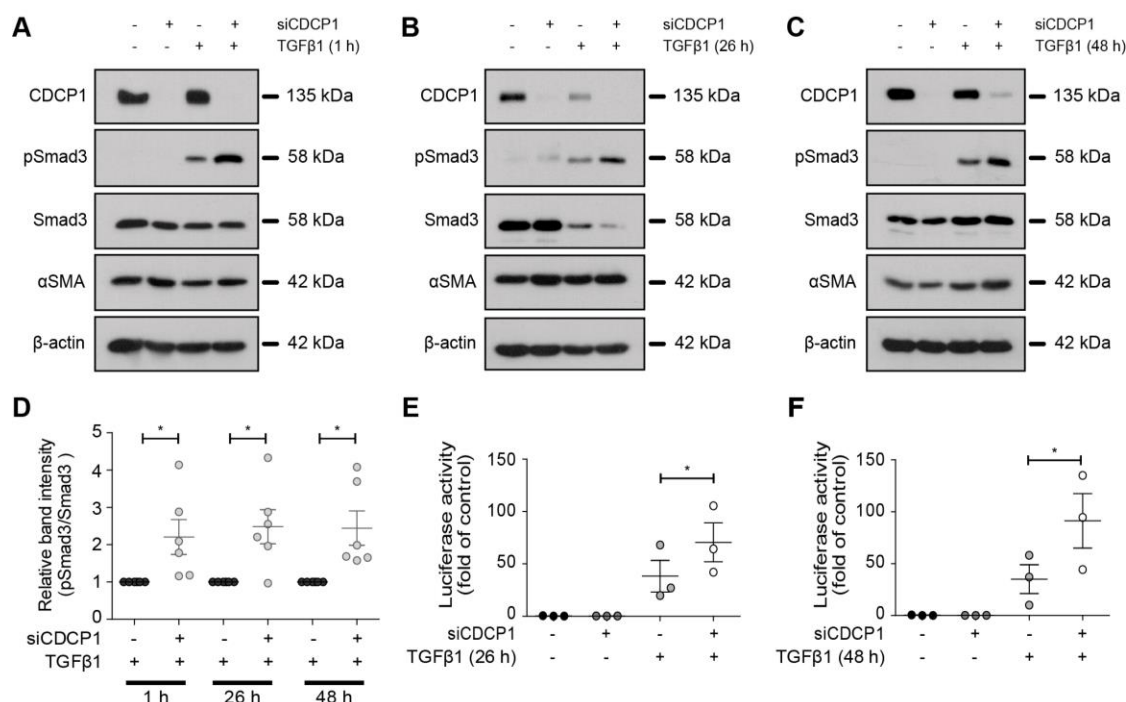


**Figure 4.16: Absence of CDCP1 enhances TGF $\beta$ -mediated Smad3 phosphorylation in pHLFs.** Reverse transfection of pHLFs with either control scrambled or CDCP1-specific siRNA was performed for 48 h, followed by cells stimulation with or without 1 ng/ml TGF $\beta$  for (A) 1 h, (B) 26 h, and (C) 48 h. Whole cell lysates were immunoblotted for CDCP1, phosphorylated and total Smad3, and  $\alpha$ SMA. Shown is one representative immunoblot out of six performed experiments (n=6). (D) Densitometric quantification of pSmad3/Smad3 ratio from (A-C) presented as mean  $\pm$  SEM. Statistical analysis: One sample t-test. \*p-value <

0.05 (E, F) Lung fibroblasts were first reversely transfected with siRNA against CDCP1 and 24h after the transfection, Smad signaling luciferase reporter or control construct were transfected to cells followed by TGF $\beta$  stimulation (1 ng/ml) for 26 h or 48 h. Luciferase activity was measured and data compared between TGF $\beta$  and siCDCP1+TGF $\beta$  treatments. All measurements were performed in four technical replicates per each condition. Data are presented as a summary of three independent experiments (n=3) with mean  $\pm$  SEM. Statistical analysis: Paired two-tailed t-test. \*p-value < 0.05.

Taken together, my data suggest that CDCP1 negatively regulates cell adhesion, ECM expression, and myofibroblasts transdifferentiation, by affecting downstream TGF $\beta$  signaling in human lung fibroblasts.

#### **4.4.5 TGF $\beta$ regulates CDCP1 expression via non-canonical TGF $\beta$ signaling pathway**

Finally, I wanted to explore the molecular mechanism by which TGF $\beta$  regulates CDCP1 expression in lung fibroblasts. At first, mediators of canonical TGF $\beta$  pathway were tested by treating phLFs with SB431542, a specific inhibitor targeting Alk5 receptor, or Sis3, a specific inhibitor of Smad3 phosphorylation, together with TGF $\beta$  for 48 h. Changes in CDCP1 expression were monitored via immunoblot. The expression of CDCP1 remained decreased by TGF $\beta$  in cells treated with SB431542 or Sis3 (Figure 4.17 A, B). Thus, I next analyzed whether TGF $\beta$  decreases CDCP1 expression via non-canonical TGF $\beta$  signaling. To do so, I stimulated phLFs with inhibitors targeting pErk1/2 (UO126), PAR1, PAR2, and a broad spectrum of matrix metalloproteases, including MMP1-3, MMP7-9, MMP12, MMP14, and MMP26 (GM6001) in parallel with TGF $\beta$  for 48 h (Figure 4.17 C-F). Surprisingly, CDCP1 protein levels remained still decreased indicating that TGF $\beta$  regulates CDCP1 expression via another, unknown mechanism.

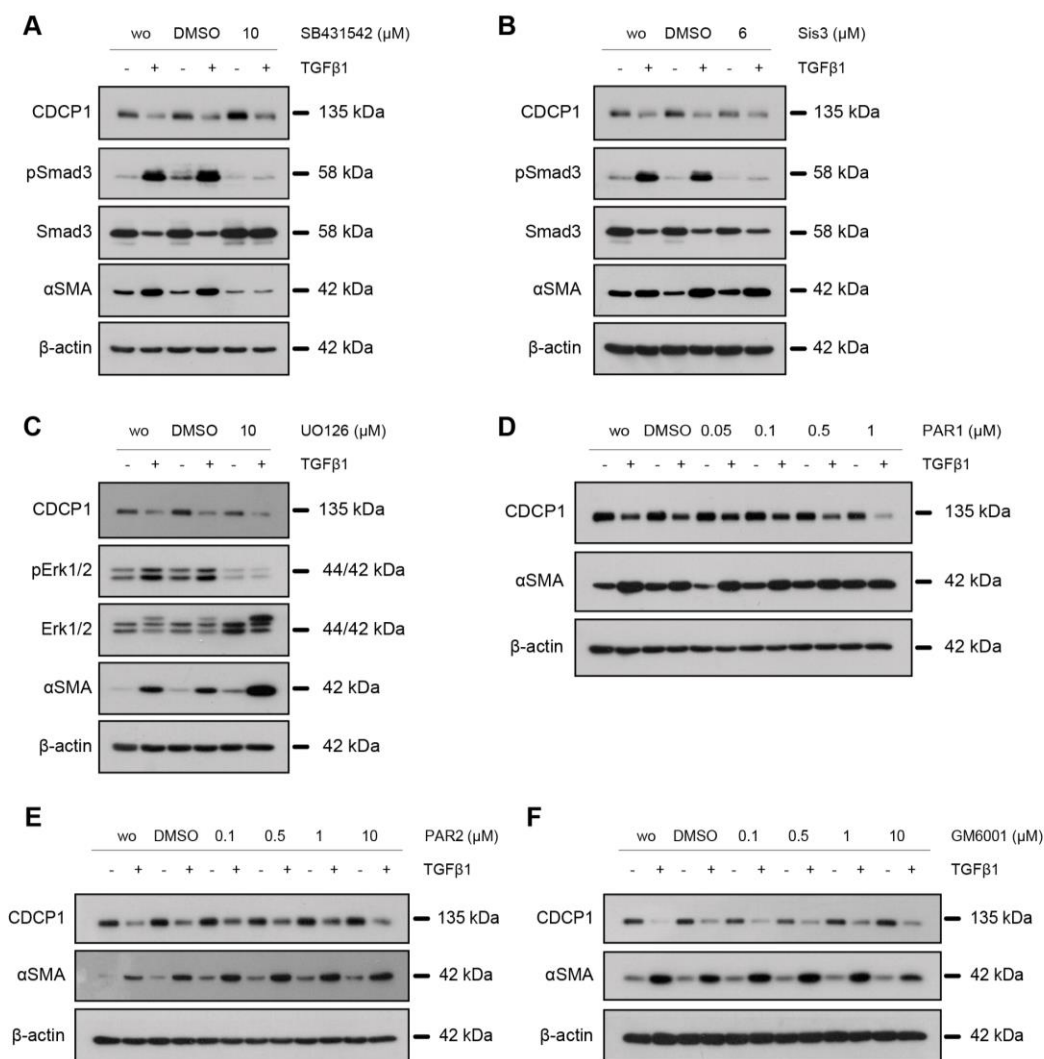


**Figure 4.17: TGFβ attenuates CDCP1 expression via non-canonical signaling.** Primary human lung fibroblasts were incubated with 1 ng/ml TGFβ together with specific inhibitors or antagonists targeting (A) Alk5 receptor, (B) phosphorylated Smad3, (C) phosphorylated Erk1/2, (D) PAR1 receptor, (E) PAR2 receptor, and (F) a broad range of MMPs every 24 h for a total 48 h. The whole protein lysates were immunoblotted for CDCP1, αSMA, phosphorylated and total Smad3, phosphorylated and total Erk1/2. Equal loading was confirmed by probing each membrane for β-actin. Shown are representative blots out of three independent experiments (n=3). Non-treated cells were marked as "wo".

#### 4.4.6 TGFβ decreases CDCP1 expression levels via ubiquitin-independent proteasomal degradation

Autophagy and the ubiquitin-proteasome pathway are well-known as the major protein degradation systems in eukaryotic cells [Lilienbaum, 2013]. Hence, I speculated that TGFβ decreases CDCP1 expression in phLFs via one of these mechanisms.

First, I tested whether TGF $\beta$  enhances CDCP1 downregulation via autophagy. Therefore, pHLFs were treated with Bafilomycin, an inhibitor of the late phase of autophagy together with TGF $\beta$  for 48 h and expression changes of CDCP1 upon treatment analyzed via immunoblot. CDCP1 expression levels, however retained decreased in the presence of Bafilomycin together with TGF $\beta$  (Figure 4.18 A). Additionally, Smad3 phosphorylation levels remained unchanged between non-stimulated and Bafilomycin-stimulated cells in the presence of TGF $\beta$ , indicating that TGF $\beta$  does not mediate CDCP1 degradation via autophagy (Figure 4.18 A).

I next tested whether TGF $\beta$  mediates downregulation of CDCP1 expression by proteasomal degradation. PhLFs were treated with the proteasome inhibitor Bortezomib in a concentration-dependent manner (1-10 nM) together with TGF $\beta$  for 48 h and changes in CDCP1 expression upon treatment monitored via immunoblot (Figure 4.18 B). Ten nM of Bortezomib prevented downregulation of CDCP1 expression in the presence of TGF $\beta$  (Figure 4.18 C) indicating that TGF $\beta$  potentially drives CDCP1 degradation in the proteasome. For proteasomal degradation proteins are tagged with ubiquitin molecules. This polyubiquitin chain functions as a signal and gets bound by the proteasome. Thus, I next tested whether CDCP1 is more ubiquitinated in the presence of TGF $\beta$ . To do so, pulldown of CDCP1 from the whole protein lysates treated with 10 nM of Bortezomib together with TGF $\beta$  for 48 h was performed and ubiquitination status of CDCP1 addressed via immunoblot (Figure 4.18 D). Immunoblotting indicated a high enrichment of CDCP1 via immunoprecipitation, however no ubiquitination of CDCP1 was detected upon treatment (Figure 4.18 D). Interestingly, Bortezomib treatment in the presence of TGF $\beta$  restored CDCP1 expression already on the mRNA level (Figure 4.18 E). Of note, 10 nM of Bortezomib also counteracted TGF $\beta$ -mediated increase of  $\alpha$ SMA protein (Figure 4.18 C) and gene (Figure 4.18 E) expression. We conclude that CDCP1 degradation by TGF $\beta$  does not occur due to protein ubiquitination but involves a more complex, and yet unknown mechanism.

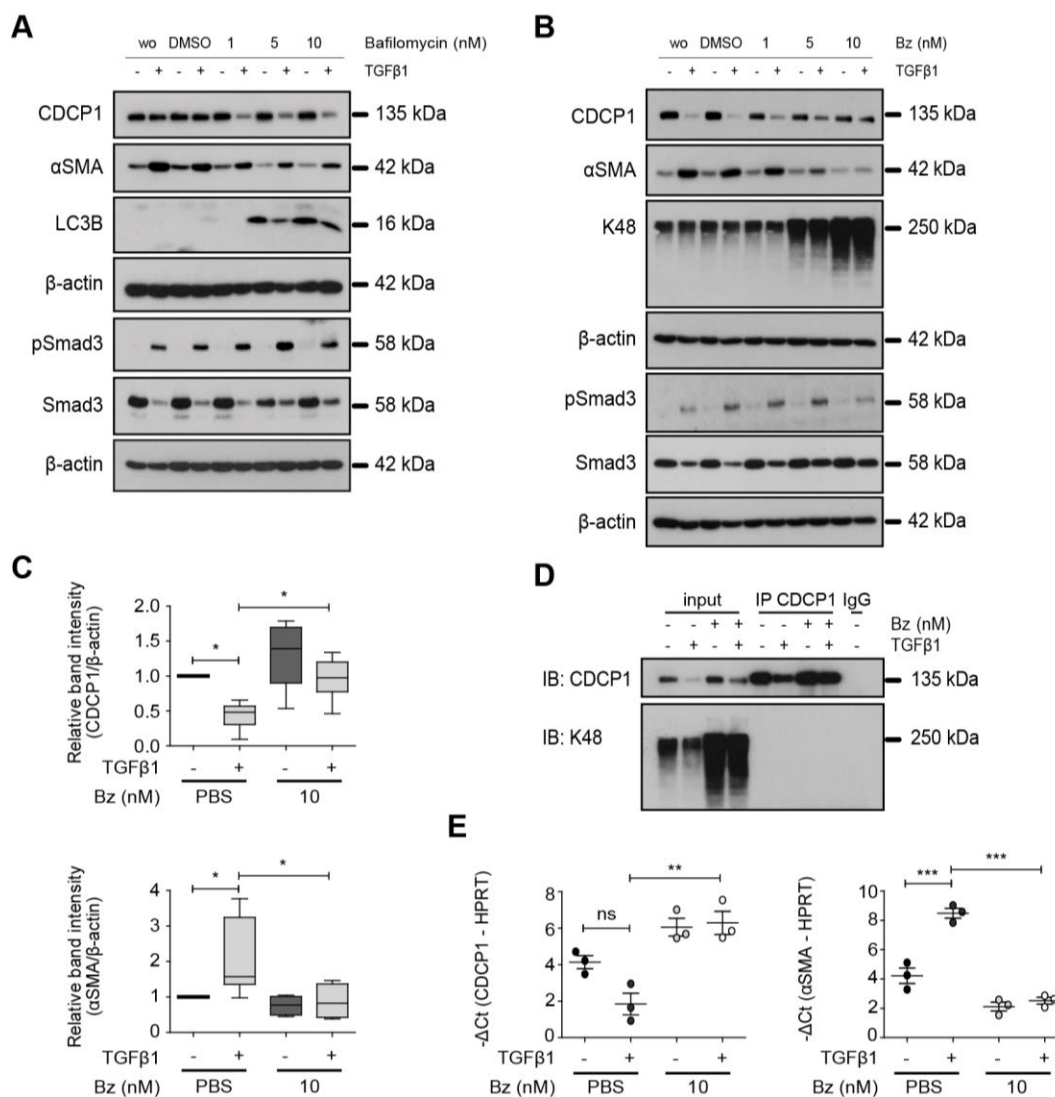


**Figure 4.18: TGFβ potentially attenuates CDCP1 expression via a complex proteasomal degradation.** Immunoblot of entire protein lysates from pHLFs treated for 48 h with 1 ng/ml TGFβ together with increasing concentrations (wo, DMSO, 1-10 nM) of (A) Bafilomycin and (B) Bortezomib. (A, B) Membranes were probed for CDCP1, αSMA, phosphorylated Smad3, and Smad3 as indicated. (A) LC3B was used as a positive control of the effective autophagy inhibition. Shown is one representative immunoblot out of three performed experiments (n=3). (B) UbiK48 was used as a positive control of the effective proteasome inhibition. Shown is one representative blot out of six independent experiments (n=6). Equal protein loading in (A, B) was confirmed by probing membranes for β-actin. (C) Densitometric quantification of CDCP1 and αSMA total protein levels from (B) with data presented as mean ± SEM. (D) PhLFs were stimulated in the presence or absence of TGFβ together with 10 nM Bz for 48 h and direct interaction of CDCP1 and ubiquitin in immunoprecipitants from the whole protein lysates analyzed via immunoblot. One representative blot out of three independent experiments is shown (n=3). (E) qRT-PCR analysis of CDCP1 and αSMA gene expression from pHLFs treated with TGFβ together with 10 nM Bz for 48 h. HPRT was used as a housekeeping gene. Data are depicted as mean ± SEM from three independent experiments (n=3). Statistical analysis: One-way ANOVA with Bonferroni's Multiple Comparison Test. \*\*\*p-value < 0.001, \*\*p-value < 0.01, \*p-value < 0.1, ns = non-significant. Bz = Bortezomib.

## 5 DISCUSSION

Myofibroblasts are characterized as essential effector cells in IPF, since they belong to the main ECM producing cell types, highly proliferating and by this maintaining the fibrotic pathological state. The cytokine TGF $\beta$  is the main effector driving transdifferentiation of cells into this active  $\alpha$ SMA expressing cell phenotype. Myofibroblasts are specified by intracellular marker expression of collagen, fibronectin, or desmin. The surface proteome, however, has only little been characterized. In an unbiased surface proteome analysis of primary human lung fibroblasts, our research group identified that the surface proteome of primary human lung fibroblasts is intensively regulated by TGF $\beta$ . Two of the top downregulated candidates, PDGFR $\alpha$  and CDCP1, have been in the focus of my thesis to characterize in detail the functional outcome of this regulation in the context of lung fibrosis.

We first confirmed protein expression and localization on the surface of fibroblasts in general and its downregulation by TGF $\beta$ . Further, my work described for the first time a potential PDGFR $\alpha$ /TGF $\beta$  cross-talk in lung fibroblasts. PDGF-AB predominantly activated PDGFR $\alpha$ , whereas PDGF-DD activated PDGFR $\beta$  receptor. Interestingly, PDGFR $\alpha$ -depleted cells displayed an increase in PDGFR $\beta$  expression indicating a compensatory effect between the two receptors. Further, the invasion capacity of lung fibroblasts is regulated by PDGF-AB ligand in a PDGFR $\alpha$ -dependent manner. Importantly, tyrosine kinase inhibitor Nintedanib decreased TGF $\beta$ -induced collagen V and  $\alpha$ SMA expression, but surprisingly this effect was largely attenuated in the absence of PDGFR $\alpha$ . Finally, I could show that Nintedanib also enhanced total collagen secretion in PDGFR $\alpha$ -depleted cells.

CDCP1 is exclusively localized on the surface of pHLFs. Mechanistic studies revealed that TGF $\beta$  decreases CDCP1 expression via an ubiquitin-independent pathway, but not via Smad or MAPK signaling. I also showed for the very first time that CDCP1 impacts downstream TGF $\beta$  signaling as demonstrated by increased Smad3 phosphorylation in CDCP1-depleted cells treated with TGF $\beta$  and which in consequence enhances  $\alpha$ SMA, collagen III and collagen V total protein expression. Moreover, I showed that loss of CDCP1 positively impacts TGF $\beta$ -mediated cell adhesion of lung fibroblasts.

### 5.1 Fibroblasts cell-surface proteome in response to profibrotic TGF $\beta$

To date, characterization of the fibroblasts surface proteome under basal as well as growth factor stimulation is not clearly assessed despite its essential importance in understanding how activated fibroblasts contribute to pathological processes in IPF [Laurent et al., 2008; Tschumperlin and Drazen, 2006; Kendall and Feghali-Bostwick, 2014]. TGF $\beta$  is one of the most intensively studied profibrotic growth factors driving fibroblasts to myofibroblasts differentiation and maintaining this phenotype in IPF [Kendall and Feghali-Bostwick, 2014; Serini and Gabbiani, 1999]. Therefore, our research group initially investigated changes in the surface

proteome of primary human lung fibroblasts under normal and TGF $\beta$ -stimulated conditions [Heinzelmann et al., 2016].

There is an emerging need to uncover specific myofibroblast surface markers in disease [Hinz et al., 2007b; Baum and Duffy, 2011]. Surface proteins represent easy accessible targets for specific pharmacological compounds compared to intracellular molecules [Hinz et al., 2007b; Ivarsson et al., 1998]. To date, there are only few studies characterizing fibroblasts surface proteome under basal and growth factor stimulation. Recently, Slany and colleagues performed a proteomics analysis of IL-1 $\beta$ -stimulated control tumor-free and tumor-associated primary human fibroblasts isolated from skin, lungs, and bone marrow using LC-MS/MS [Slany et al., 2014]. Within the intracellular proteome fraction (cytoplasm, nuclear extract, and secretome) of tumor-associated fibroblasts, they identified IGF-II, PAI-1, and PLOD2 among the top upregulated proteins by IL-1 $\beta$ , and further proposed that their upregulation may contribute to tumor development during early stages of chronic inflammation. Another study by Predic and co-authors investigated the changes of human lung fibroblasts' proteome in the presence and absence of endothelin-1, identifying Rab3a, Rab14, and Sox5 among its main targets [Predic et al., 2002]. Moreover, Pilling and colleagues aimed to analyze expression profiles of selected markers via immunostainings to specifically discriminate between human monocytes, macrophages, fibrocytes, and fibroblasts [Pilling et al., 2009]. Study by Halfon and colleagues aimed to uncover new gene and surface protein markers which are differentially expressed between mesenchymal stem cells (MSCs) and dermal fibroblasts which would be beneficial for assessing the purity of MSCs expanded *in vitro* [Halfon et al., 2011]. Surface marker profiling of fibroblasts have been previously described by Walmsley and colleagues [Walmsley et al., 2015]. Here, authors showed that freshly isolated, uncultured dermal fibroblasts showed different surface marker profile compared to cultured fibroblasts [Walmsley et al., 2015]. Nevertheless, the expression analysis of lung fibroblast surface proteome remains rare, as specific fibroblast surface markers have not been identified to date. Moreover, most studies were performed in mouse, and thus it is questionable if all data can be transferred to human system. Further studies are also required to uncover which of those identified markers play a role in disease.

## 5.2 TGF $\beta$ effect on PDGF receptor expression in phLFs

PDGFR $\alpha$  is a tyrosine kinase receptor and its expression has been described in different cell types including fibroblasts, fibrocytes and platelets [Vassbotn et al., 1994; Heldin and Westermark, 1999; Aono et al., 2014]. Importantly, the overall expression levels of PDGF receptors are not constant in the cells, but rather vary in response to various stimuli. Here I showed that profibrotic cytokine TGF $\beta$  decreases cell surface and total protein expression levels of PDGFR $\alpha$ , whereas PDGFR $\beta$  surface and total protein levels increased upon the treatment in primary human lung fibroblasts (Figure 4.1 and Figure 4.2). Our data confirm previous data by Bonner and colleagues, who also reported downregulation of PDGFR $\alpha$  gene expression by TGF $\beta$  in human

lung fibroblasts [Bonner et al., 1995]. A decrease in PDGFR $\alpha$  gene expression by TGF $\beta$  has also been described in 3T3 mouse fibroblasts, in neonatal human foreskin fibroblasts, and in mesothelial cells [Langerak et al., 1996; Gronwald et al., 1989; Paulsson et al., 1993]. These studies, however, have predominantly focused on changes in PDGFR $\alpha$  expression on the transcript rather than protein levels. In contrast, PDGFR $\alpha$  gene and protein expression has been shown to be upregulated by TGF $\beta$  in scleroderma fibroblasts [Yamakage et al., 1992]. On the other hand, it has been described in the experimental model of liver fibrosis that PDGFR $\beta$  expression levels are highly increased by TGF $\beta$  [Bissell et al., 1995]. Likewise, we observed an increase in PDGFR $\beta$  surface and total protein expression by TGF $\beta$  (Figure 4.2 and Figure 4.9 B), and importantly, an upregulation of PDGFR $\beta$  after knockdown of PDGFR $\alpha$  (Figure 4.8 and Figure 4.9).

### 5.3 PDGF ligand-receptor binding affinities in phLFs

PDGF signaling plays a critical role in various cellular responses of fibroblasts, including cell proliferation, migration, and the ECM synthesis, which are all essential for processes of normal wound healing [Alvarez et al., 2006]. However, aberrant PDGF signaling has been linked to several lung diseases, including lung fibrosis [Bonner, 2004a]. PDGF signaling is activated by binding of specific PDGF ligands to their PDGF receptors. Whether a specific ligand-receptor interaction impacts pathological mechanisms in disease has not been clarified yet in the field. [Donovan et al., 2013]. We analyzed ligand-binding affinities of PDGF-AB and PDGF-DD to PDGF receptors in human lung fibroblasts and found that PDGF-AB binds with the highest affinity to PDGFR $\alpha$  whereas PDGF-DD binds to PDGFR $\beta$  (Figure 4.9 A).

The binding affinities of PDGF ligands towards their receptors have been controversially discussed in the literature [Donovan et al., 2013; Bergsten et al., 2001; Heldin et al., 1988]. In line with our findings, it has been previously shown in *in vitro* studies that PDGF-AB ligand binds PDGFR $\alpha$ , whereas PDGF-DD showed higher binding affinities exclusively towards PDGFR $\beta$  receptor [Heldin et al., 2002; Chen et al., 2013; Kanakaraj et al., 1991]. Donovan and colleagues compared PDGF ligand-receptor-specific binding patterns in dermal *versus* lung fibroblasts by analyzing phosphorylation status of PDGFR $\alpha$  and PDGFR $\beta$  receptors in the presence of single PDGF ligands [Donovan et al., 2013]. Interestingly, they observed that all tested PDGF ligands, including PDGF-DD increased phosphorylation of PDGFR $\alpha$  receptor in human lung fibroblasts [Donovan et al., 2013], which is in contrast with our findings (Figure 4.9 A). Little information exists regarding binding affinities of PDGF-AB and PDGF-DD ligands to PDGF receptors *in vivo* [Andrae et al., 2008]. Here, PDGF-DD have been recently described to bind PDGFR $\alpha\beta$  receptor, but its functional significance remains the subject of ongoing investigations [Heldin and Lennartsson, 2013]. PDGF-AB has not been investigated in this context to date.

#### 5.4 PDGF signaling in human lung fibroblasts

It has been thought for a long time that growth factors, including PDGFs transduce signals solely via their specific receptors. Generally, PDGFs signal intracellularly via two different and independent signaling pathways, namely MAPK cascade via phosphorylation of RAF, MEK, and ERK [Monje et al., 2003] and on the other hand PI3K pathway via phosphorylation of Akt and mTOR [Razmara et al., 2013]. Nevertheless, recent studies indicate that PDGF signaling extensively cross-talks with other signaling pathways, such as EGFR, Wnt or AngII signaling [Mendelson et al., 2010; Miller et al., 2012; Linseman et al., 1995; Heeneman et al., 2000].

In this study I demonstrated that PDGF signaling cross-talks with TGF $\beta$  signaling, as shown by increased phosphorylation of Akt when cells were treated in the combination with TGF $\beta$  and PDGF ligands (Figure 4.7 and 4.9) and, on the other hand, decreased Smad3 phosphorylation in the absence of PDGFR $\beta$  (Figure 4.9 A, E). To my knowledge, this has not been previously reported in primary human lung fibroblasts or in lung fibrosis. Interestingly, a cross-talk between PDGFR $\beta$  and TGF $\beta$  signaling have recently been described in primary dermal fibroblasts [Porsch et al., 2014]. Here, authors demonstrated that PDGFR $\beta$  and TGF $\beta$ RI receptors physically interact via either the extracellular or transmembrane domain of PDGFR $\beta$  receptor. Additionally, they showed that PDGF-BB induces TGF $\beta$  signaling as shown by increased Smad2 phosphorylation and expression of TGF $\beta$  responsive gene *PAI-1*, however the exact mechanism behind PDGF-BB-induced TGF $\beta$  signaling remains unclear [Porsch et al., 2014]. Lastly, their study demonstrated that TGF $\beta$  controls PDGF-BB-mediated cell migration as treatment of primary human dermal fibroblasts with GW6604, a TGF $\beta$  kinase inhibitor, led to a decrease in wound closure compared to PDGF-BB-treated cells [Porsch et al., 2014]. Interestingly, Murray-Rust and colleagues had speculated that PDGF-BB might directly bind to the TGF $\beta$  receptor as PDGFs and TGF $\beta$  shared topological similarities [Murray-Rust et al., 1993]. Liu and co-workers studied the role of PDGFR $\alpha$  and PDGFR $\beta$  in TGF $\beta$  signaling of primary human hepatic stellate cells [Liu et al., 2014]. They observed that knockdown of PDGFR $\alpha$ , but not PDGFR $\beta$ , attenuates TGF $\beta$ -mediated Smad2 phosphorylation as well as accumulation of Smad2 in the cell nucleus of hepatic stellate cells. We, in contrast, found that knockdown of PDGFR $\beta$  led to a decrease in Smad3 phosphorylation under basal as well as PDGF-AB and -DD stimulation in human lung fibroblasts (Figure 4.9 A, E).

#### 5.5 PDGF signaling in cell invasion

PDGF signaling regulates various cellular processes, including cell proliferation, and migration via specific receptor-ligand interactions [Kimani et al., 2009; Noskovičová et al., 2015; Boström et al., 2002]. However, the invasion potential of fibroblasts due to ligand dependent signaling has not been characterized to date. Here, I showed that PDGF-AB increases cell invasion properties of primary human lung fibroblasts in a

PDGFR $\alpha$ -dependent manner (Figure 4.6). To my knowledge, the role of PDGF signaling in modulating invasion properties of primary human lung fibroblasts has not been investigated to date. Although, it has been recently published in our laboratory, that PDGF-BB stimulation enhances the invasion properties of fibroblasts, the study was performed with mouse lung fibroblasts [Oehrle et al., 2015]. There is an increased evidence that PDGF signaling plays a role in invasion and metastasis of cancer cells [Andrae et al., 2008]. Neri and colleagues reported that cancer cells undergoing epithelial-to-mesenchymal transition (EMT) activate subpopulation of cancer-associated fibroblasts (CAFs) which possess abilities to remodel collagen matrix and thus facilitate cancer cell invasion via PDGF-BB/PDGFR $\beta$  axis [Neri et al., 2016].

### 5.6 Targeting PDGF signaling in IPF

Pharmacological treatment options of IPF patients are still very limited to date. In 2014 Nintedanib (BIBF1120) was approved by the US Food and Drug Administration (FDA) for IPF therapy [Richeldi, 2014; Spagnolo et al., 2015]. Nintedanib inhibits kinase activity of PDGF, VEGF, and FGF receptors by occupying their intracellular ATP-binding sites which in turn results in a blockage of receptors' autophosphorylation and thus downstream signaling [Wollin et al., 2015]. Imatinib mesylate is another tyrosine kinase inhibitor which blocks the activity of PDGFR $\alpha$  and PDGFR $\beta$  receptors, discoidin domain receptors (DDR1 and DDR2), c-kit, and c-Abl [Day et al., 2008; Buchdunger et al., 2002] in a similar mechanism as Nintedanib [Radford, 2002]. In my studies I analyzed the inhibitory effect of tyrosine kinase inhibitors Imatinib and Nintedanib on downstream PDGF signaling in primary lung fibroblasts and observed that Akt phosphorylation levels were decreased by both drugs in a concentration dependent-manner (Figure 4.10). Thereby, all tested doses used were in the physiological range and consistent with those previously published [Knüppel et al., 2017; Hostettler et al., 2014; Dewar et al., 2003; Zhang et al., 2003]. Wollin and colleagues showed that Nintedanib inhibited downstream PDGF signaling as shown by decreased phosphorylation of Akt and Erk in mouse lung tissues [Wollin et al., 2014] which is consistent with my observations in primary human lung fibroblasts (Figure 4.10 and Figure 4.11). Additionally, they showed that Nintedanib blocked PDGF-BB-mediated autophosphorylation of PDGFR $\alpha$  and PDGFR $\beta$  in primary human lung fibroblasts isolated from donor lungs as well as in mouse lung tissue [Wollin et al., 2014]. Interestingly, in my study Nintedanib did not block PDGFR $\beta$ -mediated signaling in the absence of PDGFR $\alpha$  since phosphorylation levels of Akt still remained increased (Figure 4.11 A) indicating that the inhibitory effect of Nintedanib on PDGF signaling is attenuated in the absence of PDGFR $\alpha$ .

We also observed that PDGFR $\alpha$ -depleted cells displayed an increase in the expression levels of collagen V and  $\alpha$ SMA (Figure 4.12 A), and this effect was even more prominent in the presence of TGF $\beta$ . The role of PDGFR $\alpha$  in myofibroblasts differentiation has been previously investigated in systemic sclerosis [Liu et al., 2013]. Here, authors showed that siRNA-mediated depletion of PDGFR $\alpha$  led to a downregulation of  $\alpha$ SMA

expression on mRNA and protein levels in dermal fibroblasts. Additionally, we observed that PDGFR $\alpha$  knockdown enhanced the effect of TGF $\beta$  on collagen V secretion in primary human lung fibroblasts (Figure 4.12 B). Interestingly, Nintedanib did not diminish TGF $\beta$ -mediated increase of collagen V and  $\alpha$ SMA expression (Figure 4.12 A). The effect of Nintedanib alone on ECM expression has been previously investigated by Wollin and colleagues who showed that Nintedanib reduced collagen I expression in primary human lung fibroblasts treated with TGF $\beta$  [Wollin et al., 2014]. Furthermore, they observed that Nintedanib administration significantly decreased fibrosis and total lung collagen levels in the lungs of bleomycin-treated mice [Wollin et al., 2014]. In line with this study, Rangarajan and colleagues reported a decline in collagen I expression levels in primary human IPF lung fibroblasts treated with Nintedanib in a dose- and time-dependent manner [Rangarajan et al., 2016]. It has also been shown that collagens, including collagen V can interact with PDGF ligands and thus regulate cellular functions [Somasundaram and Schuppan, 1996; Scotton and Chambers, 2007]. Similarly, several studies reported that Nintedanib blocked TGF $\beta$ -mediated myofibroblasts transdifferentiation of primary human lung fibroblasts from IPF patients as determined by decreased expression of  $\alpha$ SMA on mRNA and protein levels [Wollin et al., 2014; Lehtonen et al., 2016]. I could not confirm these data. Our observations might indicate a potential role of PDGF signaling via receptor  $\alpha$  in modulating Nintedanib function. In summary, my data indicate that TGF $\beta$  alters the effect of tyrosine kinase inhibitor Nintedanib probably via the potential cross-talk between PDGF and TGF $\beta$  signaling which in the end may lead to the observed activation of fibroblasts and thus enhanced ECM expression.

### 5.7 TGF $\beta$ -mediated expression changes of CDCP1 in phLFs

CDCP1 is a cell surface glycoprotein which expression has been extensively characterized in epithelial cells of various organs including the lung, colon, pancreas, and breast [Orchard-Webb et al., 2014; Miyazawa et al., 2010; Ikeda et al., 2009; Wright et al., 2016]. My data showed for the first time CDCP1 expression and surface localization in primary human lung fibroblasts (Figure 4.3). Hooper and colleagues reported that microvascular endothelial cells and dermal fibroblasts do not express CDCP1 [Hooper et al., 2003]. Additionally, CDCP1 was also found to be expressed on the surface of hematopoietic progenitor cells, liver hepatocytes and primary cultures of dermal keratinocytes [Brown et al., 2004a; Siva et al., 2008; Buhning et al., 2004; Takeda et al., 2010].

Little information exists about regulators of CDCP1 expression. Here, I showed that CDCP1 mRNA and protein expression levels are significantly downregulated by TGF $\beta$  in primary human lung fibroblasts (Figure 4.4). The impact of TGF $\beta$  on CDCP1 expression has been previously investigated by Miura and colleagues, but their study was performed with human pancreatic cell lines [Miura et al., 2014]. In contrast

with this study they showed an upregulation of CDCP1 mRNA and protein expression by TGF $\beta$ , and also BMP4 and HGF, indicating a cell type and organ specific regulation of CDCP1 by TGF $\beta$ .

### 5.8 TGF $\beta$ potentially drives an ubiquitin-independent degradation of CDCP1 in the proteasome

TGF $\beta$  can exert its cellular functions via the classical Smad signaling pathway, or via different non-canonical signaling, including Ras-Erk-MAPK, JNK/p38, and PI3K/Akt pathway [Massagué, 2012; Mulder, 2000; Mu et al., 2012]. My data showed that TGF $\beta$  regulates CDCP1 expression neither via non-Smad3 nor the non-canonical MAPK pathway, but potentially reduces CDCP1 levels via proteasomal degradation of CDCP1 (Figure 4.17 and 4.18). TGF $\beta$  has recently been described to mediate an ubiquitin-proteasome degradation of parathyroid hormone-related protein (PTHrP) in human hepatocarcinoma cell lines [Li et al., 2015]. Moreover, Petrel and Brueggemeier showed that the proteasome inhibitor MG132 blocked TGF $\beta$ -mediated decrease in the estrogen receptor alpha (ER $\alpha$ ) in several breast cancer cell lines [Petrel and Brueggemeier, 2003]. We observed a clear accumulation of CDCP1 when blocking proteasomal entrance with Bortezomib. Interestingly, we did not detect any enriched ubiquitination of CDCP1, neither in the presence of TGF $\beta$ 1 alone nor in the presence of Bortezomib (Figure 4.18 D). Proteins subjected for proteasomal degradation must undergo prior ubiquitin modification, which can be mediated via addition of one (monoubiquitination) or several ubiquitins (polyubiquitination) [Farràs et al., 2005; Glickman and Raveh, 2005; Glickman and Ciechanover, 2002]. Therefore, if CDCP1 is ubiquitinated only with few ubiquitins, the antibody used might not detect the ubiquitinated protein complex. Moreover, it has also been suggested that the proteasomal degradation is not always followed by a detectable increase in the ubiquitination of the substrate. This might be due to various reasons, including the fact that the pool of free ubiquitins in the cell is limited and only the kinetically favored proteins can undergo increased ubiquitination [Jariel-Encontre et al., 2008]. Another possible explanation might be that TGF $\beta$ 1-mediated proteasomal degradation of CDCP1 occurs via an ubiquitin-independent mechanism, as it has been described before for tumor suppressor p53 [Asher et al., 2005]. Here, authors showed that ubiquitin-independent degradation of p53 in the proteasome is mediated by the enzymatic activity of NAD(P)H-quinone oxidoreductases (NQO-1). Moreover, Kong and colleagues reported that the histone deacetylase (HDAC) TSA moderates HIF-1 $\alpha$  degradation via the ubiquitin-independent proteasome pathway in RCC4 cells as they showed lack of HIF-1 $\alpha$  ubiquitination in the presence of the proteasome inhibitor MG132. Instead, they suggested that hyperacetylation of HIF-1 $\alpha$  chaperon protein HSP-70 due to loss of HDAC-6 results in accumulation and further degradation of instable HIF-1 $\alpha$ /HSP70 complex in the proteasome [Kong et al., 2006].

We also observed that mRNA levels of CDCP1 decrease upon Bortezomib stimulation in the presence or absence of TGF $\beta$  (Figure 4.18 E). Our data thus indicate that decreased CDCP1 expression by TGF $\beta$  is

restored already on transcription level indicating a more complex mechanism involving different cellular levels. Another possible explanation of this effect might be that in the presence of TGF $\beta$ , a positive regulator of CDCP1 transcription is subjected for an ubiquitin-dependent proteasomal degradation. A similar pattern has been shown for TAL1/SLC, a basic helix-loop-helix transcription factor critical for hematopoietic and endothelial cell differentiation [Terme et al., 2009]. Here, TGF $\beta$  induced a polyubiquitination, and thus proteasome-mediated degradation of TAL1/SLC in HeLa and Jurkat cells, leading to a downregulation of TAL1/SLC expression in leukemic cells. To date, limited information exists about CDCP1's transcriptional regulation. Not long ago, Emerling and colleagues identified HIF-2 $\alpha$  as a novel regulator of CDCP1 transcription in MRC10A cells [Emerling et al., 2013]. However, it has been reported that HIF-2 $\alpha$  expression is upregulated by TGF $\beta$  in human mesangial 441 cells [Hanna et al., 2013] suggesting that another transcriptional regulator may be involved in this process.

### 5.9 CDCP1 as a negative regulator of TGF $\beta$ signaling

Cross-talk between TGF $\beta$  pathway and other signaling pathways has been intensively studied during the last decade [Vert and Chory, 2011; Guo and Wang, 2009]. My data indicate that CDCP1 interferes with TGF $\beta$  signaling since CDCP-depleted primary human lung fibroblasts displayed an increase in Smad3 phosphorylation in the presence of TGF $\beta$  (Figure 4.16). TGF $\beta$  and its activated downstream signaling is one of the main drivers of fibroblasts to myofibroblasts transdifferentiation in IPF. One of the main phenotypical features of activated myofibroblasts is increased expression of  $\alpha$ SMA [Hinz, 2016] primarily regulated via TGF $\beta$ 's downstream Smad2/3 signaling [Feng and Derynck, 2005; Massagué et al., 2005]. I observed an increase of  $\alpha$ SMA in the absence of CDCP1 (Figure 4.15 A, B), and further showed that  $\alpha$ SMA-positive myofibroblasts accumulating in fibroblastic foci of IPF lungs, display a hardly detectable CDCP1 expression, whereas interstitial lung fibroblasts within the healthy lung were clearly CDCP1-positive with no detectable  $\alpha$ SMA expression (Figure 4.15 D). Limited information exists about CDCP1 signaling in general. Ligands binding CDCP1 are largely unknown to date [Wortmann et al., 2009]. To our knowledge, a possible cross-talk to TGF $\beta$  signaling has not been described yet. Further studies identifying mediators of CDCP1 signaling will provide a closer insight how CDCP1 interferes with TGF $\beta$  signaling.

I also demonstrated that CDCP1 inhibits TGF $\beta$ -mediated cell adhesion of primary human lung fibroblasts (Figure 4.14) which, to my knowledge, has not been reported to date. Several studies have shown that CDCP1 plays a role in regulating cell-matrix adhesion of cancer cells [Brown et al., 2004b; Deryugina et al., 2009; Uekita et al., 2008a; Orchard-Webb et al., 2014]. Benes and colleagues demonstrated that the tyrosine phosphorylation of CDCP1 negatively controls adhesion of cancer cells to fibronectin-coated tissue culture plates [Benes et al., 2012]. Moreover, Bhatt and colleagues observed that overexpression of CDCP1 led to changes in cell shape and thus detachment of MDA-468 breast cancer cells [Bhatt et al., 2005].

In IPF, activated myofibroblasts regulate connective tissue remodeling by producing and secreting excessive amounts of ECM components such as collagens and fibronectin. Recently, a study of Miyazawa *et al.* presented that absence of CDCP1 expression abolished ECM degradation through decreased secretion of MMP-9 protease in pancreatic cancer cells [Miyazawa *et al.*, 2010]. Therefore, I investigated the impact of CDCP1 on ECM expression in human lung fibroblasts and found that knockdown of CDCP1 led to an increase in collagen III and collagen V protein expression in a TGF $\beta$ -dependent manner (Figure 4.15 A, B). The expression of collagen III is well-known to be highly enriched in IPF [Kenyon *et al.*, 2003], whereas the expression of collagen V in IPF and its impact on ECM composition has not been described as intensively yet [Gelse *et al.*, 2003; Erler and Weaver, 2009]. Therefore, future studies are necessary to uncover the special role of collagen V in this context.

In sum, I showed that transmembrane glycoprotein CDCP1 negatively regulates TGF $\beta$ -mediated signaling events in primary human lung fibroblasts, since absence of CDCP1 enhances Smad3 phosphorylation, cellular adhesion, and total protein expression of  $\alpha$ SMA, collagen III, and collagen V. Furthermore, I observed that TGF $\beta$  downregulates CDCP1 expression on the cell surface as well as total protein and mRNA levels and that this effect might be mediated via increased ubiquitin-independent degradation of CDCP1 in the proteasome. Therefore, my data suggest that a negative feedback loop between CDCP1 and TGF $\beta$  signaling exists by which CDCP1 negatively regulates TGF $\beta$  signaling in the context of fibroblasts to myofibroblasts transdifferentiation.

Taken together, my thesis revealed that TGF $\beta$  alters the expression of the surface proteins PDGFR $\alpha$  and CDCP1 which in turn impacts their downstream signaling and finally cellular functions in lung fibroblasts strongly contributing to a profibrotic phenotype.

This study thus highlights the importance of transmembrane proteins in fibroblasts biology, including processes essential to wound healing and their pathophysiological consequences in lung fibrosis.

## 6 CONCLUSION AND FUTURE DIRECTIONS

In my thesis I identified PDGFR $\alpha$  and CDCP1, two markers originally detected in a surface proteome analysis of phLFs in the presence/absence of TGF $\beta$ , to essentially take part in myofibroblast differentiation and strongly supporting the profibrotic phenotype, thereby interfering with TGF $\beta$  signaling. I investigated the consequence of their impaired expression by TGF $\beta$  on downstream signaling, and/or functional role in primary human lung fibroblasts.

In particular, my data show that TGF $\beta$  alters not only the expression, but also downstream PDGFR $\alpha$  signaling which in turn leads to fibroblasts activation and thus enhanced ECM expression and secretion. Importantly, this effect occurs via a synergic cross-talk between PDGF and TGF $\beta$  signaling pathways. In the presence of TGF $\beta$ , Nintedanib was not able to block PDGF signaling which also resulted in increased ECM production and myofibroblasts differentiation. It is therefore important to test in future studies if patients with high TGF $\beta$  levels might respond to Nintedanib or instead need a special medical treatment additionally targeting TGF $\beta$ . In future, more mechanistic studies unraveling the cross-talk between PDGF and TGF $\beta$  signaling are necessary to identify signal transducers taking part in this process.

In the second part of my thesis, my data indicate that a negative feedback loop between CDCP1 and TGF $\beta$  pathway exists by which CDCP1 contributes to fibroblasts activation and increased ECM expression. However, there is still limited information regarding CDCP1 signaling and its impact on fibroblast function. Therefore, further work is required to investigate the mechanism behind CDCP1 and TGF $\beta$  pathway interaction, in particular which signal transducers mediate downstream CDCP1 signaling and take part in cross-talk with TGF $\beta$  pathway. This would be addressed by performing phosphoproteomics of CDCP1-depleted cells and identification of novel molecules and kinases of downstream CDCP1 signaling in primary human lung fibroblasts. Additionally, of importance is to investigate how TGF $\beta$  downregulates CDCP1 expression on a transcription level. This would be addressed by using specific inhibitors or antagonists targeting CDCP1 transcription factors, in particular those regulated by TGF $\beta$ , such as GR, C/EBP beta, or PPAR gamma and would further provide an insight whether TGF $\beta$  regulates CDCP1 expression on different cellular levels in primary human lung fibroblasts.

PDGF signaling is a well-known profibrotic signaling pathway in IPF, and therefore several tyrosine kinase inhibitors, including Nintedanib were designed to block the kinase activity of PDGF receptors in lung fibrosis. On the other hand, the clinical relevance of CDCP1 in IPF has not been investigated to date. Therefore, overexpression of CDCP1 in lung fibroblasts followed by immunoblot analysis of total protein levels of  $\alpha$ SMA and ECM components in the presence or absence of TGF $\beta$  would be interesting to do. Finally, a clinical relevance of CDCP1 could be translated in *in vivo* situation by administrating bleomycin to CDCP1-homozygous or heterozygous mice with subsequent analysis whether CDCP1 depletion protects or promotes manifestation of lung fibrosis in those mice.

Although TGF $\beta$  is one of the most intensively studied profibrotic cytokine in IPF, it might be interesting to explore if other well-known cytokines taking part in IPF, such as PDGF, Wnt, or EGF ligands, interact with CDCP1 in pHLFs. My data also confirmed and supported existing data that the surface proteome essentially contributes to a profibrotic phenotype of fibroblasts and is significantly regulated by cytokines. The surface proteome screen revealed the surface proteins Layilin, Glypican 1, FLRT3, and FERMT2, all of them not associated yet with fibroblasts or fibrosis. Thus, their role and importance in lung fibrosis have to be uncovered. Finally, future studies analyzing signaling and protein dynamics on the surface are important to identify specific fibroblasts surface markers involved in chronic lung diseases.

## 7 REFERENCES

- Abdollahi A, Li M, Ping G, Plathow C, Domhan S, Kiessling F, Lee LB, McMahon G, Gröne H-J, Lipson KE, Huber PE. 2005. Inhibition of platelet-derived growth factor signaling attenuates pulmonary fibrosis. *J. Exp. Med.* 201: 925–35.
- Alder JK, Chen JJ-L, Lancaster L, Danoff S, Su S -c., Cogan JD, Vulto I, Xie M, Qi X, Tudor RM, Phillips JA, Lansdorp PM, Loyd JE, Armanios MY. 2008. Short telomeres are a risk factor for idiopathic pulmonary fibrosis. *Proc. Natl. Acad. Sci.* 105: 13051–13056.
- Allen JT, Spiteri MA. 2002. Growth factors in idiopathic pulmonary fibrosis: relative roles. *Respir. Res.* 3: 13.
- Alvarez RH, Kantarjian HM, Cortes JE. 2006. Biology of Platelet-Derived Growth Factor and Its Involvement in Disease. *Mayo Clin. Proc.* 81: 1241–1257.
- American Thoracic Society, European Respiratory Society. 2002. American Thoracic Society/European Respiratory Society International Multidisciplinary Consensus Classification of the Idiopathic Interstitial Pneumonias. This joint statement of the American Thoracic Society (ATS), and the European Respiratory Society (ERS) was adopted by the ATS board of directors, June 2001 and by the ERS Executive Committee, June 2001. *Am. J. Respir. Crit. Care Med.* 165: 277–304.
- Andrae J, Gallini R, Betsholtz C. 2008. Role of platelet-derived growth factors in physiology and medicine. *Genes Dev.* 22: 1276–312.
- Annes JP, Munger JS, Rifkin DB. 2003. Making sense of latent TGFbeta activation. *J. Cell Sci.* 116: 217–24.
- Annesi-Maesano I, Nunes H, Duchemann B, Valeyre D, Agabiti N, Saltini C, Porretta MA. 2013. Epidemiology of idiopathic pulmonary fibrosis in Europe--an update. *Sarcoidosis, Vasc. Diffus. lung Dis. Off. J. WASOG* 30 Suppl 1: 6–12.
- Antoniou SA. 2012. Nintedanib (BIBF 1120) for IPF: a tomorrow therapy? *Multidiscip. Respir. Med.* 7: 41.
- Aono Y, Kishi M, Yokota Y, Azuma M, Kinoshita K, Takezaki A, Sato S, Kawano H, Kishi J, Goto H, Uehara H, Izumi K, Nishioka Y. 2014. Role of PDGF/PDGFR Axis in the Trafficking of Circulating Fibrocytes in Pulmonary Fibrosis. *Am. J. Respir. Cell Mol. Biol.*
- Armanios M. 2009. Syndromes of Telomere Shortening. *Annu. Rev. Genomics Hum. Genet.* 10: 45–61.
- Armanios MY, Chen JJ-L, Cogan JD, Alder JK, Ingersoll RG, Markin C, Lawson WE, Xie M, Vulto I, Phillips JA, Lansdorp PM, Greider CW, Loyd JE. 2007. Telomerase mutations in families with idiopathic pulmonary fibrosis. *N. Engl. J. Med.* 356: 1317–26.
- Asher G, Tsvetkov P, Kahana C, Shaul Y. 2005. A mechanism of ubiquitin-independent proteasomal degradation of the tumor suppressors p53 and p73. *Genes Dev.* 19: 316–21.

- Atkins CP, Gilbert D, Brockwell C, Robinson S, Wilson AM. 2016. Fatigue in sarcoidosis and idiopathic pulmonary fibrosis: differences in character and severity between diseases. *Sarcoidosis, Vasc. Diffus. lung Dis. Off. J. WASOG* 33: 130–8.
- Attisano L, Silvestri C, Izzi L, Labbé E. 2001. The transcriptional role of Smads and FAST (FoxH1) in TGFbeta and activin signalling. *Mol. Cell. Endocrinol.* 180: 3–11.
- Azuma A, Nukiwa T, Tsuboi E, Suga M, Abe S, Nakata K, Taguchi Y, Nagai S, Itoh H, Ohi M, Sato A, Kudoh S. 2005. Double-blind, placebo-controlled trial of pirfenidone in patients with idiopathic pulmonary fibrosis. *Am. J. Respir. Crit. Care Med.* 171: 1040–7.
- Bainbridge P. 2013. Wound healing and the role of fibroblasts. *J. Wound Care* 22: 407–412.
- Bauer Y, White ES, de Bernard S, Cornelisse P, Leconte I, Morganti A, Roux S, Nayler O. 2017. MMP-7 is a predictive biomarker of disease progression in patients with idiopathic pulmonary fibrosis. *ERJ Open Res.* 3: 00074–02016.
- Baum J, Duffy HS. 2011. Fibroblasts and myofibroblasts: what are we talking about? *J. Cardiovasc. Pharmacol.* 57: 376–9.
- Behr J. 2013. The diagnosis and treatment of idiopathic pulmonary fibrosis. *Dtsch. Arztebl. Int.* 110: 875–81.
- Behr J, Günther A, Ammenwerth W, Bittmann I, Bonnet R, Buhl R, Eickelberg O, Ewert R, Gläser S, Gottlieb J, Grohé C, Kreuter M, Kroegel C, Markart P, Neurohr C, Pfeifer M, Prasse A, Schönfeld N, Schreiber J, Sitter H, Theegarten D, Theile A, Wilke A, Wirtz H, Witt C, Worth H, Zabel P, Müller-Quernheim J, Costabel U. 2013. [German guideline for diagnosis and management of idiopathic pulmonary fibrosis]. *Pneumologie* 67: 81–111.
- Benes CH, Poulogiannis G, Cantley LC, Soltoff SP. 2012. The SRC-associated protein CUB Domain-Containing Protein-1 regulates adhesion and motility. *Oncogene* 31: 653–63.
- Bergsten E, Uutela M, Li X, Pietras K, Ostman A, Heldin CH, Alitalo K, Eriksson U. 2001. PDGF-D is a specific, protease-activated ligand for the PDGF beta-receptor. *Nat. Cell Biol.* 3: 512–6.
- Beyer C, Distler JHW. 2013. Tyrosine kinase signaling in fibrotic disorders: Translation of basic research to human disease. *Biochim. Biophys. Acta* 1832: 897–904.
- Bhatt AS, Erdjument-Bromage H, Tempst P, Craik CS, Moasser MM. 2005. Adhesion signaling by a novel mitotic substrate of src kinases. *Oncogene* 24: 5333–43.
- Bissell DM, Wang SS, Jarnagin WR, Roll FJ. 1995. Cell-specific expression of transforming growth factor-beta in rat liver. Evidence for autocrine regulation of hepatocyte proliferation. *J. Clin. Invest.* 96: 447–455.
- Bonner JC. 2004a. Regulation of PDGF and its receptors in fibrotic diseases. *Cytokine Growth Factor Rev.* 15: 255–273.

- Bonner JC. 2004b. Regulation of PDGF and its receptors in fibrotic diseases. *Cytokine Growth Factor Rev.* 15: 255–73.
- Bonner JC, Badgett A, Lindroos PM, Osornio-Vargas AR. 1995. Transforming growth factor beta 1 downregulates the platelet-derived growth factor alpha-receptor subtype on human lung fibroblasts in vitro. *Am. J. Respir. Cell Mol. Biol.* 13: 496–505.
- Boström H, Gritli-Linde A, Betsholtz C. 2002. PDGF-A/PDGF alpha-receptor signaling is required for lung growth and the formation of alveoli but not for early lung branching morphogenesis. *Dev. Dyn.* 223: 155–62.
- Boucher RC. 2011. Idiopathic pulmonary fibrosis--a sticky business. *N. Engl. J. Med.* 364: 1560–1.
- Brown TA, Yang TM, Zaitsevskaja T, Xia Y, Dunn CA, Sigle RO, Knudsen B, Carter WG. 2004a. Adhesion or plasmin regulates tyrosine phosphorylation of a novel membrane glycoprotein p80/gp140/CUB domain-containing protein 1 in epithelia. *J. Biol. Chem.* 279: 14772–83.
- Brown TA, Yang TM, Zaitsevskaja T, Xia Y, Dunn CA, Sigle RO, Knudsen B, Carter WG. 2004b. Adhesion or plasmin regulates tyrosine phosphorylation of a novel membrane glycoprotein p80/gp140/CUB domain-containing protein 1 in epithelia. *J. Biol. Chem.* 279: 14772–83.
- Buhring H-J, Kuçi S, Conze T, Rathke G, Bartolović K, Grünebach F, Scherl-Mostageer M, Brümmendorf TH, Schweifer N, Lammers R. 2004. CDCP1 Identifies a Broad Spectrum of Normal and Malignant Stem/Progenitor Cell Subsets of Hematopoietic and Nonhematopoietic Origin. *Stem Cells* 22: 334–343.
- Bühring H-J, Kuçi S, Conze T, Rathke G, Bartolović K, Grünebach F, Scherl-Mostageer M, Brümmendorf TH, Schweifer N, Lammers R. 2004. CDCP1 identifies a broad spectrum of normal and malignant stem/progenitor cell subsets of hematopoietic and nonhematopoietic origin. *Stem Cells* 22: 334–43.
- Buchdunger E, O'Reilly T, Wood J. 2002. Pharmacology of imatinib (STI571). *Eur. J. Cancer* 38 Suppl 5: S28–36.
- Burgstaller G, Oehrle B, Koch I, Lindner M, Eickelberg O. 2013. Multiplex Profiling of Cellular Invasion in 3D Cell Culture Models. *PLoS One* 8: e63121.
- Cao R, Bråkenhielm E, Li X, Pietras K, Widenfalk J, Ostman A, Eriksson U, Cao Y. 2002. Angiogenesis stimulated by PDGF-CC, a novel member in the PDGF family, involves activation of PDGFR-alphaalpha and -alphabeta receptors. *FASEB J.* 16: 1575–83.
- Carrington CB, Gaensler EA, Coutu RE, FitzGerald MX, Gupta RG. 1978. Natural History and Treated Course of Usual and Desquamative Interstitial Pneumonia. *N. Engl. J. Med.* 298: 801–809.
- Casar B, Rimann I, Kato H, Shattil SJ, Quigley JP, Deryugina EI. 2014. In vivo cleaved CDCP1 promotes early tumor dissemination via complexing with activated  $\beta$ 1 integrin and induction of FAK/PI3K/Akt motility signaling. *Oncogene* 33: 255–68.

- Claesson-Welsh L, Eriksson A, Westermark B, Heldin CH. 1989. cDNA cloning and expression of the human A-type platelet-derived growth factor (PDGF) receptor establishes structural similarity to the B-type PDGF receptor. *Proc. Natl. Acad. Sci. U. S. A.* 86: 4917–21.
- Coen M, Gabbiani G, Bochaton-Piallat M-L, Chen YE. 2011. Myofibroblast-Mediated Adventitial Remodeling: An Underestimated Player in Arterial Pathology. *Arterioscler. Thromb. Vasc. Biol.* 31: 2391–2396.
- Collard HR, Ward AJ, Lanes S, Courtney Hayflinger D, Rosenberg DM, Hunsche E. 2012. Burden of illness in idiopathic pulmonary fibrosis. *J. Med. Econ.* 15: 829–35.
- Coward WR, Watts K, Feghali-Bostwick CA, Jenkins G, Pang L. 2010. Repression of IP-10 by interactions between histone deacetylation and hypermethylation in idiopathic pulmonary fibrosis. *Mol. Cell. Biol.* 30: 2874–86.
- Cronkhite JT, Xing C, Raghu G, Chin KM, Torres F, Rosenblatt RL, Garcia CK. 2008. Telomere shortening in familial and sporadic pulmonary fibrosis. *Am. J. Respir. Crit. Care Med.* 178: 729–37.
- Daccord C, Maher TM. 2016. Recent advances in understanding idiopathic pulmonary fibrosis. *F1000Research* 5.
- Daniels CE, Lasky JA, Limper AH, Mieras K, Gabor E, Schroeder DR. 2010. Imatinib treatment for idiopathic pulmonary fibrosis: Randomized placebo-controlled trial results. *Am. J. Respir. Crit. Care Med.* 181: 604–10.
- Davies M, Robinson M, Smith E, Huntley S, Prime S, Paterson I. 2005. Induction of an epithelial to mesenchymal transition in human immortal and malignant keratinocytes by TGF- $\beta$ 1 involves MAPK, Smad and AP-1 signalling pathways. *J. Cell. Biochem.* 95: 918–931.
- Day E, Waters B, Spiegel K, Alnadaf T, Manley PW, Buchdunger E, Walker C, Jarai G. 2008. Inhibition of collagen-induced discoidin domain receptor 1 and 2 activation by imatinib, nilotinib and dasatinib. *Eur. J. Pharmacol.* 599: 44–53.
- Dennler S, Itoh S, Vivien D, ten Dijke P, Huet S, Gauthier JM. 1998. Direct binding of Smad3 and Smad4 to critical TGF beta-inducible elements in the promoter of human plasminogen activator inhibitor-type 1 gene. *EMBO J.* 17: 3091–100.
- Derynck R, Feng XH. 1997. TGF-beta receptor signaling. *Biochim. Biophys. Acta* 1333: F105-50.
- Derynck R, Zhang YE. 2003. Smad-dependent and Smad-independent pathways in TGF-beta family signalling. *Nature* 425: 577–84.
- Deryugina EI, Conn EM, Wortmann A, Partridge JJ, Kupriyanova TA, Ardi VC, Hooper JD, Quigley JP. 2009. Functional role of cell surface CUB domain-containing protein 1 in tumor cell dissemination. *Mol. Cancer Res.* 7: 1197–211.
- Desmoulière A, Redard M, Darby I, Gabbiani G. 1995. Apoptosis mediates the decrease in cellularity during

- the transition between granulation tissue and scar. *Am. J. Pathol.* 146: 56–66.
- Dewar AL, Domaschek RM, Doherty K V, Hughes TP, Lyons AB. 2003. Imatinib inhibits the in vitro development of the monocyte/macrophage lineage from normal human bone marrow progenitors. *Leukemia* 17: 1713–21.
- Donovan J, Shiwen X, Norman J, Abraham D. 2013. Platelet-derived growth factor alpha and beta receptors have overlapping functional activities towards fibroblasts. *Fibrogenesis Tissue Repair* 6: 10.
- Dranoff JA, Wells RG. 2010. Portal fibroblasts: Underappreciated mediators of biliary fibrosis. *Hepatology* 51: 1438–1444.
- Dreisin RB, Schwarz MI, Theofilopoulos AN, Stanford RE. 1978. Circulating immune complexes in the idiopathic interstitial pneumonias. *N. Engl. J. Med.* 298: 353–7.
- Dugina V, Fontao L, Chaponnier C, Vasiliev J, Gabbiani G. 2001. Focal adhesion features during myofibroblastic differentiation are controlled by intracellular and extracellular factors. *J. Cell Sci.* 114: 3285–96.
- Eickelberg O, Laurent GJ. 2010. The Quest for the Initial Lesion in Idiopathic Pulmonary Fibrosis. *Am. J. Respir. Cell Mol. Biol.* 42: 1–2.
- Elmufdi F, Henke CA, Perlman DM, Tomic R, Kim HJ. 2015. Novel mechanisms and treatment of idiopathic pulmonary fibrosis. *Discov. Med.* 20: 145–53.
- Emerling BM, Benes CH, Poulogiannis G, Bell EL, Courtney K, Liu H, Choo-Wing R, Bellinger G, Tsukazawa KS, Brown V, Signoretti S, Soltoff SP, Cantley LC. 2013. Identification of CDCP1 as a hypoxia-inducible factor 2 $\alpha$  (HIF-2 $\alpha$ ) target gene that is associated with survival in clear cell renal cell carcinoma patients. *Proc. Natl. Acad. Sci. U. S. A.* 110: 3483–8.
- Engel ME, McDonnell MA, Law BK, Moses HL. 1999. Interdependent SMAD and JNK signaling in transforming growth factor-beta-mediated transcription. *J. Biol. Chem.* 274: 37413–20.
- Enomoto N, Suda T, Kato M, Kaida Y, Nakamura Y, Imokawa S, Ida M, Chida K. 2006. Quantitative analysis of fibroblastic foci in usual interstitial pneumonia. *Chest* 130: 22–9.
- Erler JT, Weaver VM. 2009. Three-dimensional context regulation of metastasis. *Clin. Exp. Metastasis* 26: 35–49.
- Farràs R, Bossis G, Andermarcher E, Jariel-Encontre I, Piechaczyk M. 2005. Mechanisms of delivery of ubiquitylated proteins to the proteasome: new target for anti-cancer therapy? *Crit. Rev. Oncol. Hematol.* 54: 31–51.
- Feng X-H, Derynck R. 2005. SPECIFICITY AND VERSATILITY IN TGF- $\beta$  SIGNALING THROUGH SMADS. *Annu. Rev. Cell Dev. Biol.* 21: 659–693.
- Feng XH, Derynck R. 1996. Ligand-independent activation of transforming growth factor (TGF) beta signaling pathways by heteromeric cytoplasmic domains of TGF-beta receptors. *J. Biol. Chem.* 271:

13123–9.

- Fernandez IE, Eickelberg O. 2012a. New cellular and molecular mechanisms of lung injury and fibrosis in idiopathic pulmonary fibrosis. *Lancet* 380: 680–688.
- Fernandez IE, Eickelberg O. 2012b. New cellular and molecular mechanisms of lung injury and fibrosis in idiopathic pulmonary fibrosis. *Lancet (London, England)* 380: 680–8.
- Fernandez IE, Eickelberg O. The Impact of TGF- $\beta$  on Lung Fibrosis.
- Fernández Pérez ER, Daniels CE, Schroeder DR, St Sauver J, Hartman TE, Bartholmai BJ, Yi ES, Ryu JH. 2010. Incidence, prevalence, and clinical course of idiopathic pulmonary fibrosis: a population-based study. *Chest* 137: 129–37.
- Flaherty KR, Mumford JA, Murray S, Kazerooni EA, Gross BH, Colby T V., Travis WD, Flint A, Toews GB, Lynch JP, Martinez FJ. 2003. Prognostic Implications of Physiologic and Radiographic Changes in Idiopathic Interstitial Pneumonia. *Am. J. Respir. Crit. Care Med.* 168: 543–548.
- Frey RS, Mulder KM. 1997. Involvement of extracellular signal-regulated kinase 2 and stress-activated protein kinase/Jun N-terminal kinase activation by transforming growth factor beta in the negative growth control of breast cancer cells. *Cancer Res.* 57: 628–33.
- Garneau-Tsodikova S, Thannickal VJ. 2008. Protein kinase inhibitors in the treatment of pulmonary fibrosis. *Curr. Med. Chem.* 15: 2632–40.
- Gelse K, Pöschl E, Aigner T. 2003. Collagens--structure, function, and biosynthesis. *Adv. Drug Deliv. Rev.* 55: 1531–46.
- Gilbertson DG, Duff ME, West JW, Kelly JD, Sheppard PO, Hofstrand PD, Gao Z, Shoemaker K, Bukowski TR, Moore M, Feldhaus AL, Humes JM, Palmer TE, Hart CE. 2001. Platelet-derived growth factor C (PDGF-C), a novel growth factor that binds to PDGF alpha and beta receptor. *J. Biol. Chem.* 276: 27406–14.
- Glanville AR, Estenne M. 2003. Indications, patient selection and timing of referral for lung transplantation. *Eur. Respir. J.* 22: 845–52.
- Glickman MH, Ciechanover A. 2002. The Ubiquitin-Proteasome Proteolytic Pathway: Destruction for the Sake of Construction. *Physiol. Rev.* 82: 373–428.
- Glickman MH, Raveh D. 2005. Proteasome plasticity. *FEBS Lett.* 579: 3214–23.
- Goldstein RH, Polgar P. 1982. The effect and interaction of bradykinin and prostaglandins on protein and collagen production by lung fibroblasts. *J. Biol. Chem.* 257: 8630–3.
- Greiffio FR, Eickelberg O, Fernandez IE. 2017. Systems medicine advances in interstitial lung disease. *Eur. Respir. Rev.* 26: 170021.
- Grice GL, Nathan JA. 2016. The recognition of ubiquitinated proteins by the proteasome. *Cell. Mol. Life Sci.* 73: 3497–3506.

- Gronwald R, Seifert R, Bowen-Pope D. 1989. Differential regulation of expression of two platelet-derived growth factor receptor subunits by transforming growth factor-beta. *J. Biol. Chem.* 264: 8120–8125.
- Gross TJ, Hunninghake GW. 2001. Idiopathic Pulmonary Fibrosis. *N. Engl. J. Med.* 345: 517–525.
- Grotendorst GR, Smale G, Pancev D. 1989. Production of transforming growth factor beta by human peripheral blood monocytes and neutrophils. *J. Cell. Physiol.* 140: 396–402.
- Guiot J, Moermans C, Henket M, Corhay J-L, Louis R. 2017. Blood Biomarkers in Idiopathic Pulmonary Fibrosis. *Lung* 195: 273–280.
- Guo X, Wang X-F. 2009. Signaling cross-talk between TGF-beta/BMP and other pathways. *Cell Res.* 19: 71–88.
- Haglund K, Dikic I. 2005. Ubiquitylation and cell signaling. *EMBO J.* 24: 3353–3359.
- Halfon S, Abramov N, Grinblat B, Ginis I. 2011. Markers distinguishing mesenchymal stem cells from fibroblasts are downregulated with passaging. *Stem Cells Dev.* 20: 53–66.
- Hall M-C, Young DA, Waters JG, Rowan AD, Chantry A, Edwards DR, Clark IM. 2003. The comparative role of activator protein 1 and Smad factors in the regulation of Timp-1 and MMP-1 gene expression by transforming growth factor-beta 1. *J. Biol. Chem.* 278: 10304–13.
- Hambly N, Shimbori C, Kolb M. 2015. Molecular classification of idiopathic pulmonary fibrosis: Personalized medicine, genetics and biomarkers. *Respirology* 20: 1010–1022.
- Hanna C, Hubchak SC, Liang X, Rozen-Zvi B, Schumacker PT, Hayashida T, Schnaper HW. 2013. Hypoxia-inducible factor-2 $\alpha$  and TGF- $\beta$  signaling interact to promote normoxic glomerular fibrogenesis. *Am. J. Physiol. Renal Physiol.* 305: F1323–31.
- Hansell DM, Bankier AA, MacMahon H, McLoud TC, Müller NL, Remy J. 2008. Fleischner Society: Glossary of Terms for Thoracic Imaging. *Radiology* 246: 697–722.
- Heeneman S, Haendeler J, Saito Y, Ishida M, Berk BC. 2000. Angiotensin II induces transactivation of two different populations of the platelet-derived growth factor beta receptor. Key role for the p66 adaptor protein Shc. *J. Biol. Chem.* 275: 15926–32.
- Heinzelmann K, Noskovičová N, Merl-Pham J, Preissler G, Winter H, Lindner M, Hatz R, Hauck SM, Behr J, Eickelberg O. 2016. Surface proteome analysis identifies platelet derived growth factor receptor-alpha as a critical mediator of transforming growth factor-beta-induced collagen secretion. *Int. J. Biochem. Cell Biol.* 74: 44–59.
- Heldin C-H. 2013. Targeting the PDGF signaling pathway in tumor treatment. *Cell Commun. Signal.* 11: 97.
- Heldin C-H, Eriksson U, Östman A. 2002. New Members of the Platelet-Derived Growth Factor Family of Mitogens. *Arch. Biochem. Biophys.* 398: 284–290.
- Heldin C-H, Lennartsson J. 2013. Structural and functional properties of platelet-derived growth factor and

- stem cell factor receptors. *Cold Spring Harb. Perspect. Biol.* 5: a009100.
- Heldin CH, Bäckström G, Ostman A, Hammacher A, Rönstrand L, Rubin K, Nistér M, Westermark B. 1988. Binding of different dimeric forms of PDGF to human fibroblasts: evidence for two separate receptor types. *EMBO J.* 7: 1387–93.
- Heldin CH, Westermark B. 1999. Mechanism of action and in vivo role of platelet-derived growth factor. *Physiol. Rev.* 79: 1283–316.
- Helling BA, Gerber AN, Kadiyala V, Sasse SK, Pedersen BS, Sparks L, Nakano Y, Okamoto T, Evans CM, Yang I V., Schwartz DA. 2017a. Regulation of *MUC5B* Expression in Idiopathic Pulmonary Fibrosis. *Am. J. Respir. Cell Mol. Biol.* 57: 91–99.
- Helling BA, Gerber AN, Kadiyala V, Sasse SK, Pedersen BS, Sparks L, Nakano Y, Okamoto T, Evans CM, Yang I V., Schwartz DA. 2017b. Regulation of *MUC5B* Expression in Idiopathic Pulmonary Fibrosis. *Am. J. Respir. Cell Mol. Biol.* 57: 91–99.
- Henderson NC, Arnold TD, Katamura Y, Giacomini MM, Rodriguez JD, McCarty JH, Pellicoro A, Raschperger E, Betsholtz C, Ruminski PG, Griggs DW, Prinsen MJ, Maher JJ, Iredale JP, Lacy-Hulbert A, Adams RH, Sheppard D. 2013. Targeting of  $\alpha$ v integrin identifies a core molecular pathway that regulates fibrosis in several organs. *Nat. Med.* 19: 1617–1624.
- Herzog EL, Bucala R. 2010. Fibrocytes in health and disease. *Exp. Hematol.* 38: 548–556.
- Hinz B. 2007. Formation and Function of the Myofibroblast during Tissue Repair. *J. Invest. Dermatol.* 127: 526–537.
- Hinz B. 2012. Mechanical Aspects of Lung Fibrosis. *Proc. Am. Thorac. Soc.* 9: 137–147.
- Hinz B. 2016. Myofibroblasts. *Exp. Eye Res.* 142: 56–70.
- Hinz B. 2015. The extracellular matrix and transforming growth factor- $\beta$ 1: Tale of a strained relationship. *Matrix Biol.* 47: 54–65.
- Hinz B, Celetta G, Tomasek JJ, Gabbiani G, Chaponnier C. 2001a. Alpha-smooth muscle actin expression upregulates fibroblast contractile activity. *Mol. Biol. Cell* 12: 2730–41.
- Hinz B, Celetta G, Tomasek JJ, Gabbiani G, Chaponnier C. 2001b. Alpha-smooth muscle actin expression upregulates fibroblast contractile activity. *Mol. Biol. Cell* 12: 2730–41.
- Hinz B, Dugina V, Ballestrem C, Wehrle-Haller B, Chaponnier C. 2003. Alpha-smooth muscle actin is crucial for focal adhesion maturation in myofibroblasts. *Mol. Biol. Cell* 14: 2508–19.
- Hinz B, Phan SH, Thannickal VJ, Galli A, Bochaton-Piallat M-L, Gabbiani G. 2007a. The Myofibroblast. *Am. J. Pathol.* 170: 1807–1816.
- Hinz B, Phan SH, Thannickal VJ, Galli A, Bochaton-Piallat M-L, Gabbiani G. 2007b. The myofibroblast: one function, multiple origins. *Am. J. Pathol.* 170: 1807–16.
- Hisatomi K, Mukae H, Sakamoto N, Ishimatsu Y, Kakugawa T, Hara S, Fujita H, Nakamichi S, Oku H,

- Urata Y, Kubota H, Nagata K, Kohno S. 2012. Pirfenidone inhibits TGF- $\beta$ 1-induced over-expression of collagen type I and heat shock protein 47 in A549 cells. *BMC Pulm. Med.* 12: 24.
- Hocevar BA, Brown TL, Howe PH. 1999. TGF- $\beta$  induces fibronectin synthesis through a c-Jun N-terminal kinase-dependent, Smad4-independent pathway. *EMBO J.* 18: 1345–56.
- Honda E, Yoshida K, Munakata H. 2010. Transforming growth factor- $\beta$  upregulates the expression of integrin and related proteins in MRC-5 human myofibroblasts. *Tohoku J. Exp. Med.* 220: 319–27.
- Hooper JD, Zijlstra A, Aimes RT, Liang H, Claassen GF, Tarin D, Testa JE, Quigley JP. 2003. Subtractive immunization using highly metastatic human tumor cells identifies SIMA135/CDCP1, a 135 kDa cell surface phosphorylated glycoprotein antigen. *Oncogene* 22: 1783–94.
- Hope-Gill BDM, Hilldrup S, Davies C, Newton RP, Harrison NK. 2003. A Study of the Cough Reflex in Idiopathic Pulmonary Fibrosis. *Am. J. Respir. Crit. Care Med.* 168: 995–1002.
- Horowitz JC, Lee DY, Waghray M, Keshamouni VG, Thomas PE, Zhang H, Cui Z, Thannickal VJ. 2004. Activation of the pro-survival phosphatidylinositol 3-kinase/AKT pathway by transforming growth factor- $\beta$ 1 in mesenchymal cells is mediated by p38 MAPK-dependent induction of an autocrine growth factor. *J. Biol. Chem.* 279: 1359–67.
- Hostettler KE, Zhong J, Papakonstantinou E, Karakiulakis G, Tamm M, Seidel P, Sun Q, Mandal J, Lardinois D, Lambers C, Roth M. 2014. Anti-fibrotic effects of nintedanib in lung fibroblasts derived from patients with idiopathic pulmonary fibrosis. *Respir. Res.* 15: 157.
- Hu B, Gharaee-Kermani M, Wu Z, Phan SH. 2010. Epigenetic Regulation of Myofibroblast Differentiation by DNA Methylation. *Am. J. Pathol.* 177: 21–28.
- Hu B, Wu Z, Phan SH. 2003. Smad3 Mediates Transforming Growth Factor- $\beta$ -Induced  $\alpha$ -Smooth Muscle Actin Expression. *Am. J. Respir. Cell Mol. Biol.* 29: 397–404.
- Hubbard R, Lewis S, Richards K, Johnston I, Britton J. 1996. Occupational exposure to metal or wood dust and aetiology of cryptogenic fibrosing alveolitis. *Lancet (London, England)* 347: 284–9.
- Humphreys BD, Lin S-L, Kobayashi A, Hudson TE, Nowlin BT, Bonventre J V., Valerius MT, McMahon AP, Duffield JS. 2010. Fate Tracing Reveals the Pericyte and Not Epithelial Origin of Myofibroblasts in Kidney Fibrosis. *Am. J. Pathol.* 176: 85–97.
- Chambers RC, Scotton CJ. 2012. Coagulation cascade proteinases in lung injury and fibrosis. *Proc. Am. Thorac. Soc.* 9: 96–101.
- Chapman HA. 2011. Epithelial-Mesenchymal Interactions in Pulmonary Fibrosis. *Annu. Rev. Physiol.* 73: 413–435.
- Chen P-H, Chen X, He X. 2013. Platelet-derived growth factors and their receptors: structural and functional perspectives. *Biochim. Biophys. Acta* 1834: 2176–86.
- Chiu K-L, Kuo T-T, Kuok Q-Y, Lin Y-S, Hua C-H, Lin C-Y, Su P-Y, Lai L-C, Sher Y-P. 2015. ADAM9

- enhances CDCP1 protein expression by suppressing miR-218 for lung tumor metastasis. *Sci. Rep.* 5: 16426.
- Chung KF, Pavord ID. 2008. Prevalence, pathogenesis, and causes of chronic cough. *Lancet* (London, England) 371: 1364–74.
- Ignatz RA, Massagué J. 1986. Transforming growth factor-beta stimulates the expression of fibronectin and collagen and their incorporation into the extracellular matrix. *J. Biol. Chem.* 261: 4337–45.
- Ikeda J, Oda T, Inoue M, Uekita T, Sakai R, Okumura M, Aozasa K, Morii E. 2009. Expression of CUB domain containing protein (CDCP1) is correlated with prognosis and survival of patients with adenocarcinoma of lung. *Cancer Sci.* 100: 429–33.
- Itoh S, Itoh F, Goumans MJ, Ten Dijke P. 2000. Signaling of transforming growth factor-beta family members through Smad proteins. *Eur. J. Biochem.* 267: 6954–67.
- Ivarsson M, McWhirter A, Borg TK, Rubin K. 1998. Type I collagen synthesis in cultured human fibroblasts: regulation by cell spreading, platelet-derived growth factor and interactions with collagen fibers. *Matrix Biol.* 16: 409–25.
- Iwai K, Mori T, Yamada N, Yamaguchi M, Hosoda Y. 1994. Idiopathic pulmonary fibrosis. Epidemiologic approaches to occupational exposure. *Am. J. Respir. Crit. Care Med.* 150: 670–675.
- Jariel-Encontre I, Bossis G, Piechaczyk M. 2008. Ubiquitin-independent degradation of proteins by the proteasome. *Biochim. Biophys. Acta - Rev. Cancer* 1786: 153–177.
- Jiang WG, Sanders AJ, Katoh M, Ungefroren H, Gieseler F, Prince M, Thompson SK, Zollo M, Spano D, Dhawan P, Sliva D, Subbarayan PR, Sarkar M, Honoki K, Fujii H, Georgakilas AG, Amedei A, Niccolai E, Amin A, Ashraf SS, Ye L, Helferich WG, Yang X, Boosani CS, Guha G, Ciriolo MR, Aquilano K, Chen S, Azmi AS, Keith WN, Bilisland A, Bhakta D, Halicka D, Newsheer S, Pantano F, Santini D. 2015. Tissue invasion and metastasis: Molecular, biological and clinical perspectives. *Semin. Cancer Biol.* 35 Suppl: S244–S275.
- Kanakaraj P, Raj S, Khan SA, Bishayee S. 1991. Ligand-induced interaction between alpha- and beta-type platelet-derived growth factor (PDGF) receptors: role of receptor heterodimers in kinase activation. *Biochemistry* 30: 1761–7.
- Katzenstein A and, Myers J. 1998. Idiopathic Pulmonary Fibrosis. *Am. J. Respir. Crit. Care Med.* 157: 1301–1315.
- Kawabata M, Imamura T, Takase M, Nishihara A, Oeda E, Hanai J, Miyazono K. 1997. Smad6 inhibits signalling by the TGF-beta superfamily. *Nature* 389: 622–626.
- Keeley EC, Mehrad B, Strieter RM. 2011. The role of fibrocytes in fibrotic diseases of the lungs and heart. *Fibrogenesis Tissue Repair* 4: 2.
- Kelley J, Fabisiak JP, Hawes K, Absher M. 1991. Cytokine signaling in lung: transforming growth factor-

- beta secretion by lung fibroblasts. *Am. J. Physiol.* 260: L123-8.
- Kelly M, Kolb M, Bonniaud P, Gauldie J. 2003. Re-evaluation of fibrogenic cytokines in lung fibrosis. *Curr. Pharm. Des.* 9: 39–49.
- Kendall RT, Feghali-Bostwick CA. 2014. Fibroblasts in fibrosis: novel roles and mediators. *Front. Pharmacol.* 5: 123.
- Kenyon NJ, Ward RW, McGrew G, Last JA. 2003. TGF-beta1 causes airway fibrosis and increased collagen I and III mRNA in mice. *Thorax* 58: 772–7.
- Khalil N, O'Connor RN, Flanders KC, Unruh H. 1996. TGF-beta 1, but not TGF-beta 2 or TGF-beta 3, is differentially present in epithelial cells of advanced pulmonary fibrosis: an immunohistochemical study. *Am. J. Respir. Cell Mol. Biol.* 14: 131–138.
- Khalil N, Whitman C, Zuo L, Danielpour D, Greenberg A. 1993a. Regulation of alveolar macrophage transforming growth factor-beta secretion by corticosteroids in bleomycin-induced pulmonary inflammation in the rat. *J. Clin. Invest.* 92: 1812–8.
- Khalil N, Whitman C, Zuo L, Danielpour D, Greenberg A. 1993b. Regulation of alveolar macrophage transforming growth factor-beta secretion by corticosteroids in bleomycin-induced pulmonary inflammation in the rat. *J. Clin. Invest.* 92: 1812–1818.
- Kimani PW, Holmes AJ, Grossmann RE, McGowan SE. 2009. PDGF-Ralpha gene expression predicts proliferation, but PDGF-A suppresses transdifferentiation of neonatal mouse lung myofibroblasts. *Respir. Res.* 10: 119.
- Kimura H, Morii E, Ikeda J-I, Ezoe S, Xu J-X, Nakamichi N, Tomita Y, Shibayama H, Kanakura Y, Aozasa K. 2006. Role of DNA methylation for expression of novel stem cell marker CDCP1 in hematopoietic cells. *Leukemia* 20: 1551–6.
- King TE, Pardo A, Selman M. 2011. Idiopathic pulmonary fibrosis. *Lancet* 378: 1949–1961.
- King TE, Tooze JA, Schwarz MI, Brown KR, Cherniack RM. 2001a. Predicting survival in idiopathic pulmonary fibrosis: scoring system and survival model. *Am. J. Respir. Crit. Care Med.* 164: 1171–81.
- King et al. 2001b. Idiopathic Pulmonary Fibrosis. *Am. J. Respir. Crit. Care Med.* 164: 1025–1032.
- Klingberg F, Hinz B, White ES. 2013. The myofibroblast matrix: implications for tissue repair and fibrosis. *J. Pathol.* 229: 298–309.
- Knüppel L, Ishikawa Y, Aichler M, Heinzelmann K, Hatz R, Behr J, Walch A, Bächinger HP, Eickelberg O, Staab-Weijnitz CA. 2017. A Novel Antifibrotic Mechanism of Nintedanib and Pirfenidone. Inhibition of Collagen Fibril Assembly. *Am. J. Respir. Cell Mol. Biol.* 57: 77–90.
- Kolodsick JE, Peters-Golden M, Larios J, Toews GB, Thannickal VJ, Moore BB. 2003. Prostaglandin E<sub>2</sub> Inhibits Fibroblast to Myofibroblast Transition via E. Prostanoid Receptor 2 Signaling and Cyclic Adenosine Monophosphate Elevation. *Am. J. Respir. Cell Mol. Biol.* 29: 537–544.

- Kong X, Lin Z, Liang D, Fath D, Sang N, Caro J. 2006. Histone Deacetylase Inhibitors Induce VHL and Ubiquitin-Independent Proteasomal Degradation of Hypoxia-Inducible Factor 1. *Mol. Cell. Biol.* 26: 2019–2028.
- Königshoff M, Kramer M, Balsara N, Wilhelm J, Amarie OV, Jahn A, Rose F, Fink L, Seeger W, Schaefer L, Günther A, Eickelberg O. 2009. WNT1-inducible signaling protein-1 mediates pulmonary fibrosis in mice and is upregulated in humans with idiopathic pulmonary fibrosis. *J. Clin. Invest.* 119: 772–87.
- Kotaru C, Schoonover KJ, Trudeau JB, Huynh M-L, Zhou X, Hu H, Wenzel SE. 2006. Regional fibroblast heterogeneity in the lung: implications for remodeling. *Am. J. Respir. Crit. Care Med.* 173: 1208–15.
- Kuang P-P, Zhang X-H, Rich CB, Foster JA, Subramanian M, Goldstein RH. 2007. Activation of elastin transcription by transforming growth factor-beta in human lung fibroblasts. *Am. J. Physiol. Lung Cell. Mol. Physiol.* 292: L944-52.
- Kumar RK, O’Grady R, Maronese SE, Wilson MR. 1996. Epithelial cell-derived transforming growth factor-beta in bleomycin-induced pulmonary injury. *Int. J. Exp. Pathol.* 77: 99–107.
- Langerak AW, van der Linden-van Beurden CA, Versnel MA. 1996. Regulation of differential expression of platelet-derived growth factor alpha- and beta-receptor mRNA in normal and malignant human mesothelial cell lines. *Biochim. Biophys. Acta* 1305: 63–70.
- LaRochelle WJ, Jeffers M, McDonald WF, Chillakuru RA, Giese NA, Lokker NA, Sullivan C, Boldog FL, Yang M, Vernet C, Burgess CE, Fernandes E, Deegler LL, Rittman B, Shimkets J, Shimkets RA, Rothberg JM, Lichenstein HS. 2001. PDGF-D, a new protease-activated growth factor. *Nat. Cell Biol.* 3: 517–21.
- Laurent GJ, McAnulty RJ, Hill M, Chambers R. 2008. Escape from the Matrix: Multiple Mechanisms for Fibroblast Activation in Pulmonary Fibrosis. *Proc. Am. Thorac. Soc.* 5: 311–315.
- Lawler S, Feng XH, Chen RH, Maruoka EM, Turck CW, Griswold-Prenner I, Derynck R. 1997. The type II transforming growth factor-beta receptor autophosphorylates not only on serine and threonine but also on tyrosine residues. *J. Biol. Chem.* 272: 14850–9.
- Lee K, Nelson CM. 2012. New Insights into the Regulation of Epithelial–Mesenchymal Transition and Tissue Fibrosis. In: *International review of cell and molecular biology.*, p 171–221.
- Lehtonen ST, Veijola A, Karvonen H, Lappi-Blanco E, Sormunen R, Korpela S, Zagai U, Sköld MC, Kaarteenaho R. 2016. Pirfenidone and nintedanib modulate properties of fibroblasts and myofibroblasts in idiopathic pulmonary fibrosis. *Respir. Res.* 17: 14.
- Lettieri CJ, Nathan SD, Barnett SD, Ahmad S, Shorr AF. 2006. Prevalence and Outcomes of Pulmonary Arterial Hypertension in Advanced Idiopathic Pulmonary Fibrosis. *Chest* 129: 746–752.
- Ley B, Collard HR. 2013. Epidemiology of idiopathic pulmonary fibrosis. *Clin. Epidemiol.* 5: 483–92.
- Li B, Wang JH-C. 2011. Fibroblasts and myofibroblasts in wound healing: Force generation and

- measurement. *J. Tissue Viability* 20: 108–120.
- Li H, He G, Yao H, Song L, Zeng L, Peng X, Rosol TJ, Deng X. 2015. TGF- $\beta$  Induces Degradation of PTHrP Through Ubiquitin-Proteasome System in Hepatocellular Carcinoma. *J. Cancer* 6: 511–8.
- Li X, Pontén A, Aase K, Karlsson L, Abramsson A, Uutela M, Bäckström G, Hellström M, Boström H, Li H, Soriano P, Betsholtz C, Heldin CH, Alitalo K, Ostman A, Eriksson U. 2000. PDGF-C is a new protease-activated ligand for the PDGF alpha-receptor. *Nat. Cell Biol.* 2: 302–9.
- Lilienbaum A. 2013. Relationship between the proteasomal system and autophagy. *Int. J. Biochem. Mol. Biol.* 4: 1–26.
- Lin S-L, Kisseleva T, Brenner DA, Duffield JS. 2008. Pericytes and Perivascular Fibroblasts Are the Primary Source of Collagen-Producing Cells in Obstructive Fibrosis of the Kidney. *Am. J. Pathol.* 173: 1617–1627.
- Linseman DA, Benjamin CW, Jones DA. 1995. Convergence of Angiotensin II and Platelet-derived Growth Factor Receptor Signaling Cascades in Vascular Smooth Muscle Cells. *J. Biol. Chem.* 270: 12563–12568.
- Liu C, Li J, Xiang X, Guo L, Tu K, Liu Q, Shah VH, Kang N. 2014. PDGF receptor- $\alpha$  promotes TGF- $\beta$  signaling in hepatic stellate cells via transcriptional and posttranscriptional regulation of TGF- $\beta$  receptors. *Am. J. Physiol. Gastrointest. Liver Physiol.* 307: G749–59.
- Liu T, Zhang J, Zhang J, Mu X, Su H, Hu X, Liu W, Zhao E, Li W. 2013. RNA interference against platelet-derived growth factor receptor  $\alpha$  mRNA inhibits fibroblast transdifferentiation in skin lesions of patients with systemic sclerosis. *PLoS One* 8: e60414.
- Macneal K, Schwartz DA. 2012. The genetic and environmental causes of pulmonary fibrosis. *Proc. Am. Thorac. Soc.* 9: 120–5.
- Maher T, Adamali TM. 2012. Current and novel drug therapies for idiopathic pulmonary fibrosis. *Drug Des. Devel. Ther.* 6: 261.
- Maher TM, Evans IC, Bottoms SE, Mercer PF, Thorley AJ, Nicholson AG, Laurent GJ, Tetley TD, Chambers RC, McAnulty RJ. 2010. Diminished Prostaglandin E<sub>2</sub> Contributes to the Apoptosis Paradox in Idiopathic Pulmonary Fibrosis. *Am. J. Respir. Crit. Care Med.* 182: 73–82.
- Martin P. 1997. Wound healing--aiming for perfect skin regeneration. *Science* 276: 75–81.
- Martinez FJ, Chisholm A, Collard HR, Flaherty KR, Myers J, Raghu G, Walsh SLF, White ES, Richeldi L. 2017. The diagnosis of idiopathic pulmonary fibrosis: current and future approaches. *Lancet. Respir. Med.* 5: 61–71.
- Massagué J. 2012. TGF $\beta$  signalling in context. *Nat. Rev. Mol. Cell Biol.* 13: 616–30.
- Massagué J, Seoane J, Wotton D. 2005. Smad transcription factors. *Genes Dev.* 19: 2783–810.
- Matsui T, Heidarani M, Miki T, Popescu N, La Rochelle W, Kraus M, Pierce J, Aaronson S. 1989. Isolation

- of a novel receptor cDNA establishes the existence of two PDGF receptor genes. *Science* 243: 800–4.
- McAnulty RJ, Hernández-Rodríguez NA, Mutsaers SE, Coker RK, Laurent GJ. 1997. Indomethacin suppresses the anti-proliferative effects of transforming growth factor-beta isoforms on fibroblast cell cultures. *Biochem. J.* 321 ( Pt 3): 639–43.
- Mejía M, Carrillo G, Rojas-Serrano J, Estrada A, Suárez T, Alonso D, Barrientos E, Gaxiola M, Navarro C, Selman M. 2009. Idiopathic Pulmonary Fibrosis and Emphysema. *Chest* 136: 10–15.
- Mendelson K, Swendeman S, Saftig P, Blobel CP. 2010. Stimulation of platelet-derived growth factor receptor beta (PDGFRbeta) activates ADAM17 and promotes metalloproteinase-dependent cross-talk between the PDGFRbeta and epidermal growth factor receptor (EGFR) signaling pathways. *J. Biol. Chem.* 285: 25024–32.
- Merrilees MJ, Sodek J. Synthesis of TGF-beta 1 by vascular endothelial cells is correlated with cell spreading. *J. Vasc. Res.* 29: 376–84.
- Miller MF, Cohen ED, Baggs JE, Lu MM, Hogenesch JB, Morrisey EE. 2012. Wnt ligands signal in a cooperative manner to promote foregut organogenesis. *Proc. Natl. Acad. Sci. U. S. A.* 109: 15348–53.
- Mishra PJ, Mishra PJ, Glod JW, Banerjee D. 2009. Mesenchymal Stem Cells: Flip Side of the Coin. *Cancer Res.* 69: 1255–1258.
- Miura S, Hamada S, Masamune A, Satoh K, Shimosegawa T. 2014. CUB-domain containing protein 1 represses the epithelial phenotype of pancreatic cancer cells. *Exp. Cell Res.* 321: 209–18.
- Miyake Y, Sasaki S, Yokoyama T, Chida K, Azuma A, Suda T, Kudoh S, Sakamoto N, Okamoto K, Kobashi G, Washio M, Inaba Y, Tanaka H. 2005. Occupational and Environmental Factors and Idiopathic Pulmonary Fibrosis in Japan. *Ann. Occup. Hyg.* 49: 259–65.
- Miyazawa Y, Uekita T, Hiraoka N, Fujii S, Kosuge T, Kanai Y, Nojima Y, Sakai R. 2010. CUB domain-containing protein 1, a prognostic factor for human pancreatic cancers, promotes cell migration and extracellular matrix degradation. *Cancer Res.* 70: 5136–46.
- Monje P, Marinissen MJ, Gutkind JS. 2003. Phosphorylation of the carboxyl-terminal transactivation domain of c-Fos by extracellular signal-regulated kinase mediates the transcriptional activation of AP-1 and cellular transformation induced by platelet-derived growth factor. *Mol. Cell. Biol.* 23: 7030–43.
- Moodley YP, Scaffidi AK, Misso NL, Keerthisingam C, McAnulty RJ, Laurent GJ, Mutsaers SE, Thompson PJ, Knight DA. 2003. Fibroblasts isolated from normal lungs and those with idiopathic pulmonary fibrosis differ in interleukin-6/gp130-mediated cell signaling and proliferation. *Am. J. Pathol.* 163: 345–54.
- Moustakas A, Souchelnytskyi S, Heldin CH. 2001. Smad regulation in TGF-beta signal transduction. *J. Cell Sci.* 114: 4359–69.
- Mu Y, Gudey SK, Landström M. 2012. Non-Smad signaling pathways. *Cell Tissue Res.* 347: 11–20.

- Mucsi I, Skorecki KL, Goldberg HJ. 1996. Extracellular signal-regulated kinase and the small GTP-binding protein, Rac, contribute to the effects of transforming growth factor-beta1 on gene expression. *J. Biol. Chem.* 271: 16567–72.
- Mulder KM. 2000. Role of Ras and Mapks in TGF $\beta$  signaling. *Cytokine Growth Factor Rev.* 11: 23–35.
- Mulugeta S, Maguire JA, Newitt JL, Russo SJ, Kotorashvili A, Beers MF. 2007. Misfolded BRICHOS SP-C mutant proteins induce apoptosis via caspase-4- and cytochrome c-related mechanisms. *Am. J. Physiol. Lung Cell. Mol. Physiol.* 293: L720-9.
- Murray-Rust J, McDonald NQ, Blundell TL, Hosang M, Oefner C, Winkler F, Bradshaw RA. 1993. Topological similarities in TGF-beta 2, PDGF-BB and NGF define a superfamily of polypeptide growth factors. *Structure* 1: 153–9.
- Nadrous HF, Pellikka PA, Krowka MJ, Swanson KL, Chaowalit N, Decker PA, Ryu JH. 2005. Pulmonary Hypertension in Patients With Idiopathic Pulmonary Fibrosis. *Chest* 128: 2393–2399.
- Nakamura Y, Suda T. 2015. Idiopathic Pulmonary Fibrosis: Diagnosis and Clinical Manifestations. *Clin. Med. Insights. Circ. Respir. Pulm. Med.* 9: 163–71.
- Nakao A, Imamura T, Souchelnytskyi S, Kawabata M, Ishisaki A, Oeda E, Tamaki K, Hanai J, Heldin CH, Miyazono K, ten Dijke P. 1997. TGF-beta receptor-mediated signalling through Smad2, Smad3 and Smad4. *EMBO J.* 16: 5353–5362.
- Nalysnyk L, Cid-Ruzafa J, Rotella P, Esser D. 2012. Incidence and prevalence of idiopathic pulmonary fibrosis: review of the literature. *Eur. Respir. Rev.* 21: 355–61.
- Neri S, Hashimoto H, Kii H, Watanabe H, Masutomi K, Kuwata T, Date H, Tsuboi M, Goto K, Ochiai A, Ishii G. 2016. Cancer cell invasion driven by extracellular matrix remodeling is dependent on the properties of cancer-associated fibroblasts. *J. Cancer Res. Clin. Oncol.* 142: 437–446.
- Nho RS, Peterson M, Hergert P, Henke CA. 2013. FoxO3a (Forkhead Box O3a) Deficiency Protects Idiopathic Pulmonary Fibrosis (IPF) Fibroblasts from Type I Polymerized Collagen Matrix-Induced Apoptosis via Caveolin-1 (cav-1) and Fas. *PLoS One* 8: e61017.
- Nicholson AG, Fulford LG, Colby T V, du Bois RM, Hansell DM, Wells AU. 2002. The relationship between individual histologic features and disease progression in idiopathic pulmonary fibrosis. *Am. J. Respir. Crit. Care Med.* 166: 173–7.
- Nishiyama O, Taniguchi H, Kondoh Y, Kimura T, Ogawa T, Watanabe F, Nishimura K. 2005. Health-related quality of life in patients with idiopathic pulmonary fibrosis. What is the main contributing factor? *Respir. Med.* 99: 408–414.
- Noble PW, Albera C, Bradford WZ, Costabel U, du Bois RM, Fagan EA, Fishman RS, Glaspole I, Glassberg MK, Lancaster L, Lederer DJ, Leff JA, Nathan SD, Pereira CA, Swigris JJ, Valeyre D, King TE. 2016. Pirfenidone for idiopathic pulmonary fibrosis: analysis of pooled data from three multinational phase

- 3 trials. *Eur. Respir. J.* 47: 243–253.
- Noble PW, Albera C, Bradford WZ, Costabel U, Glassberg MK, Kardatzke D, King TE, Lancaster L, Sahn SA, Szwarcberg J, Valeyre D, du Bois RM. 2011. Pirfenidone in patients with idiopathic pulmonary fibrosis (CAPACITY): two randomised trials. *Lancet* 377: 1760–9.
- Nogee LM, Dunbar AE, Wert SE, Askin F, Hamvas A, Whitsett JA. 2001. A Mutation in the Surfactant Protein C Gene Associated with Familial Interstitial Lung Disease. *N. Engl. J. Med.* 344: 573–579.
- Noskovičová N, Petřek M, Eickelberg O, Heinzelmann K. 2015. Platelet-derived growth factor signaling in the lung. From lung development and disease to clinical studies. *Am. J. Respir. Cell Mol. Biol.* 52: 263–84.
- Oehrle B, Burgstaller G, Irmeler M, Dehmel S, Grün J, Hwang T, Krauss-Etschmann S, Beckers J, Meiners S, Eickelberg O. 2015. Validated prediction of pro-invasive growth factors using a transcriptome-wide invasion signature derived from a complex 3D invasion assay. *Sci. Rep.* 5: 12673.
- Orchard-Webb DJ, Lee TC, Cook GP, Blair GE. 2014. CUB domain containing protein 1 (CDCP1) modulates adhesion and motility in colon cancer cells. *BMC Cancer* 14: 754.
- Patterson KC, Shah RJ, Porteous MK, Christie JD, D’Errico CA, Chadwick M, Triano MJ, Deshpande C, Rossman MD, Litzky LA, Kreider M, Miller WT. 2017. Interstitial Lung Disease in the Elderly. *Chest* 151: 838–844.
- Paulsson Y, Karlsson C, Heldin C-H, Westermark B. 1993. Density-dependent inhibitory effect of transforming growth factor- $\beta$  on human fibroblasts involves the down-regulation of platelet-derived growth factor  $\beta$ -receptors. *J. Cell. Physiol.* 157: 97–103.
- Pechkovsky D V, Prêle CM, Wong J, Hogaboam CM, McAnulty RJ, Laurent GJ, Zhang SS-M, Selman M, Mutsaers SE, Knight DA. 2012. STAT3-mediated signaling dysregulates lung fibroblast-myofibroblast activation and differentiation in UIP/IPF. *Am. J. Pathol.* 180: 1398–412.
- Perry SE, Robinson P, Melcher A, Quirke P, Bühring H-J, Cook GP, Blair GE. 2007. Expression of the CUB domain containing protein 1 (CDCP1) gene in colorectal tumour cells. *FEBS Lett.* 581: 1137–42.
- Petrel TA, Brueggemeier RW. 2003. Increased proteasome-dependent degradation of estrogen receptor- $\alpha$  by TGF- $\beta$ 1 in breast cancer cell lines. *J. Cell. Biochem.* 88: 181–90.
- Pilling D, Fan T, Huang D, Kaul B, Gomer RH. 2009. Identification of markers that distinguish monocyte-derived fibrocytes from monocytes, macrophages, and fibroblasts. *PLoS One* 4: e7475.
- Porsch H, Mehić M, Olofsson B, Heldin P, Heldin C-H. 2014. Platelet-derived growth factor  $\beta$ -receptor, transforming growth factor  $\beta$  type I receptor, and CD44 protein modulate each other’s signaling and stability. *J. Biol. Chem.* 289: 19747–57.
- Porter KE, Turner NA. 2009. Cardiac fibroblasts: At the heart of myocardial remodeling. *Pharmacol. Ther.*

123: 255–278.

- Predic J, Soskic V, Bradley D, Godovac-Zimmermann J. 2002. Monitoring of Gene Expression by Functional Proteomics: Response of Human Lung Fibroblast Cells to Stimulation by Endothelin-1 †. *Biochemistry* 41: 1070–1078.
- Radford IR. 2002. Imatinib. Novartis. *Curr. Opin. Investig. Drugs* 3: 492–9.
- Rafii R, Juarez MM, Albertson TE, Chan AL. 2013. A review of current and novel therapies for idiopathic pulmonary fibrosis. *J. Thorac. Dis.* 5: 48–73.
- Raghu G, Collard HR, Egan JJ, Martinez FJ, Behr J, Brown KK, Colby T V., Cordier J-F, Flaherty KR, Lasky JA, Lynch DA, Ryu JH, Swigris JJ, Wells AU, Ancochea J, Bouros D, Carvalho C, Costabel U, Ebina M, Hansell DM, Johkoh T, Kim DS, King TE, Kondoh Y, Myers J, Müller NL, Nicholson AG, Richeldi L, Selman M, Dudden RF, Griss BS, Protzko SL, Schünemann HJ. 2011. An Official ATS/ERS/JRS/ALAT Statement: Idiopathic Pulmonary Fibrosis: Evidence-based Guidelines for Diagnosis and Management. *Am. J. Respir. Crit. Care Med.* 183: 788–824.
- Rangarajan S, Locy ML, Luckhardt TR, Thannickal VJ. 2016. Targeted Therapy for Idiopathic Pulmonary Fibrosis: Where To Now? *Drugs* 76: 291–300.
- Ravichandran KS. 2001. Signaling via Shc family adapter proteins. *Oncogene* 20: 6322–30.
- Ravikanth M, Soujanya P, Manjunath K, Saraswathi TR, Ramachandran CR. 2011. Heterogeneity of fibroblasts. *J. Oral Maxillofac. Pathol.* 15: 247–50.
- Razmara M, Heldin C-H, Lennartsson J. 2013. Platelet-derived growth factor-induced Akt phosphorylation requires mTOR/Rictor and phospholipase C- $\gamma$ 1, whereas S6 phosphorylation depends on mTOR/Raptor and phospholipase D. *Cell Commun. Signal.* 11: 3.
- Richeldi L. 2014. Treatments for Idiopathic Pulmonary Fibrosis. *N. Engl. J. Med.* 371: 781–784.
- Richeldi L, du Bois RM, Raghu G, Azuma A, Brown KK, Costabel U, Cottin V, Flaherty KR, Hansell DM, Inoue Y, Kim DS, Kolb M, Nicholson AG, Noble PW, Selman M, Taniguchi H, Brun M, Le Maulf F, Girard M, Stowasser S, Schlenker-Herceg R, Disse B, Collard HR. 2014a. Efficacy and Safety of Nintedanib in Idiopathic Pulmonary Fibrosis. *N. Engl. J. Med.* 370: 2071–82.
- Richeldi L, Cottin V, Flaherty KR, Kolb M, Inoue Y, Raghu G, Taniguchi H, Hansell DM, Nicholson AG, Le Maulf F, Stowasser S, Collard HR. 2014b. Design of the INPULSIS™ trials: Two phase 3 trials of nintedanib in patients with idiopathic pulmonary fibrosis. *Respir. Med.* 108: 1023–30.
- Roy MG, Livraghi-Butrico A, Fletcher AA, McElwee MM, Evans SE, Boerner RM, Alexander SN, Bellinghausen LK, Song AS, Petrova YM, Tuvim MJ, Adachi R, Romo I, Bordt AS, Bowden MG, Sisson JH, Woodruff PG, Thornton DJ, Rousseau K, De la Garza MM, Moghaddam SJ, Karmouty-Quintana H, Blackburn MR, Drouin SM, Davis CW, Terrell KA, Grubb BR, O’Neal WK, Flores SC, Cota-Gomez A, Lozupone CA, Donnelly JM, Watson AM, Hennessy CE, Keith RC, Yang I V, Barthel

- L, Henson PM, Janssen WJ, Schwartz DA, Boucher RC, Dickey BF, Evans CM. 2014. Muc5b is required for airway defence. *Nature* 505: 412–6.
- Rozario T, DeSimone DW. 2010. The extracellular matrix in development and morphogenesis: a dynamic view. *Dev. Biol.* 341: 126–40.
- Ryerson et al. 2011. Cough predicts prognosis in idiopathic pulmonary fibrosis. *Respirology* 16: 969–975.
- Sakai N, Tager AM. 2013. Fibrosis of two: Epithelial cell-fibroblast interactions in pulmonary fibrosis. *Biochim. Biophys. Acta* 1832: 911–21.
- Sandbo N, Dulin N. 2011. Actin cytoskeleton in myofibroblast differentiation: ultrastructure defining form and driving function. *Transl. Res.* 158: 181–96.
- Sandbo N, Lau A, Kach J, Ngam C, Yau D, Dulin NO. 2011. Delayed stress fiber formation mediates pulmonary myofibroblast differentiation in response to TGF- $\beta$ . *Am. J. Physiol. Lung Cell. Mol. Physiol.* 301: L656–66.
- Sanders YY, Ambalavanan N, Halloran B, Zhang X, Liu H, Crossman DK, Bray M, Zhang K, Thannickal VJ, Hagood JS. 2012. Altered DNA Methylation Profile in Idiopathic Pulmonary Fibrosis. *Am. J. Respir. Crit. Care Med.* 186: 525–535.
- Sanders YY, Pardo A, Selman M, Nuovo GJ, Tollefsbol TO, Siegal GP, Hagood JS. 2008. Thy-1 Promoter Hypermethylation. *Am. J. Respir. Cell Mol. Biol.* 39: 610–618.
- Scotton CJ, Chambers RC. 2007. Molecular targets in pulmonary fibrosis: the myofibroblast in focus. *Chest* 132: 1311–21.
- Seibold MA, Wise AL, Speer MC, Steele MP, Brown KK, Loyd JE, Fingerlin TE, Zhang W, Gudmundsson G, Groshong SD, Evans CM, Garantziotis S, Adler KB, Dickey BF, du Bois RM, Yang I V., Herron A, Kervitsky D, Talbert JL, Markin C, Park J, Crews AL, Slifer SH, Auerbach S, Roy MG, Lin J, Hennessy CE, Schwarz MI, Schwartz DA. 2011. A Common *MUC5B* Promoter Polymorphism and Pulmonary Fibrosis. *N. Engl. J. Med.* 364: 1503–1512.
- Selman M, King TE, Pardo A, American Thoracic Society, European Respiratory Society, American College of Chest Physicians. 2001. Idiopathic pulmonary fibrosis: prevailing and evolving hypotheses about its pathogenesis and implications for therapy. *Ann. Intern. Med.* 134: 136–51.
- Selman M, Pardo A. 2006. Role of epithelial cells in idiopathic pulmonary fibrosis: from innocent targets to serial killers. *Proc. Am. Thorac. Soc.* 3: 364–72.
- Serini G, Bochaton-Piallat ML, Ropraz P, Geinoz A, Borsi L, Zardi L, Gabbiani G. 1998. The fibronectin domain ED-A is crucial for myofibroblastic phenotype induction by transforming growth factor-beta1. *J. Cell Biol.* 142: 873–81.
- Serini G, Gabbiani G. 1999. Mechanisms of Myofibroblast Activity and Phenotypic Modulation. *Exp. Cell Res.* 250: 273–283.

- Shi-Wen X, Parapuram SK, Pala D, Chen Y, Carter DE, Eastwood M, Denton CP, Abraham DJ, Leask A. 2009. Requirement of transforming growth factor  $\beta$ -activated kinase 1 for transforming growth factor  $\beta$ -induced  $\alpha$ -smooth muscle actin expression and extracellular matrix contraction in fibroblasts. *Arthritis Rheum.* 60: 234–241.
- Shi Y, Massagué J. 2003. Mechanisms of TGF-beta signaling from cell membrane to the nucleus. *Cell* 113: 685–700.
- Shi Y, Wang YF, Jayaraman L, Yang H, Massagué J, Pavletich NP. 1998. Crystal structure of a Smad MH1 domain bound to DNA: insights on DNA binding in TGF-beta signaling. *Cell* 94: 585–94.
- Scherl-Mostageer M, Sommergruber W, Abseher R, Hauptmann R, Ambros P, Schweifer N. 2001. Identification of a novel gene, CDCP1, overexpressed in human colorectal cancer. *Oncogene* 20: 4402–8.
- Schiller HB, Mayr CH, Leuschner G, Strunz M, Staab-Weijnitz C, Preisendörfer S, Eckes B, Moinzadeh P, Krieg T, Schwartz DA, Hatz RA, Behr J, Mann M, Eickelberg O. 2017. Deep Proteome Profiling Reveals Common Prevalence of MZB1-positive Plasma B Cells in Human Lung and Skin Fibrosis. *Am. J. Respir. Crit. Care Med.*: rccm.201611-2263OC.
- Schultz-Cherry S, Ribeiro S, Gentry L, Murphy-Ullrich JE. 1994. Thrombospondin binds and activates the small and large forms of latent transforming growth factor-beta in a chemically defined system. *J. Biol. Chem.* 269: 26775–82.
- Schwartz DA, Helmers RA, Galvin JR, Van Fossen DS, Frees KL, Dayton CS, Burmeister LF, Hunninghake GW. 1994. Determinants of survival in idiopathic pulmonary fibrosis. *Am. J. Respir. Crit. Care Med.* 149: 450–4.
- Siva AC, Wild MA, Kirkland RE, Nolan MJ, Lin B, Maruyama T, Yantiri-Wernimont F, Frederickson S, Bowdish KS, Xin H. 2008. Targeting CUB domain-containing protein 1 with a monoclonal antibody inhibits metastasis in a prostate cancer model. *Cancer Res.* 68: 3759–66.
- Slany A, Meshcheryakova A, Beer A, Ankersmit H, Paulitschke V, Gerner C. 2014. Plasticity of fibroblasts demonstrated by tissue-specific and function-related proteome profiling. *Clin. Proteomics* 11: 41.
- Somasundaram R, Schuppan D. 1996. Type I, II, III, IV, V, and VI collagens serve as extracellular ligands for the isoforms of platelet-derived growth factor (AA, BB, and AB). *J. Biol. Chem.* 271: 26884–91.
- Spagnolo P, Maher TM, Richeldi L. 2015. Idiopathic pulmonary fibrosis: Recent advances on pharmacological therapy. *Pharmacol. Ther.* 152: 18–27.
- Suganuma H, Sato A, Tamura R, Chida K. 1995. Enhanced migration of fibroblasts derived from lungs with fibrotic lesions. *Thorax* 50: 984–9.
- Swigris JJ, Kuschner WG, Jacobs SS, Wilson SR, Gould MK. 2005. Health-related quality of life in patients with idiopathic pulmonary fibrosis: a systematic review. *Thorax* 60: 588–94.

- Takeda et al. 2010. CD318/CUB-domain-containing protein 1 expression on cord blood hematopoietic progenitors. *Exp. Ther. Med.* 1: 497–501.
- Taniguchi H, Ebina M, Kondoh Y, Ogura T, Azuma A, Suga M, Taguchi Y, Takahashi H, Nakata K, Sato A, Takeuchi M, Raghu G, Kudoh S, Nukiwa T, Pirfenidone Clinical Study Group in Japan. 2010. Pirfenidone in idiopathic pulmonary fibrosis. *Eur. Respir. J.* 35: 821–829.
- Terme J-M, Lhermitte L, Asnafi V, Jalinot P. 2009. TGF- $\beta$  induces degradation of TAL1/SCL by the ubiquitin-proteasome pathway through AKT-mediated phosphorylation. *Blood* 113: 6695–6698.
- Thannickal VJ, Toews GB, White ES, Lynch III JP, Martinez FJ. 2004. Mechanisms of Pulmonary Fibrosis. *Annu. Rev. Med.* 55: 395–417.
- Thomas AQ, Lane K, Phillips J, Prince M, Markin C, Speer M, Schwartz DA, Gaddipati R, Marney A, Johnson J, Roberts R, Haines J, Stahlman M, Loyd JE. 2002. Heterozygosity for a surfactant protein C gene mutation associated with usual interstitial pneumonitis and cellular nonspecific interstitial pneumonitis in one kindred. *Am. J. Respir. Crit. Care Med.* 165: 1322–8.
- Todd NW, Luzina IG, Atamas SP. 2012. Molecular and cellular mechanisms of pulmonary fibrosis. *Fibrogenesis Tissue Repair* 5: 11.
- Tomasek JJ, Gabbiani G, Hinz B, Chaponnier C, Brown RA. 2002. Myofibroblasts and mechano-regulation of connective tissue remodelling. *Nat. Rev. Mol. Cell Biol.* 3: 349–363.
- Tsakiri KD, Cronkhite JT, Kuan PJ, Xing C, Raghu G, Weissler JC, Rosenblatt RL, Shay JW, Garcia CK. 2007. Adult-onset pulmonary fibrosis caused by mutations in telomerase. *Proc. Natl. Acad. Sci. U. S. A.* 104: 7552–7.
- Tschumperlin DJ, Drazen JM. 2006. CHRONIC EFFECTS OF MECHANICAL FORCE ON AIRWAYS. *Annu. Rev. Physiol.* 68: 563–583.
- Tukiainen P, Taskinen E, Holsti P, Korhola O, Valle M. 1983. Prognosis of cryptogenic fibrosing alveolitis. *Thorax* 38: 349–55.
- Tzouvelekis A, Bonella F, Spagnolo P. 2015. Update on therapeutic management of idiopathic pulmonary fibrosis. *Ther. Clin. Risk Manag.* 11: 359–70.
- Uekita T, Jia L, Narisawa-Saito M, Yokota J, Kiyono T, Sakai R. 2007. CUB Domain-Containing Protein 1 Is a Novel Regulator of Anoikis Resistance in Lung Adenocarcinoma. *Mol. Cell. Biol.* 27: 7649–7660.
- Uekita T, Tanaka M, Takigahira M, Miyazawa Y, Nakanishi Y, Kanai Y, Yanagihara K, Sakai R. 2008a. CUB-Domain-Containing Protein 1 Regulates Peritoneal Dissemination of Gastric Scirrhous Carcinoma. *Am. J. Pathol.* 172: 1729–1739.
- Uekita T, Tanaka M, Takigahira M, Miyazawa Y, Nakanishi Y, Kanai Y, Yanagihara K, Sakai R. 2008b. CUB-domain-containing protein 1 regulates peritoneal dissemination of gastric scirrhous carcinoma.

- Am. J. Pathol. 172: 1729–39.
- Uemura M, Swenson ES, Gaça MDA, Giordano FJ, Reiss M, Wells RG. 2005. Smad2 and Smad3 play different roles in rat hepatic stellate cell function and alpha-smooth muscle actin organization. *Mol. Biol. Cell* 16: 4214–24.
- Vaillant P, Menard O, Vignaud JM, Martinet N, Martinet Y. 1996. The role of cytokines in human lung fibrosis. *Monaldi Arch. chest Dis. = Arch. Monaldi per le Mal. del torace* 51: 145–52.
- Valeyre D, Albera C, Bradford WZ, Costabel U, King TE, Leff JA, Noble PW, Sahn SA, du Bois RM. 2014. Comprehensive assessment of the long-term safety of pirfenidone in patients with idiopathic pulmonary fibrosis. *Respirology* 19: 740–747.
- Vassbotn F, Havnen O, Heldin C, Holmsen H. 1994. Negative feedback regulation of human platelets via autocrine activation of the platelet-derived growth factor alpha-receptor. *J. Biol. Chem.* 269: 13874–13879.
- Verrecchia F, Chu ML, Mauviel A. 2001. Identification of novel TGF-beta /Smad gene targets in dermal fibroblasts using a combined cDNA microarray/promoter transactivation approach. *J. Biol. Chem.* 276: 17058–62.
- Vert G, Chory J. 2011. Crosstalk in cellular signaling: background noise or the real thing? *Dev. Cell* 21: 985–91.
- Visscher DW, Myers JL. 2006. Histologic spectrum of idiopathic interstitial pneumonias. *Proc. Am. Thorac. Soc.* 3: 322–9.
- Vittal R, Horowitz JC, Moore BB, Zhang H, Martinez FJ, Toews GB, Standiford TJ, Thannickal VJ. 2005. Modulation of prosurvival signaling in fibroblasts by a protein kinase inhibitor protects against fibrotic tissue injury. *Am. J. Pathol.* 166: 367–75.
- Waisberg DR, Barbas-Filho JV, Parra ER, Ferezlian S, Ribeiro de Carvalho CR, Kairalla RA, Capelozzi VL. 2010. Abnormal expression of telomerase/apoptosis limits type II alveolar epithelial cell replication in the early remodeling of usual interstitial pneumonia/idiopathic pulmonary fibrosis. *Hum. Pathol.* 41: 385–391.
- Walmsley GG, Rinkevich Y, Hu MS, Montoro DT, Lo DD, McArdle A, Maan ZN, Morrison SD, Duscher D, Whittam AJ, Wong VW, Weissman IL, Gurtner GC, Longaker MT. 2015. Live fibroblast harvest reveals surface marker shift in vitro. *Tissue Eng. Part C. Methods* 21: 314–21.
- Wang C, Deng L, Hong M, Akkaraju GR, Inoue J, Chen ZJ. 2001. TAK1 is a ubiquitin-dependent kinase of MKK and IKK. *Nature* 412: 346–351.
- Wells AU, Desai SR, Rubens MB, Goh NSL, Cramer D, Nicholson AG, Colby T V., du Bois RM, Hansell DM. 2003. Idiopathic Pulmonary Fibrosis. *Am. J. Respir. Crit. Care Med.* 167: 962–969.
- De Wever O, Demetter P, Mareel M, Bracke M. 2008. Stromal myofibroblasts are drivers of invasive cancer

- growth. *Int. J. Cancer* 123: 2229–2238.
- Wharton K, Derynck R. 2009. TGFbeta family signaling: novel insights in development and disease. *Development* 136: 3691–7.
- White ES. 2015. Lung extracellular matrix and fibroblast function. *Ann. Am. Thorac. Soc.*
- White ES, Lazar MH, Thannickal VJ. 2003. Pathogenetic mechanisms in usual interstitial pneumonia/idiopathic pulmonary fibrosis. *J. Pathol.* 201: 343–54.
- Wollin L, Maillet I, Quesniaux V, Holweg A, Ryffel B. 2014. Antifibrotic and anti-inflammatory activity of the tyrosine kinase inhibitor nintedanib in experimental models of lung fibrosis. *J. Pharmacol. Exp. Ther.* 349: 209–20.
- Wollin L, Wex E, Pautsch A, Schnapp G, Hostettler KE, Stowasser S, Kolb M. 2015. Mode of action of nintedanib in the treatment of idiopathic pulmonary fibrosis. *Eur. Respir. J.* 45: 1434–45.
- Wortmann A, He Y, Deryugina EI, Quigley JP, Hooper JD. 2009. The cell surface glycoprotein CDCP1 in cancer--insights, opportunities, and challenges. *IUBMB Life* 61: 723–30.
- Wright HJ, Police AM, Razorenova O V. 2016. Targeting CDCP1 dimerization in triple-negative breast cancer. *Cell Cycle* 15: 2385–2386.
- Yamakage A, Kikuchi K, Smith EA, LeRoy EC, Trojanowska M. 1992. Selective upregulation of platelet-derived growth factor alpha receptors by transforming growth factor beta in scleroderma fibroblasts. *J. Exp. Med.* 175: 1227–34.
- Yamashita M, Fatyol K, Jin C, Wang X, Liu Z, Zhang YE. 2008. TRAF6 Mediates Smad-Independent Activation of JNK and p38 by TGF- $\beta$ . *Mol. Cell* 31: 918–924.
- Yong SJ, Adlakha A, Limper AH. 2001. Circulating transforming growth factor-beta(1): a potential marker of disease activity during idiopathic pulmonary fibrosis. *Chest* 120: 68S–70S.
- Zawel L, Dai JL, Buckhaults P, Zhou S, Kinzler KW, Vogelstein B, Kern SE. 1998. Human Smad3 and Smad4 are sequence-specific transcription activators. *Mol. Cell* 1: 611–7.
- Zhang P, Gao WY, Turner S, Ducatman BS. 2003. Gleevec (STI-571) inhibits lung cancer cell growth (A549) and potentiates the cisplatin effect in vitro. *Mol. Cancer* 2: 1.
- Zoz DF, Lawson WE, Blackwell TS. 2011. Idiopathic Pulmonary Fibrosis: A Disorder of Epithelial Cell Dysfunction. *Am. J. Med. Sci.* 341: 435–438.

## 8 LIST OF TABLES

**Table 3.1:** Chemical and reagents

**Table 3.2:** Consumables

**Table 3.3:** Media

**Table 3.4:** Human siRNAs

**Table 3.5:** DNA plasmids

**Table 3.6:** Inhibitors and antagonists

**Table 3.7:** Primary antibodies for Western blot

**Table 3.8:** Secondary antibodies for Western blot

**Table 3.9:** Fluorochrome-conjugated antibodies for FACS analysis

**Table 3.10:** Isotype controls for FACS analysis

**Table 3.11:** Primary antibodies for immunofluorescence stainings

**Table 3.12:** Secondary antibodies for immunofluorescence stainings

**Table 3.13:** Antibodies for immunoprecipitation

**Table 3.14:** Sequences of human primers

**Table 3.15:** Kits

**Table 3.16:** Laboratory equipment

**Table 3.17:** Software

**Table 3.18:** Complete transfection mix per one well of a 6-well plate or one 10 cm dish

**Table 3.19:** Plasmid calculations

**Table 3.20:** Complete transfection solution per one well of a 48-well plate

**Table 3.21:** Composition of 4 % SDS-PAGE Stacking gel

**Table 3.22:** Composition of 7.5 % and 10 % SDS-PAGE Separation gels

**Table 3.23:** Deparaffinization protocol

**Table 3.24:** Mastermix for cDNA synthesis

**Table 3.25:** qPCR reaction mix per one assay

**Table 3.26:** Standard qRT-PCR protocol

## 9 LIST OF FIGURES

- Figure 1.1:** Schematic illustration of potential clinical development and progression of IPF.
- Figure 1.2:** Histopathological features of UIP.
- Figure 1.3:** Phenotypical differences between fibroblasts and myofibroblasts.
- Figure 1.4:** Myofibroblast precursor cells.
- Figure 1.5:** A schematic overview of profibrotic stimuli promoting myofibroblasts transdifferentiation in IPF.
- Figure 1.6:** A schematic illustration of Smad-dependent signaling pathway.
- Figure 1.7:** A schematic illustration of Smad-independent signaling pathway.
- Figure 1.8:** A schematic overview of PDGF receptors and PDGF/PDGFR binding patterns.
- Figure 4.1:** TGF $\beta$  downregulates PDGFR $\alpha$  expression in phLFs.
- Figure 4.2:** TGF $\beta$  decreases PDGFR $\alpha$  expression on the surface of phLFs.
- Figure 4.3:** CDCP1 co-stains with CD90 (Thy-1) on the surface of phLFs.
- Figure 4.4:** CDCP1 is downregulated by TGF $\beta$  in phLFs.
- Figure 4.5:** PDGF signaling in human lung fibroblasts.
- Figure 4.6:** PDGF-AB signaling plays a role in invasion properties of phLFs.
- Figure 4.7:** PDGF-AB and PDGF-DD enhance PDGF signaling independently of TGF $\beta$ .
- Figure 4.8:** Knockdown of PDGFR $\alpha$  and PDGFR $\beta$  decreases their expression in phLFs.
- Figure 4.9:** PDGF ligands enhance PDGF signaling in the absence of PDGFR $\alpha$ .
- Figure 4.10:** Imatinib and Nintedanib block PDGF signaling in phLFs.
- Figure 4.11:** The absence of PDGFR $\alpha$  receptor diminishes inhibitory effect of Nintedanib on PDGF signaling.
- Figure 4.12:** Knockdown of PDGFR $\alpha$  enhances  $\alpha$ SMA and collagen V expression.
- Figure 4.13:** Silencing of CDCP1 decreases its cell surface and total protein levels.
- Figure 4.14:** CDCP1 silencing negatively impacts cell adhesion of phLFs.
- Figure 4.15:** CDCP1-depleted lung fibroblasts exhibit increased  $\alpha$ SMA and ECM expression.
- Figure 4.16:** Absence of CDCP1 enhances TGF $\beta$ -mediated Smad3 phosphorylation in phLFs.
- Figure 4.17:** TGF $\beta$  attenuates CDCP1 expression via non-canonical signaling.
- Figure 4.18:** TGF $\beta$  potentially attenuates CDCP1 expression via a complex proteasomal degradation.

## ACKNOWLEDGEMENTS

Foremost, I would like to express my deepest appreciation to my supervisor Prof. Dr. Oliver Eickelberg for giving me the opportunity to perform my scientific internship and furthermore write my thesis under his supervision at the CPC. I am very thankful for his guidance, constant support, and especially for teaching me that there are no problems in life, only challenges.

Furthermore, I would very much like to thank my supervisor Dr. Katharina Heinzelmann for her excellent supervision, everlasting support inside and outside of the lab, and for her enthusiasm, kindness, and extensive scientific discussions during past three and a half years. I am extremely glad for being a part of her research team during my internship and PhD studies.

I am very grateful to Prof. Dr. Martin Petřek from the Palacky University in Czech Republic for giving me an opportunity to perform my scientific internship at the CPC and to Prof. Dr. Daniel Krappmann for critical review and discussion of my PhD project as my external thesis committee advisor.

I also appreciate a help of our collaborators from the Proteomics core facility, and clinical collaborators from the University Hospital of Munich and Asklepios Clinic (Prof. Jürgen Behr, Prof. Rudolf Hatz, Dr. Michael Lindner, Dr. Hauke Winter, and Dr. Gerhard Preissler). Furthermore, I would like to thank the CPC-M BioArchive for providing human material for this work.

My special and deep appreciation goes to all former and current members of Eickelberg lab, specifically Dr. Gerald Burgstaller, Dr. Claudia Staab-Weijnitz, Dr. Isis Fernandez, Dr. Natalia Smirnova, Dr. Nikica Mise-Racek, Dr. Viktoriya Tomiatti, Dr. Andrea Schamberger, Flavia Greiffo, Larissa Knüppel, Jessica Grün, Arunima Sengupta, Michael Gerckens, Emmanuela Gbandi, Birgitta Heckl, Katharina Lippl, Daniela Dietel, Kyra Peters, Elisabeth Hennen, Ann-Christin Beitel, Dibora Tibebe, Heike Hoffmann, Constanze Heise for their constant support, scientific discussions, excellent technical performance, and all the fun inside and outside of the lab. Moreover, I am very thankful to every single colleague from the CPC, who have always been a constant support and helped me not only with scientific performance but also outside of the lab.

I would also like to acknowledge an outstanding CPC Research School team, specifically Prof. Dr. Dr. Melanie Königshoff, Dr. Doreen Franke, Dr. Camille Beunèche, Dr. Hoeke Baarsma, and Dr. Claudia Staab-Weijnitz for their tremendous help, motivation, enthusiasm, and challenges during the whole graduate school program.

My very special and deep thanks go to Flavia Greiffo, Aina Martin Medina, Rita Costa, Carolina Ballester López, and Martina De Santis for their unconditional help, support, endless discussions, for always being there for me, and especially for all the fun and memories we made and shared together.

Also, I want to say thanks to all my former office members, specifically Dr. Deniz Bölükbaş, Vanessa Welk, Dr. Ilona Keller, Thomas Meul, Simon Christ, Christoph Mayr, and Stefanie Weiß for their help, motivation, and especially funny times we shared during our PhD.

Special gratitude also goes to my dearest friends Monika Borovská and Marián Slávik, who have always been there for me when I needed it, and who supported me during the whole PhD.

My dearest and heartiest gratitude goes to my family for their unconditional love, support, motivation, and patience during the whole PhD.

Finally, my kind and sincere thanks goes to all reviewers who dedicated their time and motivation to proofread my thesis.